Pan African University
Institute of Water
and Energy Sciences

PAN-AFRICAN UNIVERSITY
INSTITUTE FOR WATER AND ENERGY SCIENCES
(including CLIMATE CHANGE)

Master Dissertation

Submitted in partial fulfillment of the requirements for the Master degree in

[WATER ENGINEERING]

Presented by

Leopold Andre Louis Cheikh Anta Guedji NGOM

TITLE OF THESIS: AN ASSESSMENT OF CLIMATE CHANGE IMPACT ON WATER RELATED ECOSYSTEM SERVICES (WRES) INCLUDING HYDROPOWER POTENTIAL IN THE DANO CATCHMENT (VOLTA BASIN)

Defended on 00/09/2019 Before the Following Committee:

Chair:	Ghenim Abderrahmane	Professor	University of Tlemcen
Co-supervisor:	Aymar Bossa	Ph.D	WASCAL
Co-supervisor:	Yacouba Yira	Ph.D	WASCAL/IRSAT
External Examiner :	Thameur Chaibi	Professor	INRGREF
Internal Examiner	Halima Belarbi	Ph.D	Centre Universitaire de Maghnia

Declaration

I, LEOPOLD ANDRE LOUIS CHEIKH ANTA GUEDJI NGOM hereby declare that this thesis represents my personal work, realized to the best of my knowledge. I also declare that all information, material and results from other works presented here, have been fully cited and referenced in accordance with the academic rules and ethics.

Signed: Date:30/09/2019

LEOPOLD ANDRE LOUIS CHEIKH ANTA GUEDJI NGOM

Certification

The undersigned certifies that they have read and hereby recommend for the acceptance by the Pan Africa University Institute of Water and Energy Sciences, a dissertation entitled "**An assessment of climate change impact on water related ecosystem services (WRES) including hydropower potential in the Kandadji catchment in West Africa**", in fulfillment of the requirement of the award of the degree in Master of Science in Water Engineering (WE).

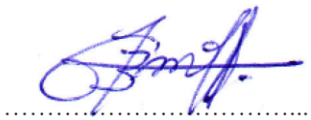

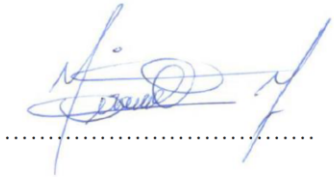

Dr. Aymar Yaovi Bossa

(Main Supervisor)

Date September 30, 2019

Dr. Yacouba YIRA

(Co-Supervisor)

Date September 30 , 2019

Abstract

This study assesses the impact of future climate change on water related ecosystem services (WRES) including hydropower potential in the Dano catchment (Volta basin). The Catchment covers an area of 196 Km² and is located in the Southwest of Burkina Faso in West Africa.

Based on hydro-meteorological variables data collection such as discharge, precipitation, temperature etc. the conceptual rainfall-runoff model HBV light was successfully calibrated and validated for the catchment. The results indicate acceptable to very good model performances during the calibration (NSE = 0.945, R^2 = 0.945, and KGE= 0.948) and validation (NSE = 0.648, R^2 = 0.798, and KGE= 0.551) for discharge demonstrating a good agreement between observed and simulated variables

The projected climate change signal in the catchment was examined using the representative concentration pathways 4.5 (HadGEM2-ES, GFDL-ESM2M) of WASCAL high-resolution regional climate simulation between a refence period and two future periods (2020-2049 & 2070-2099). Compared to the reference period of 1985-2005, both climate models (data bias corrected) show an increased temperature of 1.9 to 2.8 °C by 2020-2049, and at the end of the century 3.2 to 5.4 °C. For precipitation the trend up will increasing to 10 to 30 % in the middle of the century and between 37 to 51.4% towards 2100. The potential evapotranspiration will increase by 2.3 % 5.3% by 2049 and of 4.1 to 8.8 % at the end of the century. The projected annual discharges change signals, show an increase of 25 % to 68 % by 2049 and at the end of the century this increase reaches 80.65 % to 109 %. The analysis shows that the precipitation, temperature and evapotranspiration change indicated that streamflow is more related to precipitation than to temperature.

The effect of climate change on water related ecosystem services was assessed using discharge discharges simulated from the application of the two climate datasets (GFDL-ESM2M and HadGEM2-ES) and the validated HBV model. The simulated hydrological changes were translated into changes in WRES provision (hydropower, domestic water consumption, crop water availability even the ecological flow). The projected discharge increase will translate in an increase of all explored WRES in the future except the satisfaction of additional domestic water use that will decrease because of population growth. Therefore, the projected increase in future discharge will not be sufficient to counter balance the dd additional water demand associated to population development. These results imply adopting efficient water use techniques and harnessing the highlighted WRES potential in the catchment.

Keywords: Climate change, hydrological modelling, Water related ecosystems services, HBV light, Burkina Faso

Résumé

Cette étude a été réalisée pour évaluer l'impact du changement climatique futur sur les services écosystémiques liés à l'eau (WRES), y compris le potentiel hydroélectrique dans le bassin de Dano (bassin de la Volta). Ce bassin versant couvre une superficie de 196 km² et est situé dans le sud-ouest du Burkina Faso en Afrique de l'Ouest.

Sur la base de la collecte de données de variables hydrométéorologiques telles que les débits, les précipitations, la température, etc. Le model HBV a été calé avec succès. Les performances du model pour la calibration NSE = 0,945, R^2 = 0,945, et KGE = 0,948) ainsi que la validation (NSE = 0,648, R^2 = 0,798, et KGE = 0,551) démontrent un bon accord entre les variables observées et simulées.

Le signal de changement climatique projeté dans le bassin versant a été examiné sous le scenario d'émission RCP4.5 des deux modèles climatiques (HadGEM2-ES, GFDL-ESM2M) de WASCAL comparant deux périodes futures (2020-2049 et 2070-2099) et une période de référence. Par rapport à la période de référence 1985-2005, l'ensemble des modèles climatiques (données corrigées) montre de manière concordante une augmentation de la température de 1,9 à 2,8 ° C pour le milieu du siècle, de 3,2 à 5,4 ° C à la fin du siècle. Pour les précipitations, une augmentation de 10 à 30% au milieu du siècle et de 37 à 51,4% d'ici 2100 est projetée. L'évapotranspiration potentiel augmentera jusqu'à 5,3% d'ici 2049 et 8,8% vers la fin du siècle. Les débits annuels projetés montrent une augmentation de 25% à 68% d'ici 2049 et, à la fin du siècle, cette augmentation atteint 80,65% à 109%. L'analyse montre que les changements dans les précipitations, la température et l'évapotranspiration indiquent que le débit du cours d'eau est davantage lié aux précipitations qu'à la température.

Les débits obtenus à partir de l'utilisation de deux jeux de données climatiques de simulation (GFDL-ESM2M et HadGEM2-ES) avec le modèle approuvé HBV ont été utilisés pour évaluer l'effet du changement climatique sur les services écosystémiques liés à l'eau. Les changements hydrologiques observés se sont traduits par des changements dans la fourniture de WRES (énergie hydroélectrique, consommation d'eau domestique, disponibilité en eau des cultures et débit écologique). L'augmentation des débits futurs se traduira par une augmentation de tous les WRES explorés, à l'exception de la satisfaction des besoins supplémentaire d'eau domestique qui diminuera en raison de l'augmentation de la population. L'augmentation du débit induite par les changements climatiques ne suffit pas à compenser l'augmentation de la demande en eau liée au développement de la population. L'ensemble de ces résultats implique une adoption des techniques économes d'eau ainsi que l'exploitation du fort potentiel en WRES mis en évidence dans le bassin.

Mots-clés : changement climatique, modélisation hydrologique, services écosystémiques liés à l'eau, HBV light, Burkina Faso

Dedication

This work is dedicated

To my father Djodji Xavier NGOM and my mother Agath Marie Tine, who have unconditionally supported me,

To my brothers, sisters, friend and entire family, who heartened me to work hard in order to accomplish the best.

Acknowledgements

This research has been a triumph on account of the aggregate efforts of numerous organizations and people. I would like to offer my profound thanks to:

The Pan African University of Water and Energy Sciences, including Climate Change, the director and his team;

African Union and its German Partner GIZ for the scholarship and the research grant;

I sincerely thank my supervisor Dr Yaovi Aymar BOSSA and co-supervisors Dr. Yacouba YIRA, Dr Jean Hounkpè, for their constant support, time spent, attentive advice, and for welcoming me to the WASCAL Competence Center for my internship I will never forget;

WASCAL Competence Center, CIREG Project and their staffs (especially Dr Sylla B., Dr Salack S. and Dr Saley I.) for their availability and precious help.

Last, but not least, I thank my family for their support and motivation.

To my friends and colleagues for their helpful comments.

Table of Contents

List of Tables

List of Figures

Abbreviations and Acronyms

AET	Actual evapotranspiration
CIREG	Climate Information for Integrated Renewable Electricity Generation
DGM	National Meteorological Service of Burkina Faso
DGRE	General Directorate of Water Resources
DEM	Digital Elevation Model
FAO	Food and Agriculture Organization of the United Nations
PET	Potential Evapotranspiration
R2	Coefficient of determination
NSE	Sutcliffe criterion calculated on streamflow values
GCM	general circulation model/ Global climate model
HBV	Hydrologiska Byrans Vattenbalansavdelnin
KGE	Kling and Gupta Efficiency
IPCC	Intergovernmental Panel on Climate Change
IWRM	Integrated water resources management
MEAHA	Ministry of water and sanitation of Burkina Faso
RGPH	General Census of Population and Housing
Reff	Model efficiency
RCM	Regional circulation/climate model
RCP	Representative concentration Pathway
SDI	Streamflow Drought Index
SPI	Standardiized Precipitation Index
RDI	Reconnaissance Drought Index
SMHI	Swedish Meteorological and Hydrological Institute
WRF	Weather, Research and Forecasting
WRES	Water related Ecosystem Services
WASCAL	West African Science Service Centre on Climate Change
WHO	World Health Organisation

Chapter 1: Introduction

1.1. Background

The world is facing severe impacts of climate change and climate variability. Climate change refers to significant changes in global temperature, wind patterns, precipitation, and other measures of climate that occur over several decades or longer(United et al. 2011). Among the factors influencing remarkably climate change, are greenhouse gas emissions. The Fifth Assessment Reports of the Intergovernmental Panel on Climate Change (AR5-IPCC) indicated that the global warming is due mainly to greenhouse gas emissions(Pachauri and Leo 2014), especially the CO_2 inducted by fossil fuels consumption(Almestad 2015).

Water resources are impacted by climate variability and change. Water related ecosystem services (crop water supply, household water supply and hydropower), tributary to water resources, are therefore potentially subject the impacts of climate change. Indeed, WRES are projected to change in coming decades because of changes in the water cycle, as a consequence of changes in the spatial and temporal distribution of precipitation and the form of precipitation on the earth (Fig1.1**,** Chang and Bonnette 2016). While the development of countries and their need for WRES are increasing, the provision of water related ecosystem services is threatened by climate change. These effects of climate change on WRES are expected to be felt strongly in Africa, because the continent as a whole is one of the most vulnerable due to its high exposure and low adaptive capacity (IPCC 2013),

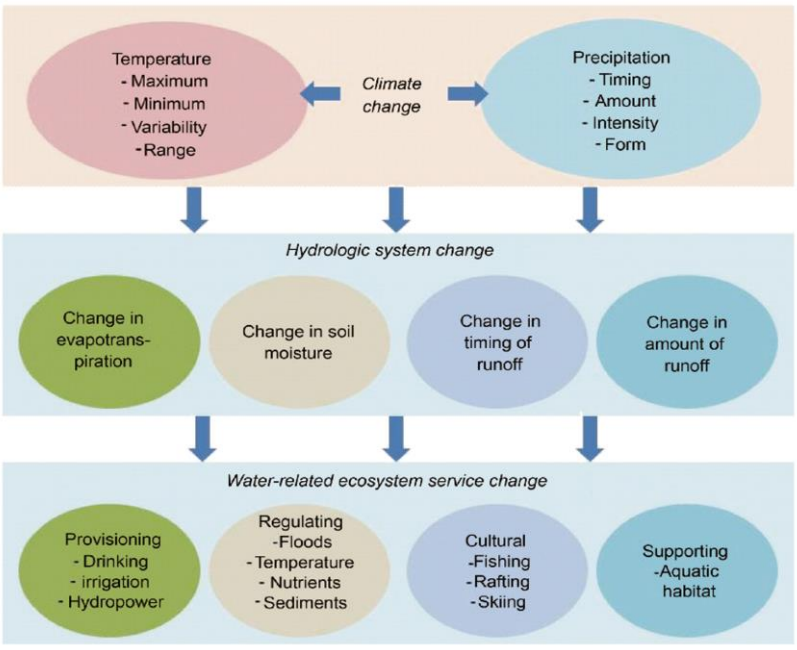

Fig1.1: Cascading effects of climate change on water related ecosystem services (Source: Chang and Bonnette, 2016)

1.2. Relevance of study /Problem statement/Justification of the study

The Volta, Mono and Niger basins are the focus area of the CIREG (Climate Information for integrated Renewable Electricity Generation, https://cireg.pik-potsdam.de/en/) project. The CIREG project intends to support by co-developing climate services and solutions to provide relevant Renewable Electricity information to stakeholders and decision-makers.

The United Nations Environment Programme (2014) reported that in the Niger and Volta basins there will be significant temperature increase, reduced rainfall (10-25% by 2025), possible increase in rainfall in sahel zone in June, July, August, increased evaporation, greater drought probabilities, more rainfall variability and unreliability, and reduced river flow. All these impacts will induce differences risks such as decrease crop productivity, induce rural communities' vulnerability, and reduced flow induce impact on hydropower generation (Fig2.2).

The impact of climate change on precipitation and water availability is therefore of major concern for policy makers in the Volta Basin of West Africa, whose economy mainly depends on rainfed agriculture and hydropower generation.(P. Taylor et al. 2010). The current study helps to resolve this concern through the assessment of climate change impact on water related ecosystem services (WRES) including hydropower potential using the medium scale catchment of Dano as case study.

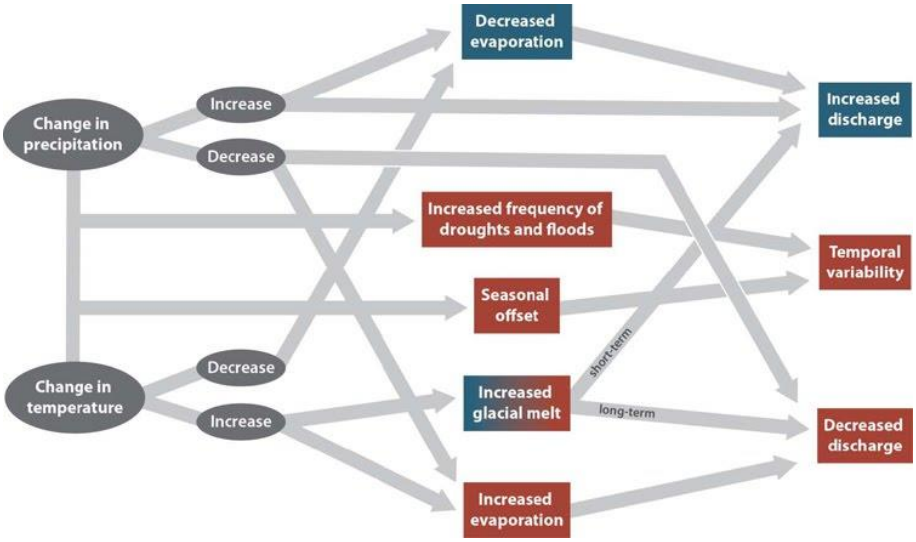

Fig1.2: Flow chart of climate change effects. Red indicates effects that are typically detrimental to hydroelectric production, and blue indicates effects that typically improve hydroelectric production potential (Ben et al. 2011)

1.3. Research questions

- How efficient is the HBV hydrological model in simulating the hydrology of the Dano catchment?
- What is projected climate change for the Dano catchment and how will it affect the catchment hydrology?
- What is the expected impact of climate change on WRES what are the future WRES demand and challenges?

1.4. Objectives of the study

From the background information and problem statement the following general and specific research objectives are formulated.

1.4.1. Main objective

The general objective of the study is to contribute the adaptation to climate change in the field of water resources management through the assessment of climate change impact on WRES in the Dano catchment.

1.4.2. Specific objectives

More specifically, the study aims to:

- To calibrate and validate the HBV hydrological model for the Dano catchment and evaluate its performances.
- Evaluate future climate trends in the study area using the WASCAL high-resolution regional climate simulation ensemble for West Africa (WASCAL-RCS) and assess their impact on the hydrology of the catchment
- To assess the impacts of climate change on specific water related ecosystem services.

1.5. Thesis organization

The thesis is organized in seven chapters including this general introduction. The remaining chapters include the Chapter 2. Study area, Chapter 3. Literature Review, Chapter 4. hydrological modelling, Chapter 5. Projected climate signal and its impact on streamflow, Chapter 6. Climate change impact on WRES And Chapter 7. General conclusion and recommendations.

Chapter 2. Study area

2.1. Geographical location of the study area

Dano is a commune located in south west of Burkina Faso in the province of Ioba. Dano includes 7 sectors and is located at a distance of 150 km from Bobo Dioulasso and 280 km from Ouagadougou. The area of the of catchment is around 196 Km² and it is between 11 ° and 12 ° north latitude and 3 ° and 4 ° west longitude.

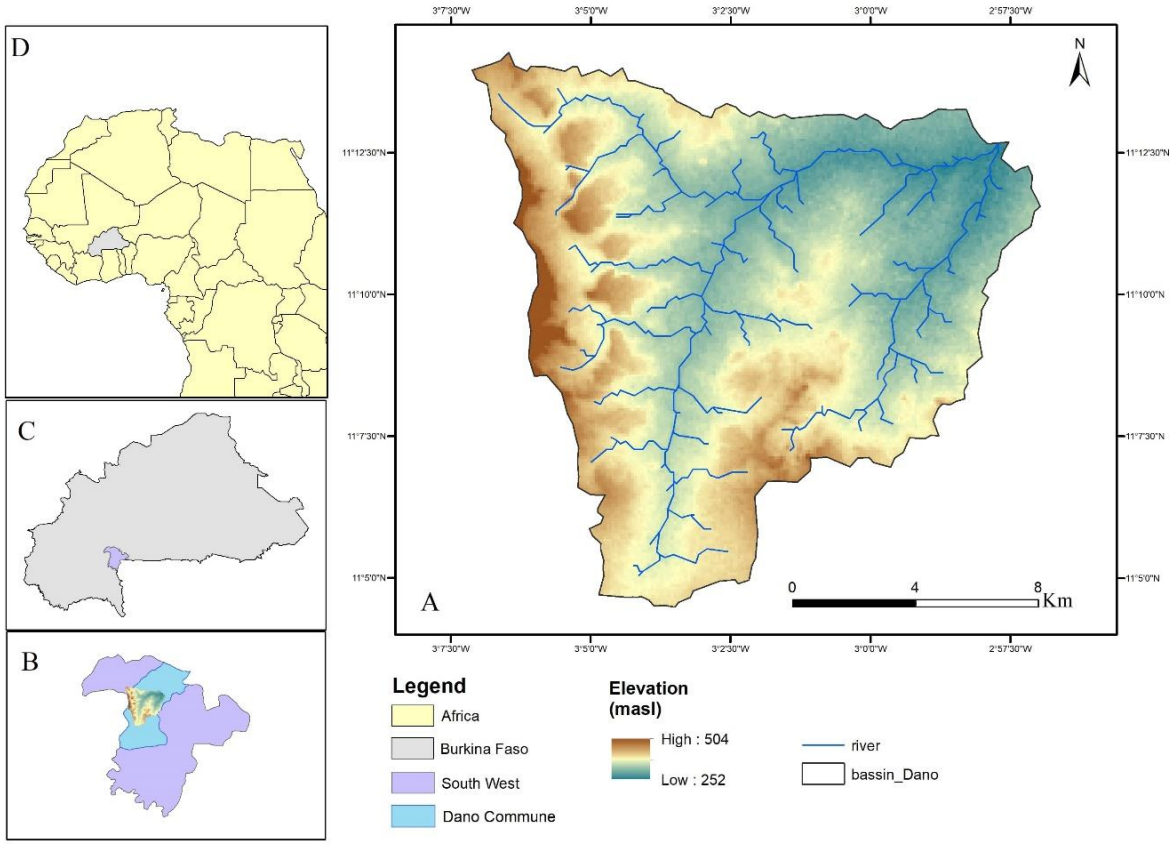

Fig 2.1: Location map. Part A shows the Dano catchment, part B indicates its position in the Dano commune and in south-west region, part C situates south-west in Burkina Faso and part D show position Burkina Faso in West Africa.

2.2. Climate

Dano is characterized by a South-Sudanian climate regime with two seasons: a dry season that lasts 7 months (from October to April) and a wet season of 5 months (from May to September). The average annual rainfall is of the order of 1000 mm.

Maximum temperatures are around 21 ° C in December and 38 ° C in March-April and daytime temperatures vary between 24.9 ° C and 30.2 ° C (P.N.G.T., 2000). Fig2.2 shows the monthly variation on temperature during one year.

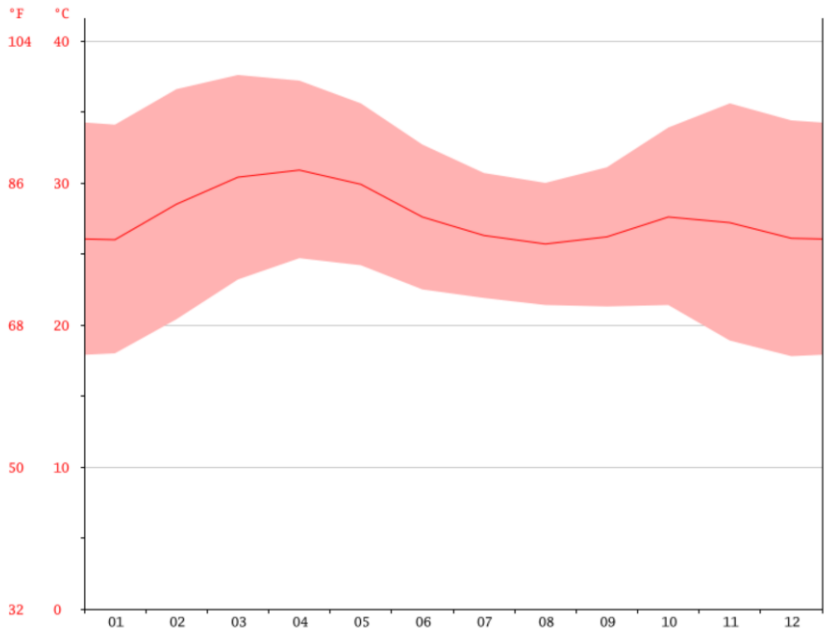

Fig2.2: Dano temperature curve (http://climate-data.org/)

Table 2.1: Dano climatic table (http://climate-data.org/)

	January	February	March	April	May	June	July	August	September	October	November	Décember
Mean temperature (°C)	26	28.5	30.4	30.9	29.9	27.6	26.3	25.7	26.2	27.6	27.2	26.1
Average minimum temperature (°C)	18	20.4	23.2	24.7	24.2	22.5	21.9	21.4	21.3	21.4	18.9	17.8
Average maximum temperature (°C)	34.1	36.6	37.6	37.2	35.6	32.7	30.7	30	31.1	33.9	35.6	34.4
Precipitation (mm)	2	3	17	42	93	128	181	255	179	48	7	3

2.3. Vegetation

The vegetation of Dano is dominated by species like *Gardenia sp, Combretum micranthum* (kinkeliba), *Parkia biglobosa* (néré), *Butyrospermum parkii* (shea) *and Bombax costatum* (kapokier). In grasses, the dominant species are *Loudetia togoensis*, *Pennicetum sp* and Andropogon sp. The vegetation cover is more or less degraded depending on the terroirs and villages.

There are four vegetation types (Monograph of the municipality of Dano, 2006).:

- woody savannah, dominated by species such as shea or “néré”;

- a savannah planted in recent;

- gallery forest along the rivers, including species such as Mitragyna inermis, Anogeissus leiocarpus (African birch), Diospynos mespiliformis (the false ebony tree), Terminalia spp, Khaya senegalensis (the caïcédrat), etc;

- a mosaic of shrubs on hillocks and hills in which Combretum spp is well represented

In addition to this natural vegetation, anthropogenic formations such as those of *Mangifera indica* (mango), *Eucalyptus camandulensis*, etc. occur in many places (Communal Development Plan, 2007).

A particular feature of Dano (and the south-western part of the country) is the intensive use of firewood to produce the local beer "dolo". About 6 442 tons of wood are used annually for the production of dolo (Blin & Sidibe, 2012). This constitutes an additional driver to the degradation of the natural vegetation

2.4. Soil Type

In Dano, there are mainly gravelly and brown soils consisting largely of leached or impregnated ferruginous soils associations with patches of lithosolic soils on ferruginous cuirass.

The main encountered types are as follows:

- soils of gravels in a state of continuous degradation; this type of soil, sandy on the surface, deep sandy-clay, occupies nearly a quarter of the communal territory and receives millet and bean crops;

- sandy-loam soils at the surface and clayey at depth are distributed over half of the municipal territory; these soils rich in organic matter are of satisfactory fertility, and suitable for the production of millet, maize, beans, peanuts, cotton;

- ferruginous soils leached sandy on the surface and clayey in depth, permeability and porosity mediocre. They occupy nearly a quarter of the territory, are sensitive to water and wind erosion, and have a low organic matter content.

The different types of soils encountered in the municipal area are located respectively in the shallows, on the old ergs and at the level of glacis.

They are weakened by wind and water erosion and are deteriorating from year to year, causing a drop in agricultural production (Monograph of the municipality of Dano, April 2006).

2.5. Hydrography

The town of Dano is crossed by the "Gbataziè", which drains the rainwater in the South-North direction. The other rivers that cross the town are Mouhoun and Po, a tributary of Bougouriba. In addition, there is a dam at Moutori and a water reservoir at Pontiéba which are exploited for agricultural purposes (Monograph of the municipality of Dano, 2006; KI 2009).

2.6. Population Dynamic

According to the General Census of Population and Housing (RGPH) in 2006, the population of the municipality of Dano is 43583 inhabitants of which 22464 women corresponding to 51.54%, and 21,119 men representing 48,46 % [Communal Development Plan, 2007].

Dano, compared to other municipalities in the region has a large population with a very high birth rate which was 52.61 $^{0}/_{00}$ in 2005 (Monograph of the municipality of Dano, 2006). Population density consequently increased from 24.9 persons per Km^2 in 1985 to 51.8 persons per Km^2 in 2006.

2.7. Economic activities

Like the country's economy, Dano is essentially agricultural. The sector employs about 86% of the population. Agriculture is mostly rainfed with poor technology and investments (Callo-concha, Gaiser, and Ewert 2012). Besides agricultural activities, women are especially active in fruit and firewood gathering, petty trade, artisanship and foodstuff trading (Callo-Concha et al., 2012). The rate of access to safe drinking water in the rural areas is about 63% (MEAHA, 2013). Therefore, a very large part of the population relies on surface water as source of supply.

Chapter 3. Literature Review

3.1. The climate variability and change

Climate change refers to a change in the state of the climate that can be identified (e.g., by using statistical tests) by changes in the mean and/or the variability of its properties and that persists for an extended period, typically decades or longer(IPCC 2018). The reasons of the global climate changes originate from both the outside components, for example, sun powered radiation and expanding ozone depleting substances, and the interior changeability of the sea environment framework. (Qian, Lu, and Zhu 2010)

Climate variability refers to variations in the mean state and other statistics (such as standard deviations, the occurrence of extremes, etc.) of the climate on all spatial and temporal scales beyond that of individual weather events(IPCC 2018). Fluctuation might be because of regular inward procedures inside the atmosphere framework (inner inconstancy), or to variations in natural or anthropogenic external forcing (external variability).(Pachauri and Leo 2014)

Description of Climate Change Scenarios, RCPs (Representative Concentration Pathway)

Anticipating the effect of environmental change on water resources, agribusiness, and different other sectors is troublesome and needs the utilization of conceivable situation changes characterized by the Intergovernmental Panel on Climate Change (IPCC) (Bodian et al. 2018)

The RCPs (Representative Concentration Pathways) describe different 21st century pathways of greenhouse gas emissions and atmospheric concentrations, land use and air pollutant emissions. The IPCC have developed four RCPs developed (RCP2.6, RCP4.5, RCP6, and RCP8.5).

Under the RCP2.6 scenario, the radiation forcing is approximately 2.6 W/m2 in 2100 (Su et al. 2015). The RCP4.5 scenario predicts the forcing to be approximately 4.5 W/m2 in 2100. (Su et al. 2015). Under the RCP8.5, the highest greenhouse gas emission scenario, the radiation forcing is approximately 8.5 W/m2 in 2100 (van Vuuren et al. 2011).

RCP2.6 is a stringent mitigation scenario, RCP4.5 is an intermediate scenario, and RCP8.5 is a scenario with very high greenhouse gas emissions.(K. E. Taylor, Stouffer, and Meehl 2012)

Table 3.1 A summary of the assessment of the four key factors used in the risk assessment United Nations Environment Programme (region: The Niger, Volta, and adjacent smaller basins)

region	Water resources status	Socio-economic status	Institutional capacity	Climate change impacts	Risk widespread
The Niger, Volta, and adjacent smaller basins	Sub-humid towards south; serious scarcity in Sahelian zone; floods in coastal belt; unpredictable rainfall with high variability; increasing water stress; water quality problems	High degree of poverty, high population growth. Political instability in many countries. High dependence on rain- fed agriculture; high gender imbalance in income;	Poor institutional capacity largely due to long period of political instability; transboundary institutions and agreements in place in key river basins; lack of human resource capacity Political	Significant temperature increase; reduced rainfall (10 – 25% by 2025); possible increase in rainfall in Sahel zone in June, July, August; increased evaporation; greater drought probabilities; more rainfall variability and unreliability; reduced groundwater recharge and river flow	Rural communities vulnerable to decreased crop productivity; reduction in key wetland areas; reduced flow will impact on hydropower generation; resurgence of malaria in Togo and Niger; upsurge of measles and meningitis expected;

(United Nations Environment Programme 2014)

Critical/very poor status/severe impacts/high risk
Poor status/moderate impacts/moderate risk

3.2. Water related ecosystem services (WRES)

Crop water supply

Water abstraction for irrigation is increasing with the population growth. Most dam are built for irrigation and an estimation of 30 to 40% of the total land are irrigated through the world (Tazen 2015). Crop water supply is in fact the most consumer of water, as it refers to water used for agricultural production (FAO-AQUASTAT, 2013;Mdemu et al. 2009). In rainfed agricultural systems, crop water stress is a major limitation to crop production (IWMI 2007).

Household water supply

This is the amount of water distributed to household consumption (drinking and non-drinking purposes) after extraction in surface water or groundwater and before treatment. (European Commission 2013).

Hydropower

It is a systems using the energy released when water falls due to gravity, this energy is converted into electricity (Fallis 2013). It is among the non-polluting and economically attractive renewable energy (Mul et al. 2015). The potential of hydropower can be estimated depending on the flow rate and shape of the area. (European Small Hydropower Association 2004).

3.3. Hydrological modelling

A model is a simplified representation of the real-world system according to (Sorooshian et al. (2008), Hydrological model are a tool that can help to understand the functionate of our environment and the water resource management (Devia, Ganasri, and Dwarakish 2015). There are Metric models, Conceptual models (HBV model, TOPMODEL) and Physics-based models (SHE or MIKESHE model, SWAT) (Sorooshian et al. 2008)). However, there are always trade-offs among the models, and selection of the most appropriate one depends upon the objectives and data availability. The current work applies the HBV model.

- **Description of the HBV model**

The Swedish HBV model (Hydrologiska Byrans Vatten balansavdelning), (Achleitner, Rinderer, and Kirnbauer 2009) developed by SMHI (Swedish Meteorological and Hydrological Institute) has become a widely used tool in the world for flow prediction for ungauged watersheds. This model is an example of semi distributed conceptual model (Sten 1976). The entire catchment is divided into sub catchments, which are further divided into different elevation and vegetation zones (Seibert and Vis 2012). It runs on daily and monthly rainfall data, air temperature and evaporation (Devia, Ganasri, and Dwarakish 2015).

This model is known for its robustness, despite its relative simplicity. To further simplify the model, some components may be rendered inactive. This model simulates daily flow using as inputs daily temperatures, precipitation, and flows, as well as monthly estimates of potential evapotranspiration. It takes into account the topographic characteristics such as area and altitude for the spatial discretization of the study area in homogeneous zones for the semi-distributed version (OUICI 2018)

The general water balance equation used is:

$$P - E - Q = \frac{d}{dt}(SP + SM + UZ + LZ + lakes)$$

Where P is precipitation (mm), E is evaporation, Q is runoff, SP is the snow pack, SM is the soil moisture, UZ and LZ are the upper and lower ground water zone and lakes represent the volume of lake.

3.4. Climate impact on WRES assessment

The climate impact assessment can be investigated through the application of climate simulation products to a hydrological simulation model over different time periods (fig3.1)

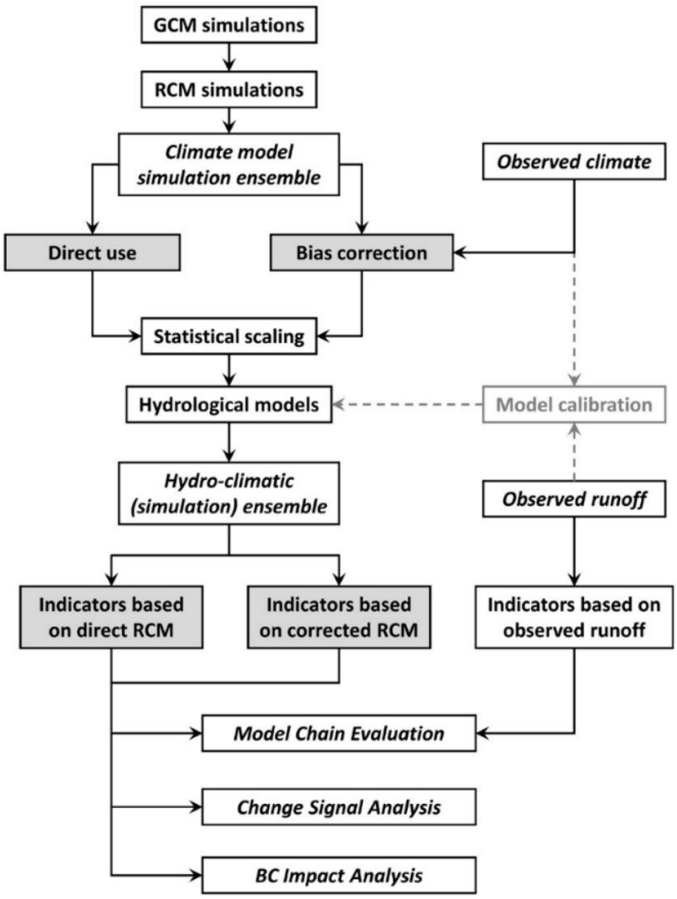

Fig3.1: Workflow Climate change hydrological impact assessment

- WASCAL high-resolution regional climate simulation**.**

WASCAL aims to enhance the resilience of human and environmental systems to climate change and increased variability in the region of west Africa. The institution made available a high-resolution regional climate simulation ensemble for West Africa. Three regional climate models (WFR V 3.5.1, COSMO-CLM 4.18, REGCM4) and three earth system models (MPI-ESM, GFDL-ESM2M and HadGEM2-ES) from the CMIP5 project are downscaled by each of the regional models, over the period of 1980 - 2010. The Representative Concentration Pathways considered in the simulation is the RCP4.5 scenario from 2020 to 2050 and from 2070 to 2100 (Heinzeller et al. 2018). The simulation outputs are provided at the resolution of 12km and 60km. It is covering all west Africa region from 25W to 25E and 5S to 25N (Heinzeller et al. 2018).

- Climate data bias correction

A bias is defined as long term average difference between model and observation (Wilcke, Mendlik, and Gobiet 2013). Bias correction uses mathematical/statistical methods (Hagemann, Haerter, and Piani 2010). The output of GCM and RCM can't be directly used in hydrology because there are systemics errors (biases) causes by the climate models (biases like: limited spatial resolution,

numerical schemes, simplified physics and thermodynamic processes, or incomplete knowledge of climate system processes). Errors in GCM simulations, relatively to historical observations are large (Ramirez-Villegas et al. 2013).

Bias correction applied on GCM simulations enhance the skills of the GCM projections (Amengual et al. 2012). However, bias correction is not a purely statistical problem and cannot overcome fundamental deficiencies in climate models (Maraun et al. 2017). There are several bias correction method like the delta approach, the Linear Scaling method and the quantile approaches (N'Tcha M'Po 2016).Table 3.1, shows different application of these methods to correct RCM simulated data.

Table 3.1: Overview of methods used to correct RCM-simulated precipitation and/or temperature data, for more information on the methods see Teutschbein and Seibert (2012) and the specified references (Teutschbein and Seibert 2013)

Method	**Variable**	**Short description**	**Advantages (+) and Disadvantages (-)**	**references**
Raw RCM Output Data	Precipitation Temperature	RCM-simulated time series are used directly without any bias correction	+ simplest way to use RCM data – systematic model errors are ignored – can cause substantial errors in impact studies	
Precipitation Threshold	Precipitation	-an RCM-specific threshold is calibrated such that the number of RCM-simulated days exceeding this threshold matches the number of observed days with precipitation • rarely used as a "stand-alone" method but often combined with other correction proce- dures	+ wet-day frequencies are corrected – mean, standard deviation (variance) and wet-day intensities are not adjusted	Schmidli et al. (2006)
Delta-Change Correction	Precipitation Temperature	• RCM-simulated future change signals (anomalies) are superimposed upon observational time series • usually done with a multiplicative correction for precipitation and an additive correction for temperature	+ observations are used as a basis, which makes it a robust method + corrects the mean – standard deviation (variance), wet-day frequencies and intensity ies are not corrected – potential future changes in climate dynamics and variability are not accounted for – all events change by the same amount	Gellens and Roulin (1998) Graham et al. (2007a, b) Johnson and Sharma (2011) Lettenmaier et al. (1999) Mpelasoka and Chiew (2009) Middelkoop et al. (2001) Moore et al. (2008) Rasmussen et al. (2012) Shabalova et al. (2003)
Linear Transformation	Precipitation Temperature	• adjusts RCM time series with correction val- ues based on the relationship between long- term monthly mean observed and RCM control run values	+ corrects the mean + variability ofcorrected data is more consistent with original RCM data – standard deviation (variance), wet-day frequencies and intensities are not corrected	Lenderink et al. (2007)

		• precipitation is typically corrected with a factor and temperature with an additive term	– all events are adjusted with the same correction factor	
Local Intensity Scaling (LOCI)	Precipitation	combines a precipitation threshold with linear scaling (both described above)	+ corrects mean, wet-day frequencies and intensities + variability ofcorrected data is more consistent with original RCM data – standard deviation (variance) is not corrected – all events are adjusted with the same correction factor	Schmidli et al. (2006) +
Power Transformation	Precipitation	• a precipitation threshold can be introduced a priori to avoid too many drizzle days (i.e., very low but non-zero precipitation) • is a non-linear correction in an exponential form (a×Pb) that combines the correction of the coefficient of variation (CV) with a linear scaling	+ corrects mean and standard deviation (variance) + events are adjusted non-linearly + variability ofcorrected data is more consistent with original RCM data ± adjusts wet-day frequencies and intensities only to some extend	Leander and Buishand (2007) Leander et al. (2008)
Variance Scaling	Temperature	combines standard linear scaling with a scaling based on standard deviations	+ corrects mean and standard deviation (variance) + variability ofcorrected data is more consistent with original RCM data – all events are adjusted with the same addends and correction factor	Chen et al. (2011)
Distribution Mapping/ Quantile mapping	Precipitation Temperature	matches the distribution functions of observations and RCM-simulated climate values • a precipitation threshold can be introduced to avoid substantial distortion of the distribution caused by too many drizzle days (i.e., very low but non-zero precipitation) • also known as “quantile-quantile mapping”, “probability mapping”, “statistical downscaling” or “histogram equalization”	+corrects mean, standard deviation (variance), wet-day frequencies and intensities + events are adjusted non-linearly + variability ofcorrected data is more consistent with original RCM data	Block et al. (2009) Boe et al. (2007) Déqué et al. (2007) Ines and Hansen (2006) Johnson and Sharma (2011) Piani et al. (2010) Rojas et al. (2011) Sennikovs and Bethers (2009) Sun et al. (2011)

Chapter 4. Hydrological modelling

4.1. Introduction

Hydrological forecasts are essential, both for the prevention of floods and for water resources planning (Johansson, Andreasson, and Jansson 2003). As described by et al 2007) a model can help to represent the real world system, as for the process of runoff and nowadays it is considered that a model is an important and necessary tool for water and environment resource management and prediction. Their application are found in water resources management, hydrological risk analysis (Patil 2008) ; (Harlin and Lindström 1992), flood and low-water forecasting (Bruen, 1999, Randrianasolo et al. 2010), the reconstruction of hydrological series, the design of hydraulic structures (Bergström et al. 1992), the study of the impact of change in land use and vegetation cover on hydrological cycles (Hundecha, 2005),the assessing the impact of land use on hydrology (Viney et al. 2009), and the study of the impact of climate change on hydrological cycles (Gardelin et al., 2001, Bergström et al., 2001) Similar to the above mentioned studies, the following on climate impact assessment on WRES applies a hydrological model.

4.2. Methodology

4.2.1. Data source and processing

Temperature, precipitation, wind speed, relative humidity, solar radiation, discharges, DEM, are the different climatological et hydrological data used in this research. The climate data were retrieved from the Boromo and the Gaoua stations of the national meteorological service (DGM) of Burkina Faso. The dataset covers the period of 2002-2014. As for discharges is was measured between 2011 to 2014 and readily available at the WASCAL competence Center.

Wind speed, relative humidity, solar radiation, and temperature were used to calculate the potential evapotranspiration following the Penman–Monteith equation using the version 3.2 of the FAO ETO CALCULATOR.

Table 4.1: resumes of the data sources and characteristic

Type of data	Sources	UNIT	Type of data	Periode of data
Temperature	the national meteorological service (DGM) du Burkina Faso	°C	Mean daily	2002-2014
Precipitation		mm / h	Mean Daily	2002-2014
Wind speed		m/s	Daily	2002-2014
Relative humidity		1/1	Daily	2002-2014
Solar radiation		Wh/m²	Daily	2002-2014
discharges		m3/s	Daily	2011-2014
discharges	Direction Générale des ressources en eau (DGRE) du Burkina Faso	m3/s	Daily	2011-2014
DEM	http://srtm.csi.cgiar.org/		DEM - SRTM 90 West Africa	

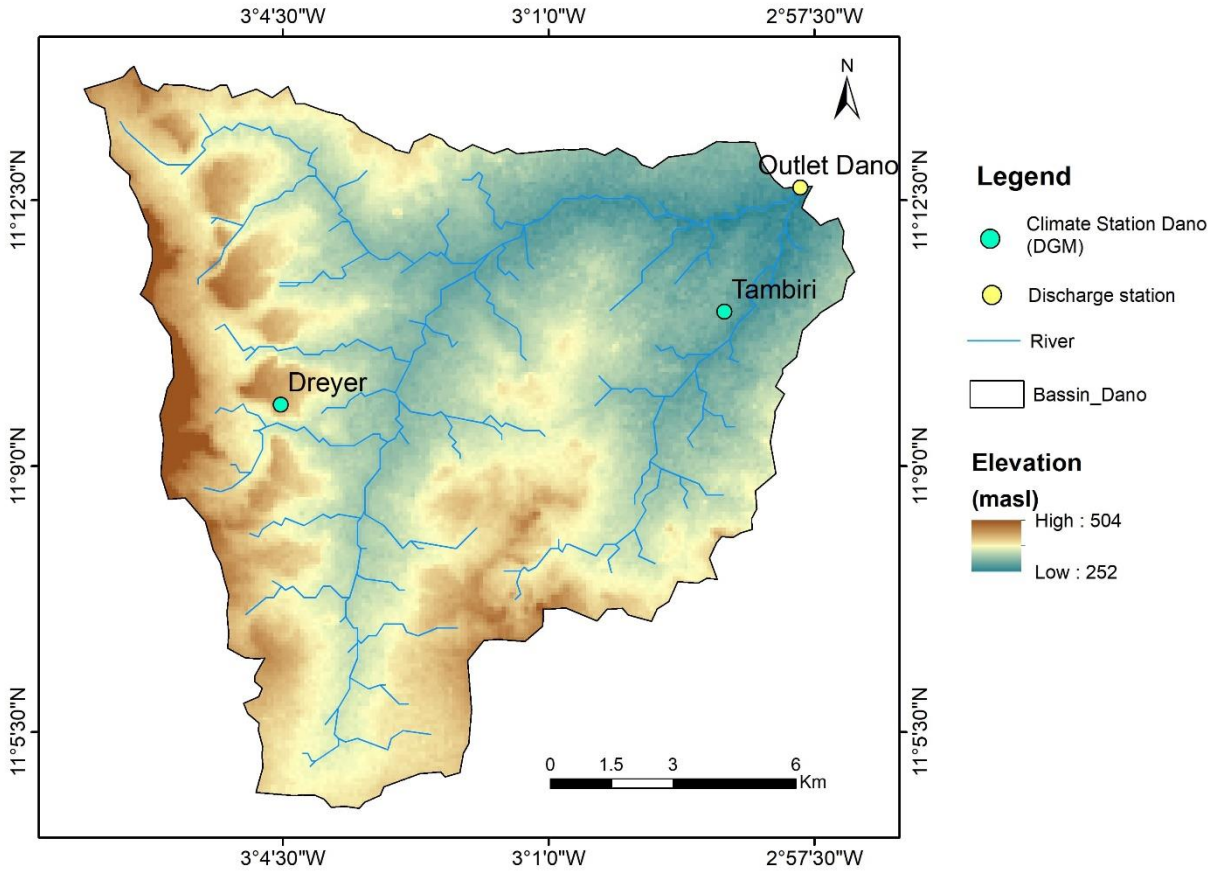

Fig4.1: representation of Dano catchment and climates stations

4.2.2. Hydrological model.

In this study the version 4.0.0.22 of the HBV light was applied to perform the hydrological modelling. This version of HBV can be used for free. The HBV model is a simple conceptual rainfall-runoff model, it can be classified as a semi-distributed rainfall-runoff model of catchment hydrology, it is suitable for different purposes, such as simulation of long streamflow records,

streamflow forecasting and hydrological process research (Driessen et al. 2010). It depends on the daily rainfall, air temperature, and long-term monthly mean potential evapotranspiration as input data to simulate the daily streamflow at a basin outlet (Bergstrom, 1995; SMHI, 2012). It has been applied in many different catchments, including the Rhine (Linde et al., 2008; Hundecha and Bardossy, 2004)(Driessen et al. 2010) and the Meuse (Akhtar, Ahmad, and Booij 2008). HBV-Light uses a warming-up period to set variable values according to the preceding meteorological conditions (Bhattarai et al. 2018) There are two differences between this HBV Light and the other versions: the model initialization should be done using a warming-up period in HBV Light, and a routing parameter that can take all real values instead of just integer values (Seibert, 2005(Driessen et al. 2010).

HBV can be used as a fully global or semi-distributed model by dividing the catchment into sub-basins. In a global model, it is assumed that the study area (watershed) is one unit (zone) and the parameters do not change in the catchment area(OUICI 2018). For the currentor study HBV light at the global scale for the Dano watershed.

The model has 15 parameters that need to be parameterized for calibration. The model is subdivided into three routines; snow and glacier routine, soil moisture routine and runoff generation routine (Bhattarai et al. 2018).

4.2.3. Model structure

Input data are observations of precipitation, temperature, discharge and estimates of potential evapotranspiration. The time step is usually one day, but it is possible to use shorter time steps. The evaporation values used are normally monthly averages although it is possible to use daily values. A daily time step was used in this study. The fig 4.2, 4.3 & 4.4 gives an overview of the structure of the different routines within the model

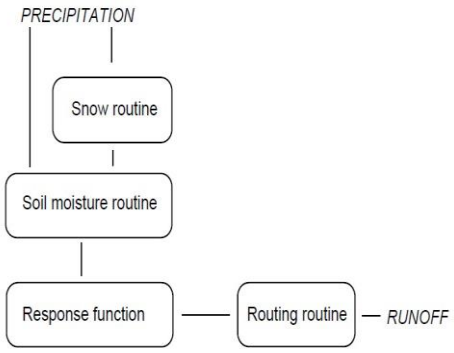

Fig 4.2: overview of the structure of the different routines within the model

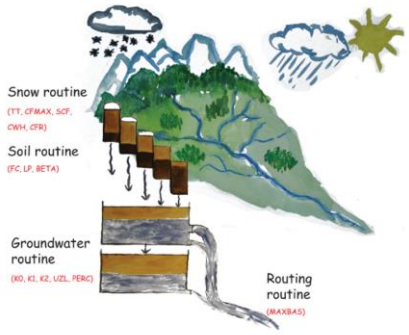

Fig 4.3: Schematic structure of the HBV model (Seibert and Vis 2012a)

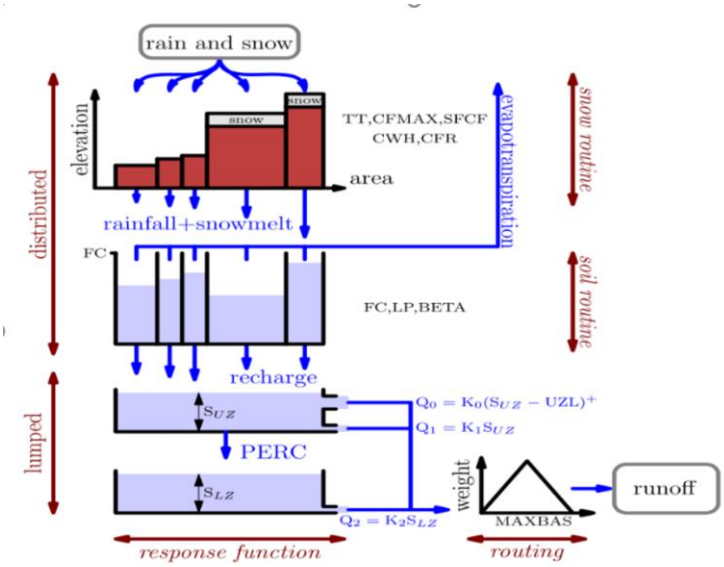

Fig 4.4 detailed structure of the HBV model (Driessen et al. 2010)

Input Data files ()

The folder structure for a catchment is as follows:

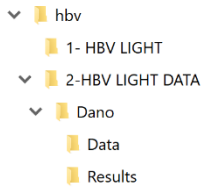

The name of the parent folder, in this case DANO, is used by HBV-light as the name of the catchment. This folder should at least contain a subfolder 'Data'. The subfolder 'Results' will be created automatically during the simulations if it does not exist. The 'Data' folder should contain the following files in order to be able to open the catchment in HBV-light: - PTQ file - Evaporation file

The PTQ-file (ptq.dat) contains time series of daily precipitation [mm/day], temperature [ºC] and discharge [mm/day]. The name of the input file is ptq.txt and the format is as follows:

a) a header of two lines, the first one contains a name for the catchment (no comma allowed in this line), the second line is not used by the program. b) Date (YYMMDD or YYYYMMDD), precipitation, temperature, discharge in one row per day (separated by commas) c) Precipitation and temperature series need to be complete, i.e. no missing values are allowed. In case of missing discharge data, any negative number (e.g. -9999) can be used as no data value.

Evaporation file

The evaporation-file contains values for the potential evaporation [mm/Δt]. The evaporation file may contain a) 365 values, i.e., long-term daily mean values b) As many values as time steps in the PTQ-file, i.e., one value for each time step The file has the following format: one line (header) followed by the values (one value per row)

Output data files

-Result files

The results file stores the model state for all the days within the simulation period. The following variables are included in the file:

• **Date**	-	
• **Qsim**	mm Δt^{-1}	simulated runoff
• **Qobs**	mm Δt^{-1}	observed runoff (read from the PTQ file)
• **Precipitation**	mm Δt^{-1}	
• **Temperature**	ºC	
• **AET**	mm Δt^{-1}	
• **PET**	mm Δt^{-1}	
• **Snow**	mm	water equivalent of the snow pack
• **Snowcover**	-	fraction of (sub)catchment covered with snow
• **SM**	mm	water content of the soil box
• **Recharge**	mm Δt^{-1}	
• **Glacier** (*)	mm	change in glacier water content
• **S*XZ*** (**)	mm	storage in the specific zone
• **Q*N*** (***)	mm Δt^{-1}	runoff generated by the specific outflow component
• **Qsim_rain**	mm	contribution of rain to the simulated runoff
• **Qsim_snow**	mm	contribution of snow to the simulated runoff
• **Qsim_glacier** (*)	mm	contribution of glacier to the simulated runoff

Summary file

The Summary file contains summary statistics of the catchment. These are divided in two categories, 'Water Balance' statistics and 'Goodness of Simulation' statistics**.**

Water Balance includes the following variables:

• **Sum Qsim**	**mm Δt^{-1}**	**summation of simulated runoff**
• **Sum Qobs**	mm Δt^{-1}	summation of observed runoff
• **Sum Precipitation**	mm Δt^{-1}	summation of precipitation
• **Sum AET**	mm Δt^{-1}	summation of AET
• **Sum PET**	mm Δt^{-1}	summation of PET
• **Contribution of Q*N***	-	portion of runoff generated by the corresponding outflow component, with *N* either 0, 1 or 2

Goodness of fit includes the following variables:

• **Coefficient of determination**	-	
• **Model efficiency**	-	
• **Efficiency for log(Q)**	-	
• **Mean difference**	mm $year^{-1}$	
• **Efficiency based on intervals of *n* days**	-	where *n* is the time step of the interval. Presence of this variable depends on the Efficiency based on intervals of n days settings on the Model Settings form.
• **Efficiency for specified season**	-	Presence of this variable depends on the Efficiency for specified season settings on the Model Settings form.
• **Efficiency based on weighted Q**	-	Presence of this variable depends on the Efficiency based on weighted Q settings on the Model Settings form.
• **Efficiency for peak flows**	-	Presence of this variable depends on the Efficiency for peak flows settings on the Model Settings form.

- Eto-calculator

- Calculation of the Standard precipitation Index (SPI)

The Standardised Precipitation Index (SPI) was used to assess whether the calibration and validation period of the study are normal or not. SPI was developed by McKee et al. (1993) to serve as a “versatile tool in drought monitoring and analysis”. The SPI calculation for any location is based on the long-term precipitation record for a desired period. This long-term record is fitted to a probability distribution, which is then transformed into a normal distribution so that the mean SPI for the location and desired period is zero (Edwards and McKee, 1997). Positive SPI values indicate greater than median precipitation, and negative values indicate less than median precipitation. Since SPI is normalized, wetter and drier climates can be represented in the same way. Although SPI can

monitor wet periods, it is typically used to assess the length and magnitude of drought events.(D Tigkas, Vangelis, and Tsakiris 2013).

Table 4.2: Classification of drought conditions according to the SPI (D Tigkas, Vangelis, and Tsakiris 2013)

SPI values	Classification
2.0+	Extremely Wet
1.5 to 1.99	Very Wet
1.0 to 1.49	Moderately Wet
-.99 to .99	Near Normal
-1.0 to -1.49	Moderately Dry
-1.5 to -1.99	Severely Dry
-2 and less	Extremely Dry

The DrinC (Drought Indices Calculator) software was used for that purpose. The software aims at providing a user-friendly tool for the calculation of several drought indices, with emphasis on two recently developed ones: the Reconnaissance Drought Index (RDI) and the Streamflow Drought Index (SDI). Also, the widely used Standardised Precipitation Index (SPI) and the Rainfall Deciles can be calculated. The common characteristic of the selected indices is that they require relatively small number of data for their calculation and the results can be easily interpreted and used in strategic planning and operational applications. DrinC has full graphical user interface functionality (GUI) and runs on MS Windows operating systems (Dimitris Tigkas 2013). The version 1.5.73 (2014) of the software was applied.

4.2.4. Calibration and validation

The calibration procedure for rainfall-runoff models essentially involves (Patil 2008):

1. Modelling of discharge time series using the model under consideration, hydrological inputs and initial values model parameters.

2. Estimation of objective function (OF) which is a statistical measure (e.g. root mean squared error, correlation etc.) of goodness fit between observed dis- charge time series (Qob) and the modelled discharge time series (Qca).

3. Searching for the best model parameters by optimizing the objective function in a systematic way.

4. Validation, where the performance of the calibrated model parameters is cross- checked for the part of the data which is not used for the calibration

The current study followed a similar process. The discharge data was available form 01/01/2011 to 31/12/2014. The data was split into two sets for calibration and validation Daily records of mean

daily flow, temperature, precipitation and potential evapotranspiration from 31/10/2012 to 31/10/2013 were used as input for model calibration and records from 31/10/2013 to 31/12/2014 have been used for model validation. Warming-up period from 01/01/2011 to 31/10/2012 has been used to allow for adjustments to the initial and boundary conditions and it was needed to get appropriate initial values of the different state variables for the start of the simulation period, the simulations during the 'warming-up'- period are neither stored nor used for any further analysis (Seibert 1998). Calibration has been done to obtain the best process parameters for the basin.

Different model parameters are included and used in the calibration processes, see Seibert (2000) for details and parameter ranges. The calibration is carried out using the inbuilt GAP optimization tool (Genetic Algorithm and Powell), that refers to a genetic algorithm to approximate the solution of the optimization problem (Seibert, 2000) and to a routine using Powell's quadratically convergent method for local optimization of the problem (Press et al., 1992). The genetic algorithm starts with one or more populations of 50 randomly generated parameter sets that are located within the given ranges.(Driessen et al. 2010).

Table 4.3 shows the simulations parameters used for the Dano catchment. It also shows the default, and of parameter used during the calibration phase.

Table 4.3: simulation parameters

Name	Unit	Valid range	Default value	Description
PERC	mm/Δt	[0, inf)	1	treshold parameter
UZL	mm	[0, inf)	20	treshold parameter
K0	1/Δt	[0,1)	0.2	storage (or recession) coefficient 0
K1	1/Δt	[0,1)	0.1	storage (or recession) coefficient 1
K2	1/Δt	[0,1)	0.05	storage (or recession) coefficient 2
MAXBAS	Δt	[1,100]	1	length of triangular weighting function
PCALT	%/100m	(-inf,inf)	10	change of precipitation with elevation
TCALT	°C/100m	(-inf,inf)	0.6	change of temperature with elevation
TT	°C	(-inf,inf)	0	threshold temperature
CFMAX	mm/Δt °C	[0,inf)	3	degree-Δt factor
SP	-	[0,1]	1	seasonal variability in degree-Δt factor
SFCF	-	[0, inf)	1	snowfall correction factor
CFR	-	[0, inf)	0.05	refreezing coefficient
CWH	-	[0, inf)	0.1	water holding capacity
FC	mm	(0, inf)	200	maximum soil moisture storage
LP	-	[0,1]	1	soil moisture value above which AET reaches PET
BETA	-	(0, inf)	1	parameter that determines the relative contribution to runoff from rain or snowmelt

Model performance criteria

It is highly important to have a good method to evaluate the results of the calibration process (SMHI, 2012. User manual). To assess the performance of the model, different coefficients were used: Coefficient of determination (R^2), Model efficiency (R_{eff}), Kling-Gupta efficiency (KGE)

-Model efficiency (Reff or NSE)

The coefficient of efficiency, Reff, was used for assessment of simulations by the HBV model.

$$R_{eff} = 1 - \frac{\sum (Q_{Sim}(t) - Q_{Obs}(t))^2}{\sum (Q_{Obs}(t) - \overline{Q}_{Obs})^2}$$

R_{eff} compares the prediction by the model with the simplest possible prediction, a constant value of the observed mean value over the entire period.

R_{eff} = 1	**Perfect fit, QSim(t)= QObs(t)**
R_{eff} = 0	Simulation as good (or poor) as the constant-value prediction
R_{eff} < 0	Very poor fit

-Coefficient of determination (R^2)

$$R^2 = \frac{\sum_{i=1}^{n} (Q_{i,calc} - \overline{Q}_{obs})^2}{\sum_{1=1}^{n} (Q_{i,obs} - \overline{Q}_{obs})^2}$$

The value of R2 describes the proportion of the variance of the observed flow rates compared to the simulated flow rates. Authors such as Moriasi D. N et al. 2007 suggest that any R2 value greater than 0.5 for daily flow comparisons is an acceptable threshold for hydrological simulation.

- Kling-Gupta efficiency (KGE)

Kling-Gupta efficiency between sim and obs, with treatment of missing values. This goodness-of-fit measure was developed by Gupta et al. (2009) to provide a diagnostically interesting decomposition of the Nash-Sutcliffe efficiency (and hence MSE), which facilitates the analysis of the relative importance of its different components (correlation, bias and variability) in the context of hydrological modelling(https://www.rforge.net/doc/packages/hydroGOF/KGE.html)

$$KGE = 1 - \sqrt{\left(CC - 1\right)^2 + \left(\frac{cd}{rd} - 1\right)^2 + \left(\frac{cm}{rm} - 1\right)^2}$$

CC is the Pearson coefficient value and

cm is the average of observed values and

rm is average of forecast values and

cd is standard deviation of observation values

rd is standard deviation of forecast values

4.3. Result and discussion

4.3.1. Calibration results

The parameters that were optimized during the calibration are presented in table 4.4. Table 4.4 also presents the optimum value of each parameter using the the Model Efficiency as objective function. The achieved NSE equals 0.94. The corresponding water balance and other statistical quality measures are shown in table 4.5.

Table 4.4: Calibrated parameter range and optimum value

Parameters	Lower limit	Upper limit	Optimum value
TT	-2	0.5	-0.2
CFMAX	0.5	4	2.2
SP	1	1	1
SFCF	0	5	3.205
CFR	0	5	4.486
CWH	0	5	2.718
FC	1	5000	333.204
LP	0**.3**	1	0**0.995**
BETA	1	1**00**	13.308
PERC	0	250	18.605
UZL	0	250	180.041
K0	0	0.99999	0.043
K1	0	0.99999	0.304
K2	5 E-05	0.99999	0.529
MAXBAS	1	100	2.109
PCALT	1	100	-0.202
TCALT	0	100	2.221

Table 4.5: results of 'Water Balance' statistics and 'Goodness of Simulation' statistics for calibration period of simulation

Dano Catchment	
	Calibration
Water Balance [mm/year]:	
Sum Qsim	143.704
Sum Qobs	149.388
Sum Precipitation	803.128
Sum AET	819.352
Sum PET	1752.171
Goodness of fit:	
Coefficient of determination R^2	**0.945**
Model efficiency R_{eff}/ NSE	**0.945**
Kling-Gupta efficiency KGE	**0.948**

Fig 4.5: presents the observed and simulated discharges during the calibration period. A close analysis of the hydrographs indicates a strong proximity between observed and simulated runoff, meaning a very good simulation of the of observed daily flow by the model. This translates into Model efficiency, coefficient of determination and Kling-Gupta Efficiency close to 1 (fig 4.5). Such a model is deemed well calibrated. Nevertheless, it can be noticed that the model constantly underestimates peak flows.

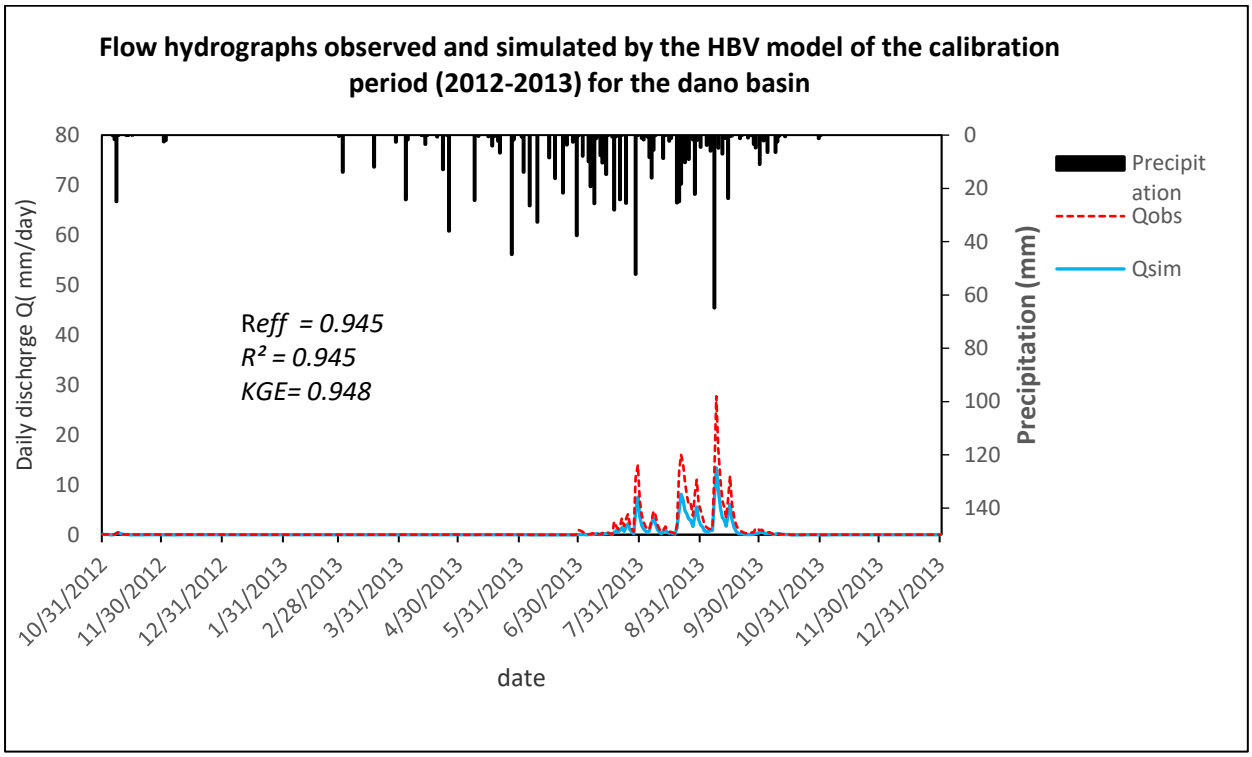

Fig 4.5: Observed and simulated discharges for the calibration period (2013) at the outlet. Reff , R2, and KGE refer to Model efficiency, Coefficient of determination and Kling-Gupta Efficiency respectively.

4.3.2. Validation results

The calibrated set of the parameters was tested against the observed flow of the validation period (31/10/2013 to 31/12/2014). Graph fig 4.6 shows the resulting comparison between observed and simulated discharges. A model efficiency of 0.64 was achieved, indicating an acceptable validation. It is worth noting that peak flows are still underestimated. The water balance of the validation period as well as the goodness of fit measures are summarized in Table 8.

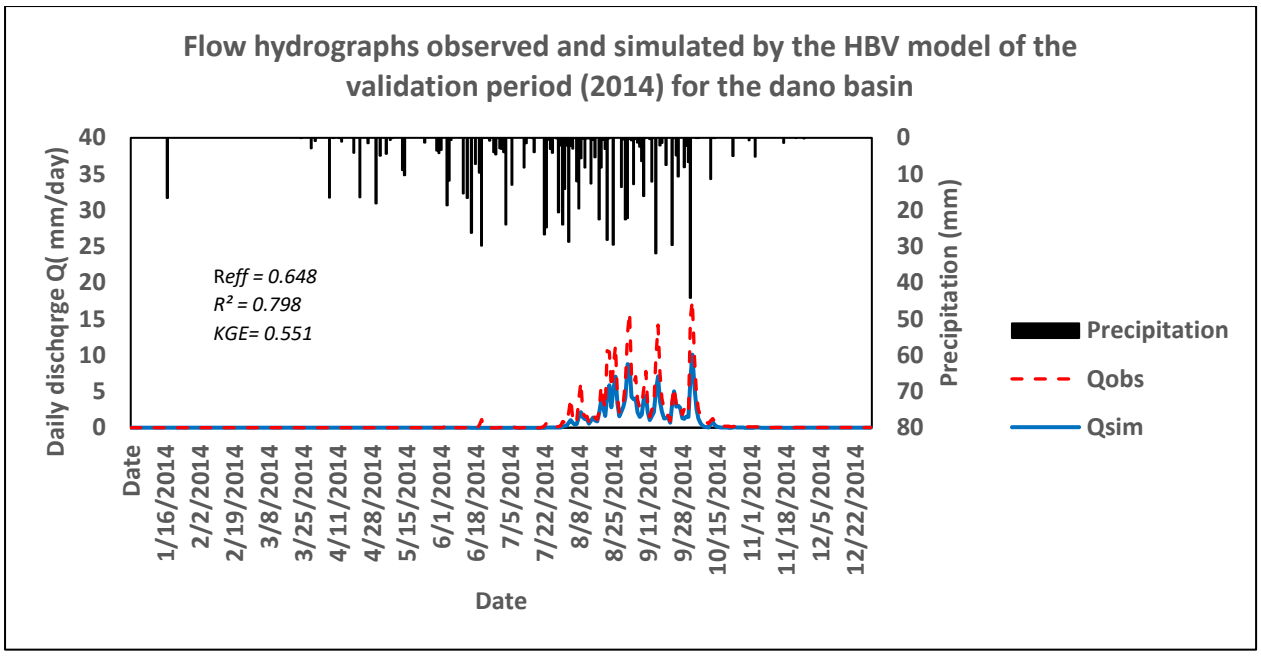

Fig 4.6: Observed and simulated discharges for the validation period (2014) at the outlet. Reff, R2, and KGE refer to Model efficiency, Coefficient of determination and Kling-Gupta Efficiency respectively.

Table 4.5: results of 'Water Balance' statistics and 'Goodness of Simulation' statistics for validation period

Dano	Validation
Water Balance [mm/year]:	
Sum Qsim	189.675
Sum Qobs	140.689
Sum Precipitation	919.406
Sum AET	714.993
Sum PET	1774.439
Goodness of fit :	
Coefficient of determination	**0.798**
Model efficiency	**0.648**
Kling-Gupta efficiency	**0.551**

The results of the Standard Precipitation Index (spi) indicate that the years of calibration (2012-2013) were very humid (SPI=2) while the validation year (2014) was y near to normal (SPI=-0.8). This difference in the climatology of the calibration and validation periods might explained the drop in the model efficiency during the validation.

2011 - 2012	0.8
2012 - 2013	2.0
2013 - 2014	-0.8

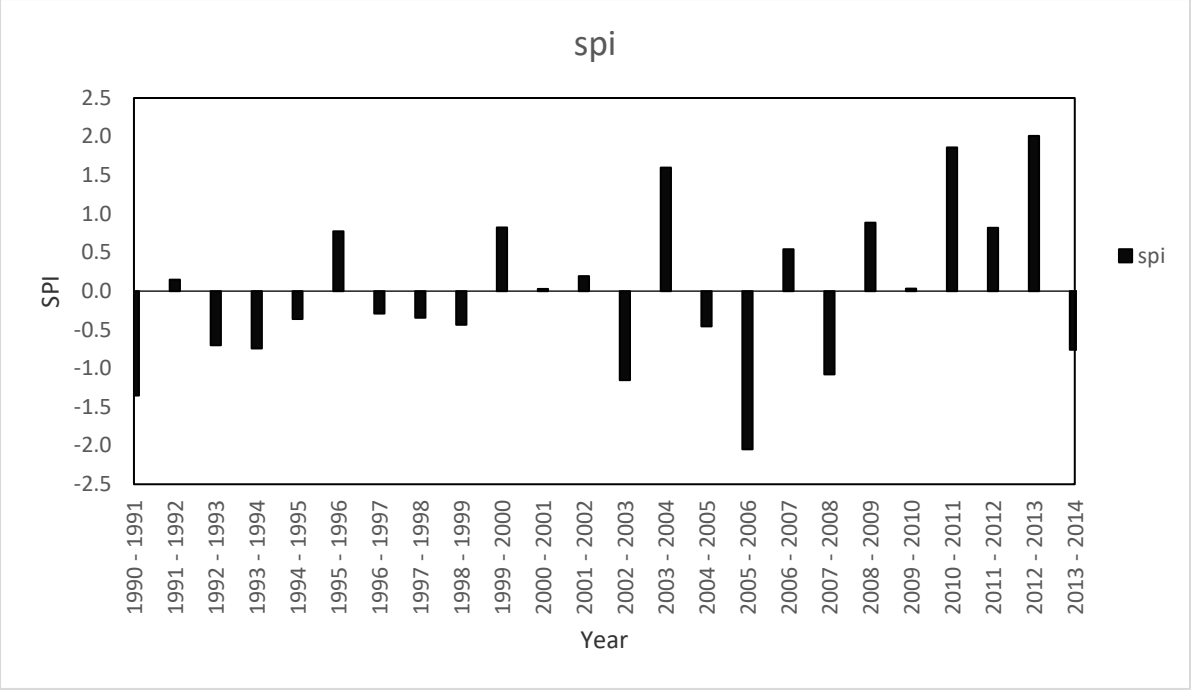

Fig 4.7: Standardized precipitation index (SPI) in the Dano catchment (1990-2014).

4.4. Discussion

The results for the calibration and validation of the HBV model give a good performance for the Dano Catchment. The achieved coefficients (Model efficiency, Coefficient of determination and Kling-Gupta Efficiency) were above 0.9 and 0.55 during the calibration and validation phases, respectively. These results indicate an overall good ability of the model to reproduce the hydrology of the Dano catchment.

It is however noted a poor representation of peaks, as simulated discharges constantly underestimated observations. Several studies have also noted the difficulties for the HBV model to reproduce peaks. Indeed Hundecha (2005) reported the same problem for the case of the sub-basins of the Rhine in Germany (Hundecha 2005).

Looking at the values of the SPI obtained, one notes that the calibration period (spi = 2) is a wet period and the validation period (Spi = - 0.8) corresponds to a normal period. This difference in the climatology of the calibration and validation periods might explained the drop in the model efficiency during the validation. Paradoxically, this result indicates the ability of the model to perform under different climatic conditions.

4.5. Conclusion

In this chapter, the hydrological behaviour of the DANO catchment was modeled using the the HBV Light model developed by the Swedish Meteorological and Hydrological Institute (SMHI) at the daily time step. The applied criteria for the evaluation of the model performance were the:

Coefficient of determination, the Model efficiency and the Kling-Gupta efficiency. The model was successfully validated for these three coefficients although an underestimation of peak flows was noted. Furthermore, the achieved Water Balance was consistent with the one reported for similar basin in the region. Overall, based on these result

it can be concluded that the HBV model as parameterized gives good results, simulates the hydrology of the catchment in an acceptable way and suitable for impact assessment.

Chapter 5: Projected climate signal and its impact on streamflow

5.1. Introduction

Availability of freshwater in sub-Saharan Africa is fundamental to economic growth and social development (Kankam-Yeboah et al. 2013) . Water is essential to economic and social activities such as water supply and sanitation, agriculture, hydropower generation, urban development, industry and fisheries etc...(Kankam-Yeboah et al. 2013).

(Bodian et al. 2018) highlighted that the streamflow is one of the major components to determine the water availability. However, hydrological cycle can be altered by human activities and climate change(Milano et al. 2013).Therefore, it is primordial to have knowledge on streamflow in order to better assess the quantity of existing water for multiple purposes currently and for the future (Bodian et al. 2018) as the major effect of climate change is likely to be alterations in hydrologic cycles and changes in water availability (Setegn et al. 2011). Nearly most regions of the world are expected to experience a net negative impact of climate change on water resources and freshwater ecosystems according to the Intergovernmental Panel on Climate Change (IPCC)(IPCC 2007). Precipitation and temperature are the key drivers for the hydrological regime of rivers, and climate change has its main impact through changes in these two variables.(Aich et al. 2014).

The objective of this chapter is to investigate the impact of future climate change on the streamflow in the Dano catchment, in order to support a better management of its water resources. It is done in the first step by correcting the dataset of RCM, followed by the analysis of climate change trend by comparing the historical climate and projected ones (RCM), and finally the application of climate simulations to a hydrological model and assessing the impacts.

5.2. Materials and Methodologies

5.2.1. Data sources

- Observed dataset

The observed climate data used in the study were collected from different source and for different period of time. (table 5.1)

Table 5.1: Applied climate data

Type of data	Sources	UNIT	Type of data	Periode of data	Stations
Température	the national meteorological service (DGM)	°C	Mean daily	2002-2014	-Dreyer Foundation -Tambiri -Boromo
Precipitation		mm / h	Mean Daily	2002-2014	-Dreyer Foundation -Tambiri
Wind speed		m/s	Daily	2002-2014	
Relative humidity		1/1	Daily	2002-2014	
Solar radiation		Wh/m²	Daily	2002-2014	
discharge		m3/s	Daily	2011-2014	

- Simulated climate Data

The applied simulated data of the future period come from the The WASCAL high-resolution regional climate simulation ensemble for West Africa. All data are made available to the public at the CERA long-term archive of the German Climate Computing Center (DKRZ) with a subset available at the PANGAEA Data Publisher for Earth & Environmental Science portal (https://doi.pangaea.de/10.1594/PANGAEA.880512).(Heinzeller et al. 2018).

These regional climate projections are generated at high (12 km) and intermediate (60 km) resolution using the Weather Research and Forecasting Model (WRF). The simulations cover the validation period 1980–2010 and the two future periods 2020–2050 and 2070–2100. (Heinzeller et al. 2018) In this study two products of WASCAL high-resolution regional climate simulation ensemble for West Africa were used the GFDL-ESM2M and HadGEM2-ES, those models are based on a 365-day (no-leap year) and a 360-day (12×30 days) calendar, respectively

5.2.2. Data evaluation and correction

The observed and simulated data need to be analysed to find missing, wrong and discrepancy in the dataset According to the standards for estimation of missing data set by World Meteorological Organization (WMO) (1966), all the missing data required for scientific use should be 10% of the total records

- Graphical comparison

Different graphical comparisons between observed and simulation climate data ware adopted. These included Cumulative Distribution Function, mean monthly averages etc.

- Bias correction of climatic data (Quantile mapping)

Quantile mapping is the most effective in correcting the biases of daily precipitation. The method of quantile mapping can be used to correct biases of precipitation projections for modelling the future availability of water resources (N'Tcha M'Po 2016).

To correct systematic biases inherent in all RCM models, the quantile mapping method was employed. In the current study, it was done for the periods 1980 to 2005, 2020-2049, 2070-2099. The different output of climate model, (temperature, precipitation, wind and relative humidity) were corrected for all periods of time following the Quantile Mapping.

The software R studio was used for the correction of the different variables of the model climate outputs (rcp4.5: GFDLESM, HadGEM2). The method needs a period of overlap year between observed and simulated as un period of calibration. To show the effectiveness of the correction, R studio can give us as a result the data corrected but also graphs that help to see and evaluate the correction of bias data

5.2.3. Hydrological modelling

a) HBV model, calibration, validation

The Observed and the two RCM–GCM datasets (HadGEM2-ES and GFDL-ESM2M) uncorrected and bias corrected are used as climate input for HBV light model. The Calibration and validation of the HBV are detailed in Chapter 4**.** A split sample test approach was adopted and the performances of the model were as follows: Coefficient of determination R^2 = 0.945, Model efficiency Reff/ NSE = 0.945 and Kling-Gupta efficiency KGE = 0.948 for the calibration phase and Coefficient of determination = 0.798, Model efficiency = 0.648 and Kling-Gupta efficiency 0.551 for the validation.

b) Eto calculation

The potential evapotranspiration is needed as an input in HBV light model, so the estimation was done for the different periods of time of the simulated climate (historical (1980-2005) and projected (2020-2049, 2070-2099), the different RCM datasets (HadGEM2-ES and GFDL-ESM2M), and for the uncorrected and bias corrected data. This was done using version 3.2 of the software Eto calculator by FAO

c) Signal change and magnitude

To do the assessment of climate change impact on the streamflow and the other parameters (temperatures, precipitation, potential evapotranspiration) the difference of mean between the results of models HBV-light outputs for the projected periods (2020-2049, 2070-2099) and the

historical one (1980-2005) are be analysed. Both uncorrected and bias corrected output are compared as bias correction can potentially affect climate change signal

5.3. Results and discussion

5.3.1. Data evaluation and correction

The simulated climate data (Precipitation, temperature, relative humidity, Wind speed) of the two datasets (HadGEM2-ES and GFDL-ESM2M) was compared to observations prior and post correction (Fig 5.1, 5.2,5.3 & 5.4). The results indicate important biases before correction. The results further highlight the effectiveness of the bias correction method (quantile Mapping method) as represented in the graphs fig. 5.1, 5.2,5.3 & 5.4 (for all other variables please refer to graphs in appendix 1)

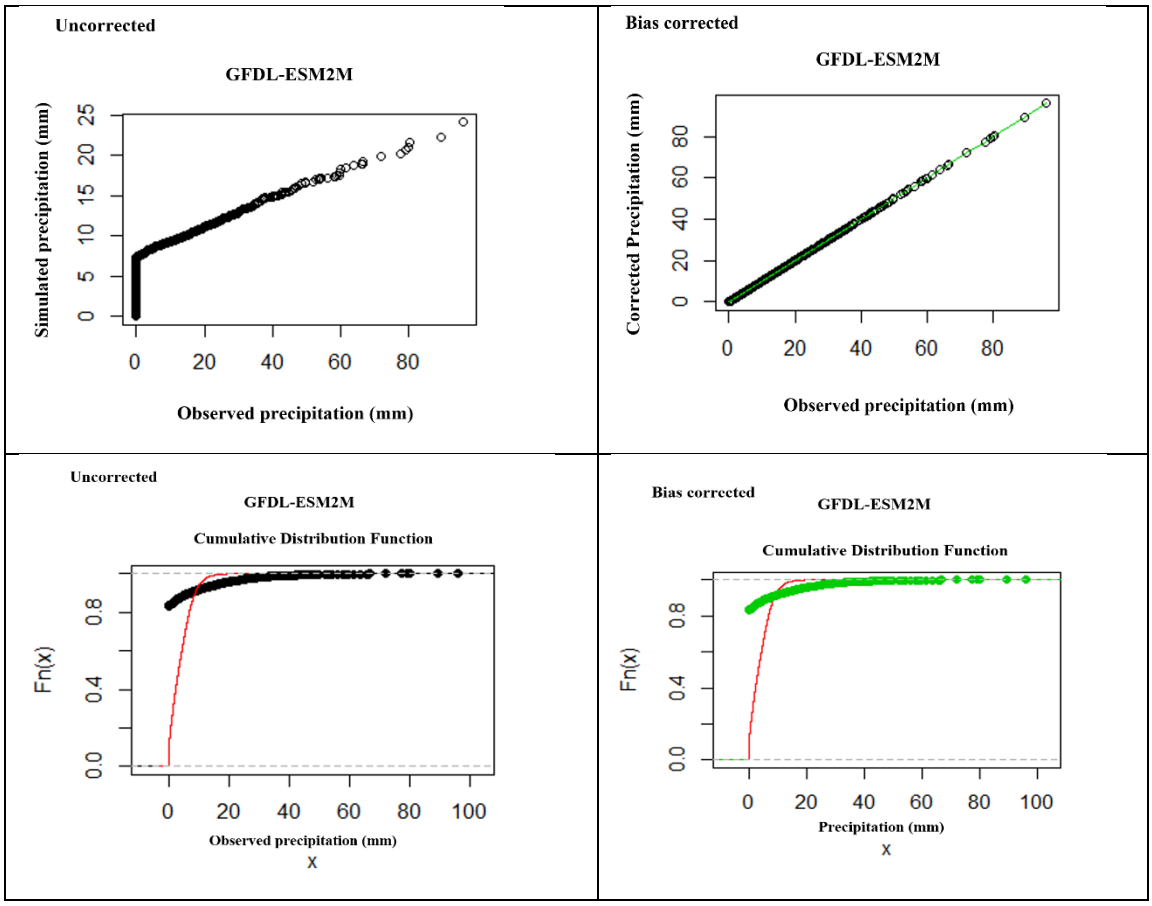

Fig.5.1: comparative graphs showing before and after correction of the values of precipitation (GFDL-ESM2M), in RStudio with the method of quantile mapping

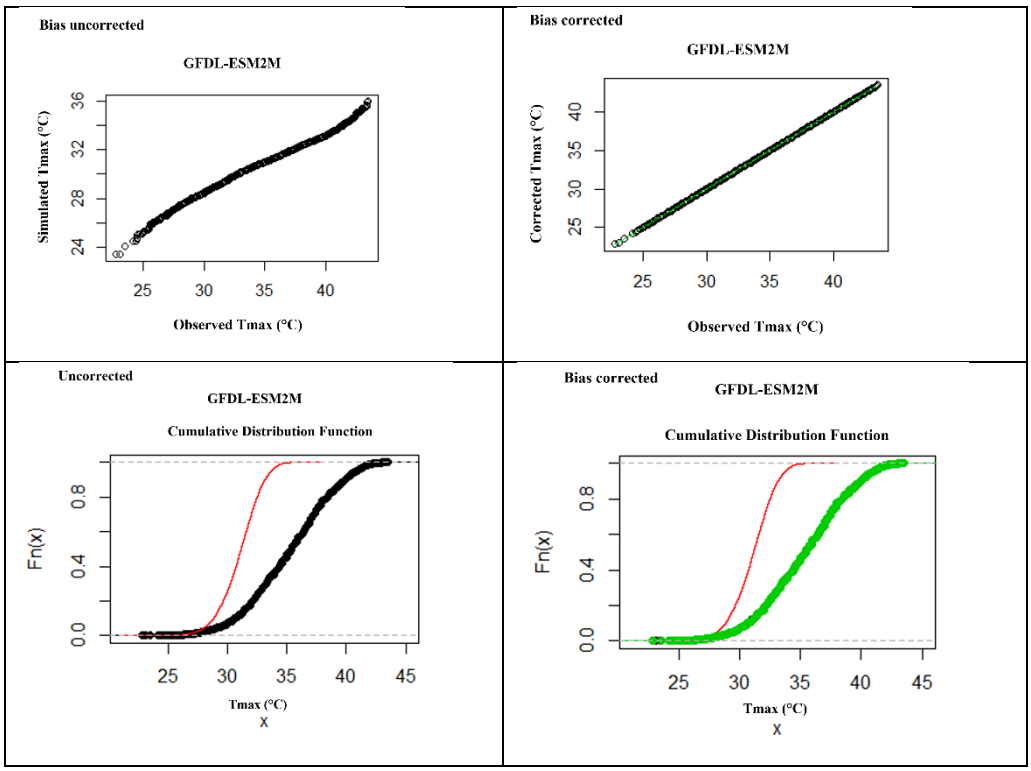

Fig. 5.2: comparative graphs showing before and after correction of the values of temperature maximum Tmax (GFDL-ESM2M), in RStudio with the method of quantile mapping

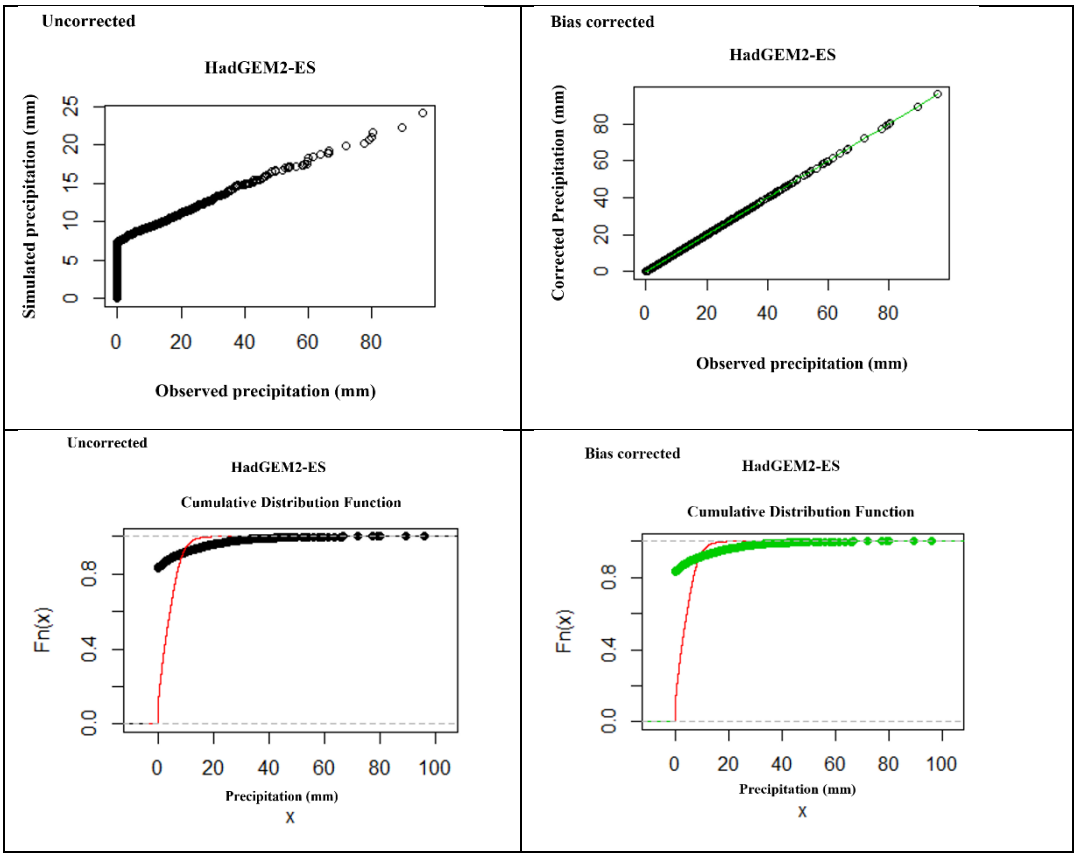

Fig 5.3: comparative graphs showing before and after correction of the values of precipitation (HadGEM2-ES), in RStudio with the method of quantile mapping

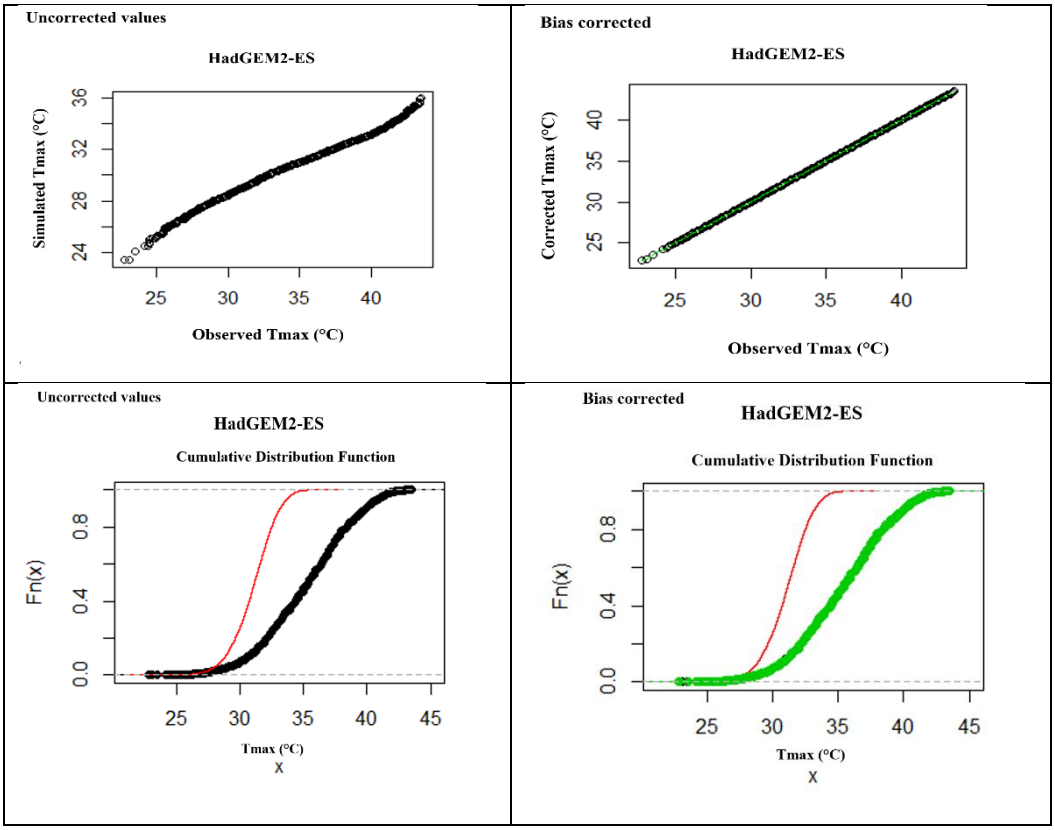

Fig 5.4: comparative graphs showing before and after correction of the values of maximum temperature Tmax (HadGEM2-ES), in RStudio with the method of quantile mapping

The comparison between simulated historical climate products RCP 4.5 (HadGEM2-ES, GFDL-ESM2M) and observed (provided by the National Meteorological Service-DGM) for precipitation, mean temperature, relative humidity and wind Speed was also done for the reference period of 1980-2005 or 2002-2005 using average monthly values as shown in graph fig 5.5

This fig 5.5 indicates (HadGEM2-ES, GFDL-ESM2M) before correction that for the majority of the months there is an overestimation of precipitation and wind speed, whereas for the other parameters (temperature, relative humidity) there is an underestimate compared to the observed data (reference). After bias correcting (bias correct), the set of simulated data matches the observed data in general. However, for the precipitation and the relative humidity of the HadGEM2-ES one still notices that the observed and simulated graph still show deviations from observations.

.

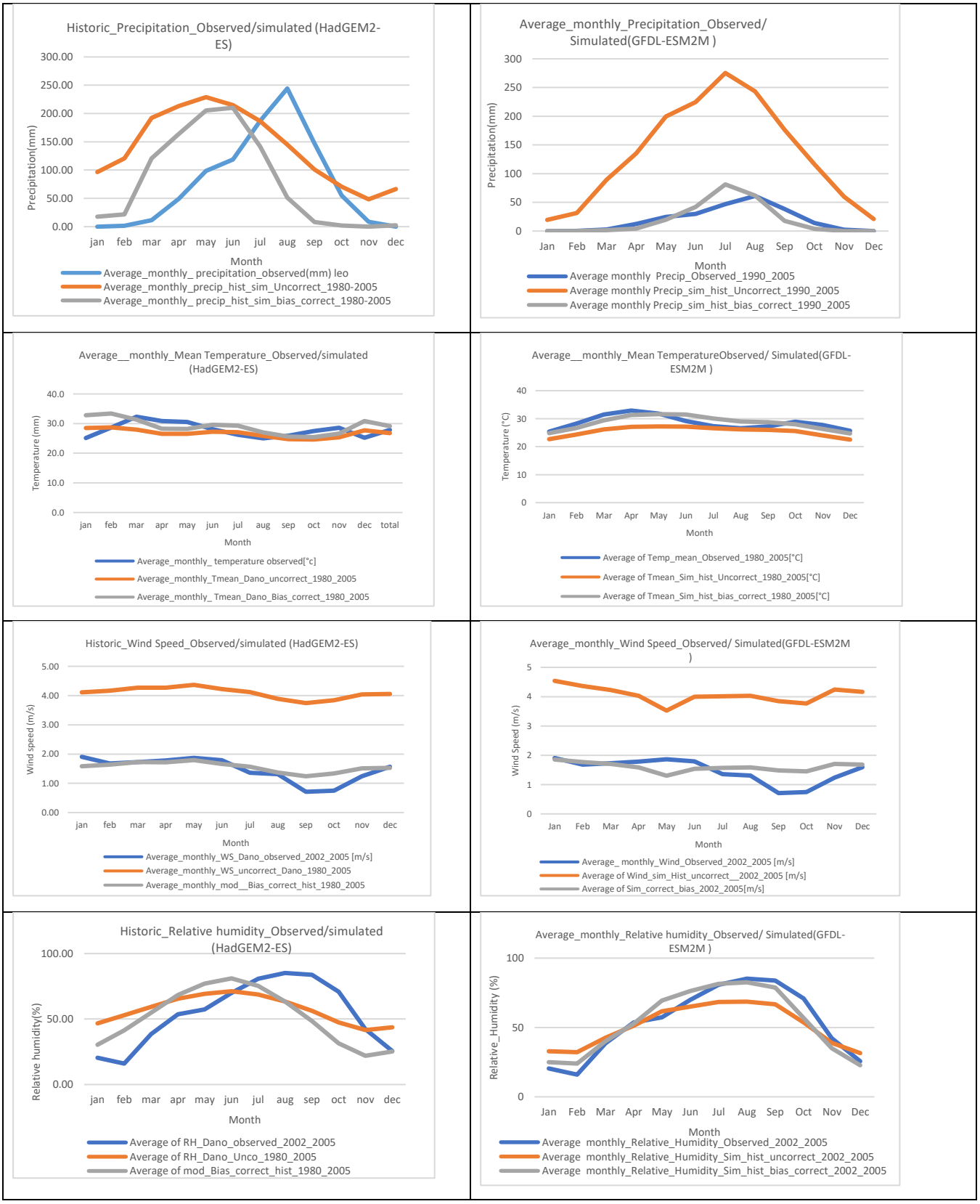

Fig 5.5: Graph mean monthly of Comparison between the historic period of observed and simulated (uncorrected /bias corrected) climate models ensemble ((HadGEM2-ES, GFDL-ESM2M).

5.3.2. Scenario Application in hydrological modelling, trend, Signal change and magnitude

Fig 5.6 compares the historical (1980-2005) and projected (2020-2049 and 2070-2099) Precipitation, mean Temperature, AET, PET and discharges.

Precipitation:

One notes for bias corrected data that the average monthly precipitation shows a trend up compared to the historic (1980-2005) period. A projected annual precipitation increases for GFDL-ESM2M of 97.85 mm (10.5 %) is expected the for the period 2020-2049, while this increase reaches 345.5 mm (37%) in the period 2070-2099.

Compared to the bias corrected data, the precipitation changes with non-bias corrected climate data show a similar trend (with however differences in magnitude). Comparing uncorrected data and bias corrected data one notices that the number of rainiest months are reduced. so the rainiest months are July and August with maximum monthly rains of up to 316 mm and 366 mm respectively by the middle of the century and around the end of the century

Mean Temperature

F***ig.5.6*** also shows that the temperatures have a trend up for the projected 1(2020-2049) and projected 2 (2070-2099) respectively compared to the historical period (1980-2005). The result shows an increase of 1.9 °C by 2049 and at the end of the century 3.2°C. The maximum/ minimum temperature for the projected 1 (2020-2049) are 34.4°C / 25.8 °C and for the projected 2 (2070-2099) the graph shows 35.5 °C / 26.75 °C. The uncorrected data have the same trend up compared to the historical period, but the bias correction permitted to correct the underestimation of the temperature.

Actual Evapotranspiration (AET)

Fig 5.6 shows that the AET have a trend up for the projected 1(2020-2049) and projected 2 (2070-2099 compared to the historical period (1980-2005). Increases of 20.9 mm (3.2%) by 2049 and 104.4 mm (16%) by the end of the century are projected.

Compared to the uncorrected bias, bias correction reduces the overestimation of AET so the maximum monthly AET is up to 105 mm and 113 mm in the month of august respectively by the middle of the century and around the end of the century. For the minimum AET one notices that the values are almost the same for all period of time (historical and projected). For the average monthly AET, it can be noticed that a general decrease from August to April before an increase is observed from May to July.

Potential Evapotranspiration

Fig 5.6 shows for the projected periods of GFDL-ESM2M that the PET has a trend up compared to the historical period (1980-2005). Increases of 39.3 mm (2.3%) by 2049 and 71.8 mm (4.1 %). at the end of the century are shown.

The uncorrected data have the same trend up compared to the bias corrected data but the bias correction permitted to correct the overestimation of the PET. The maximum monthly PET is up to 189.1 mm and 191.5 mm in the month of March respectively by the middle of the century and around the end of the century. For the minimum PET one notices that the values are almost the same 119.1 mm for September for all period of time historical and projected. On average, monthly PET shows a decrease in general from March to September followed by an increase from October to February.

Discharges

Discharges of historical (1980-2005) and projection (2020-2049 and 2070-2099) for the climate products GFDL-ESM2M in shown on Fig 5.6.

The results of hydrological modelling with HBV light show a projected change in annual discharge for the periods of 2020– 2049 and 2070 and 2099 compared to the reference period. Fig.18 present a trend up with different magnitude, compared to historical period. The average annual discharges show an increase of 74 mm (25 %) by 2049 and at the end of the century this increase reaches 238.8 mm (80.65 %).

The flows are starting by April for all historic and projected periods and increase until August where the maximum values of 154.98 mm occur for projected 1 (2020-2049) and 221.5 mm for projected 2 (2070-2099). After august, the discharges decrease until November to reach zero. Between the months of November and March the discharges are almost null or equal to zero during the dry season. The uncorrected data have the same trend up compared to bias corrected data but the magnitudes are different and bias correction permitted to correct the underestimation of the flow rate.

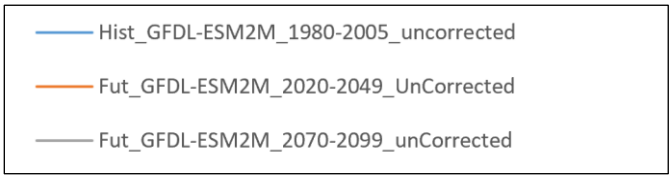
Hist_GFDL-ESM2M_1980-2005_uncorrected
Fut_GFDL-ESM2M_2020-2049_UnCorrected
Fut_GFDL-ESM2M_2070-2099_unCorrected

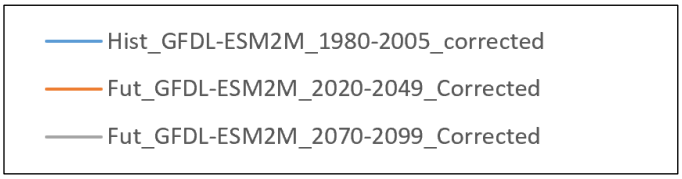
Hist_GFDL-ESM2M_1980-2005_corrected
Fut_GFDL-ESM2M_2020-2049_Corrected
Fut_GFDL-ESM2M_2070-2099_Corrected

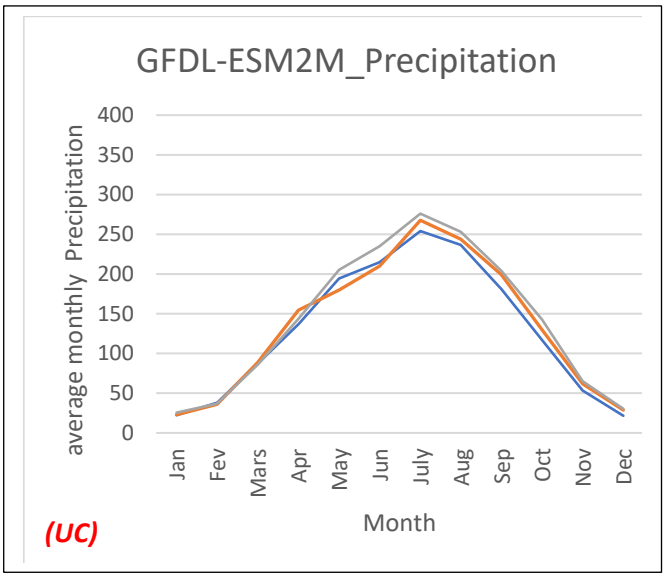
GFDL-ESM2M_Precipitation
average monthly Precipitation
400
350
300
250
200
150
100
50
0
Jan
Fev
Mars
Apr
May
Jun
July
Aug
Sep
Oct
Nov
Dec
Month
(UC)

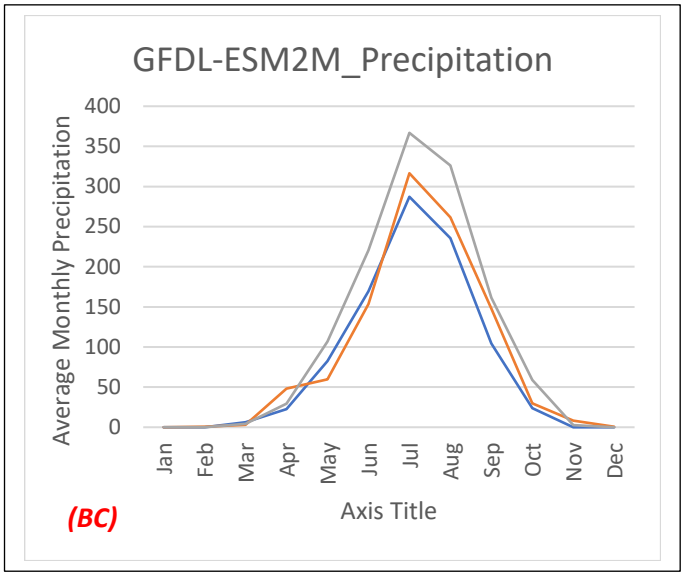
GFDL-ESM2M_Precipitation
Average Monthly Precipitation
400
350
300
250
200
150
100
50
0
Jan
Feb
Mar
Apr
May
Jun
Jul
Aug
Sep
Oct
Nov
Dec
Axis Title
(BC)

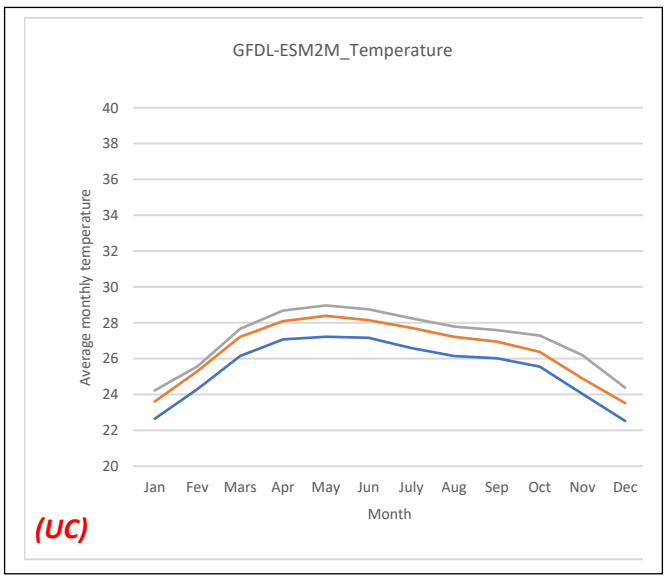
GFDL-ESM2M_Temperature
Average monthly temperature
40
38
36
34
32
30
28
26
24
22
20
Jan
Fev
Mars
Apr
May
Jun
July
Aug
Sep
Oct
Nov
Dec
Month
(UC)

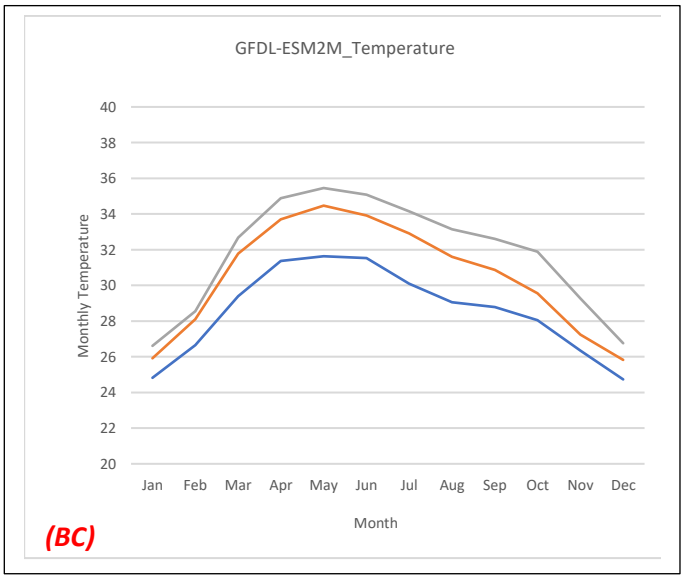
GFDL-ESM2M_Temperature
Monthly Temperature
40
38
36
34
32
30
28
26
24
22
20
Jan
Feb
Mar
Apr
May
Jun
Jul
Aug
Sep
Oct
Nov
Dec
Month
(BC)

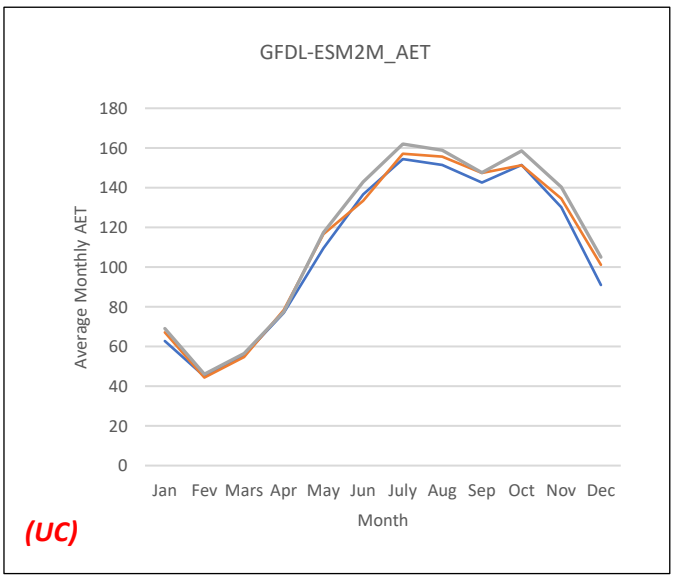
GFDL-ESM2M_AET
Average Monthly AET
180
160
140
120
100
80
60
40
20
0
Jan
Fev
Mars
Apr
May
Jun
July
Aug
Sep
Oct
Nov
Dec
Month
(UC)

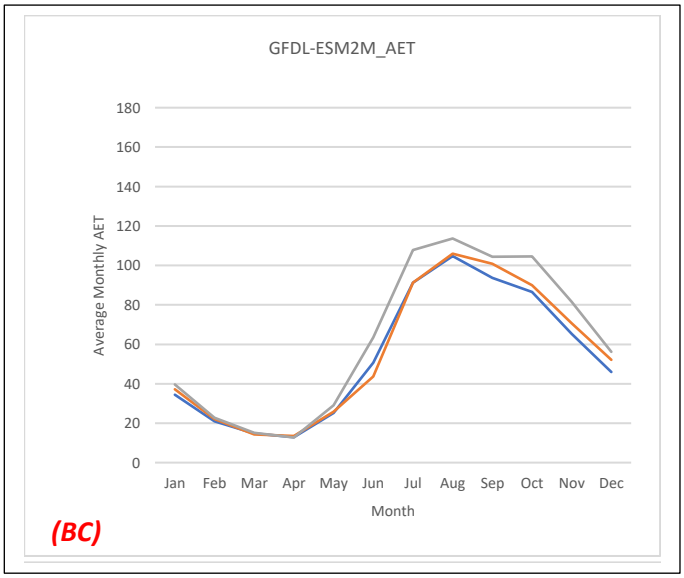
GFDL-ESM2M_AET
Average Monthly AET
180
160
140
120
100
80
60
40
20
0
Jan
Feb
Mar
Apr
May
Jun
Jul
Aug
Sep
Oct
Nov
Dec
Month
(BC)

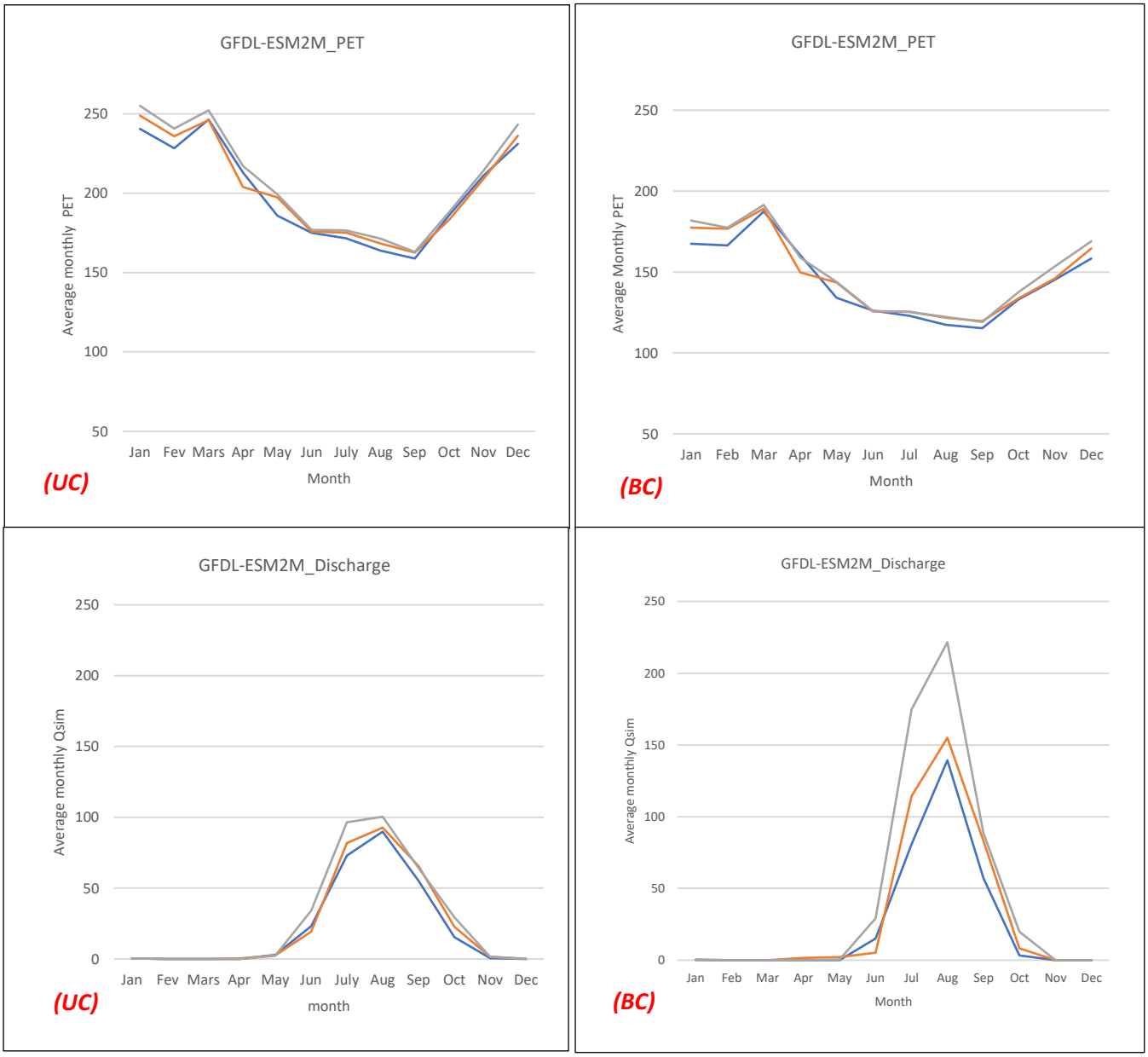

Fig 5.6: Graphs comparing Historical (1980-2005) and projected (2020-2049 and 2070-2099) Average nonthly precipitation, temperature, Potential evapotranspiration (PET), Actual Evapotranspiration (AET) nd discharges (Qsim) under emission scenarios RCP4.5

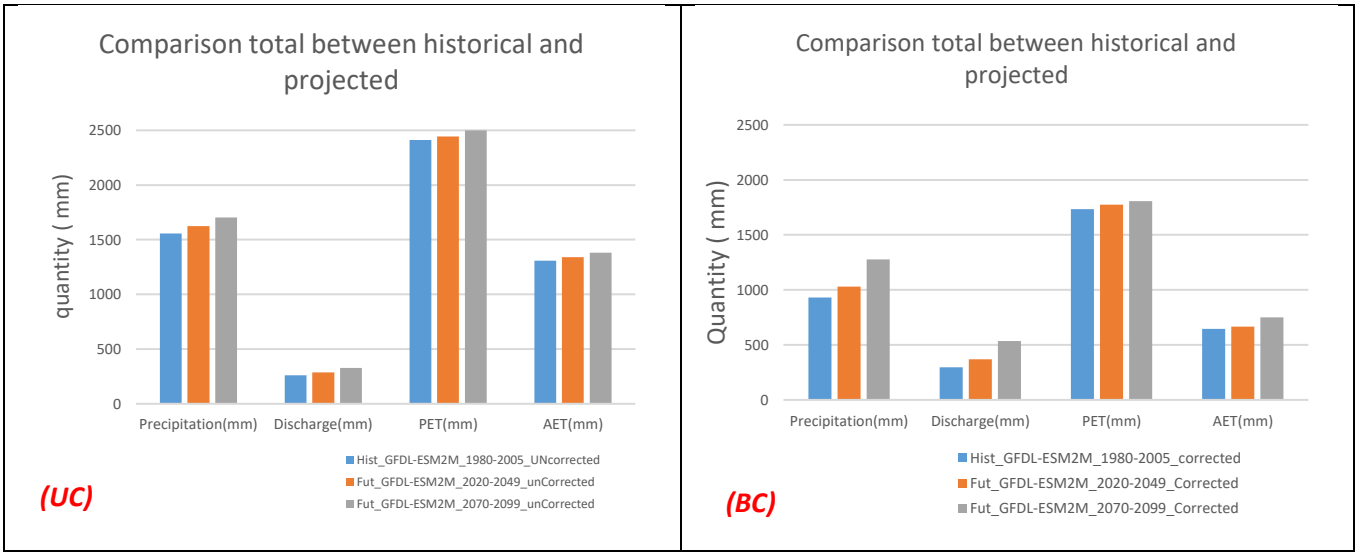

Fig 5.7: Comparison between the historical (1980-2005) and projected (2020-2049 and 2070-2099) average monthly precipitation, PET, AET and discharges simulated of climate model GFDL-ESM2M

Fig 5.8 presents the historical (1980-2005) and projected (2020-2049 and 2070-2099) Precipitation, mean Temperature, AET, PET and discharges forHadGEM2-ES Under RCP4.5. In general, the trends of all parameter (Precipitation, mean Temperature, AET, PET and discharges) are the same compared to climate model GFDL-ESM2M. The differences are found in the magnitude between the historical and projected climate data. The results of biases correction and uncorrected data are on the same trend as well, only the magnitudes are different.

Precipitation:

Fig 5.8 indicates for bias corrected data that the average monthly precipitation shows a trend up compared to the historic period (1980-2005). The projected precipitation will increase by 286.9mm/year (30.4 %) for projected period 2020-2049 and by 484.2 mm (51,4%) for projected period 2070-2099.

Compared to the uncorrected bias, bias correction reduces the number of rainiest months so the rainy months are July and August with maximum monthly rains of up to 328 mm and 391.8 mm respectively by the middle of the century and around the end of the century.

Mean Temperature

Fig 5.8 shows, that temperature has a trend up for the projected 1(2020-2049) and projected 2 (2070-2099) compared to the historical period (1980-2005). The graph shows an increase of 2.8 °C

by 2049 and at the end of the century 5.4 °C. The maximum/ minimum temperature for the projected 1 (2020-2049) are 35°C / 27 °C and for the projected 2 (2070-2099) the graph shows 37.38°C / 29°C. The uncorrected data have the same trend up compared to the historical period, with the difference that bias correction permitted to correct the underestimation of temperature.

Actual Evapotranspiration (AET)

Fig 5.8 shows, that the AET have a trend up for the projected 1(2020-2049) and projected 2 (2070-2099) compared to the historical period (1980-2005). The comparison shows an increase of 62.6 mm (10 %) by 2049 and at the end of the century 125.5 mm (19.95%).

Compared to the uncorrected bias, bias correction reduces the overestimation of AET so the maximum monthly AET is up to 105 mm and 113 mm in the month of august respectively by the middle of the century and around the end of the century. For the minimum AET one notices that the values are almost. One notice based on the annual pattern a decrease from August to April before an increase starting from May to July.

Potential Evapotranspiration PET

Fig 5.8 shows for historical (1980-2005) and projection PET for HadGEM2-ES, that PET has a trend up for the projected 1(2020-2049) and projected 2 (2070-2099). The results show an increase of 89.1 mm (5.3%) by 2049 and 146.3 mm (8.8 %).at the end of the century. The uncorrected data have the same trend compared to the bias corrected data but the bias correction permitted to correct the overestimation of the PET. The maximum / minimum monthly PET is up to 179.5 mm (March) / 110.8 mm (September) and 184.5 mm (March) / 114.8 m (September) by the middle of the century and around the end of the century, respectively. The annual pattern of PET, shows that a decrease in projected from March to September followed by an increase from October to February.

Discharges

The results of hydrological modelling with HBV light show a projected change in annual discharge for the periods of 2020– 2049 and 2070-2099 compared to the reference period .Fig 5.8 presents a trend up with different magnitude., Compared to the historical period the results an annual discharge increase of 221.8 mm (68 %) by 2049 and this increase reaches 355.3 mm (109 %). at the end of the century.

The flows are starting by May for all historic and projected periods and increase until August where the maximum values of 218 mm for projected 1 (2020-2049) and 280 mm for projected 2 (2070-2099) are found. The uncorrected data have the same trend up compared to bias corrected data

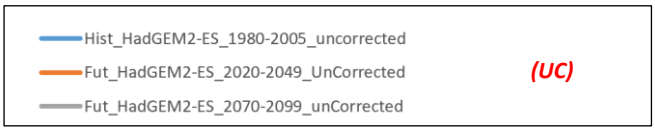
Hist_HadGEM2-ES_1980-2005_uncorrected
Fut_HadGEM2-ES_2020-2049_UnCorrected
Fut_HadGEM2-ES_2070-2099_unCorrected
(UC)

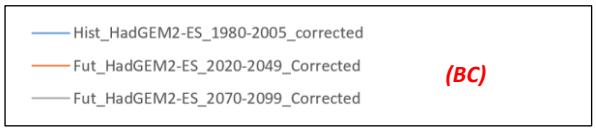
Hist_HadGEM2-ES_1980-2005_corrected
Fut_HadGEM2-ES_2020-2049_Corrected
Fut_HadGEM2-ES_2070-2099_Corrected
(BC)

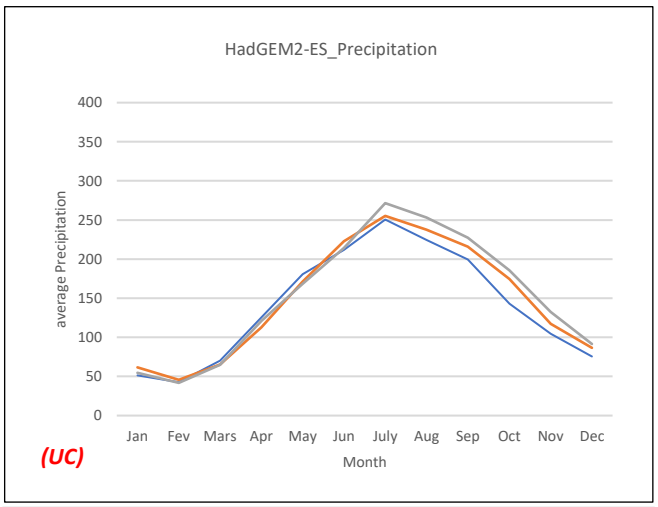
HadGEM2-ES_Precipitation
average Precipitation
0
50
100
150
200
250
300
350
400
Jan Fev Mars Apr May Jun July Aug Sep Oct Nov Dec
Month
(UC)

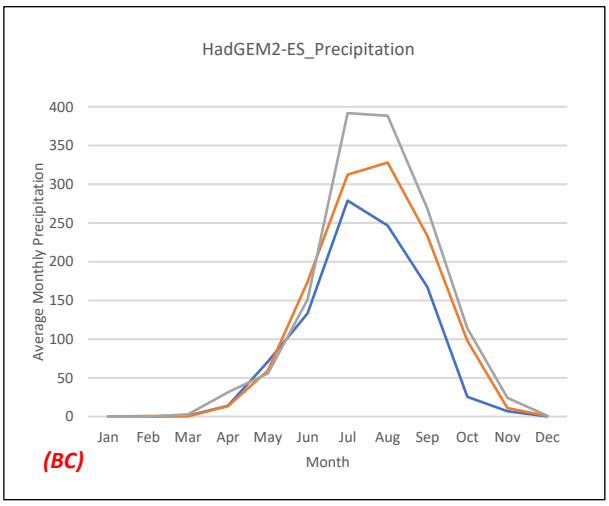
HadGEM2-ES_Precipitation
Average Monthly Precipitation
0
50
100
150
200
250
300
350
400
Jan Feb Mar Apr May Jun Jul Aug Sep Oct Nov Dec
Month
(BC)

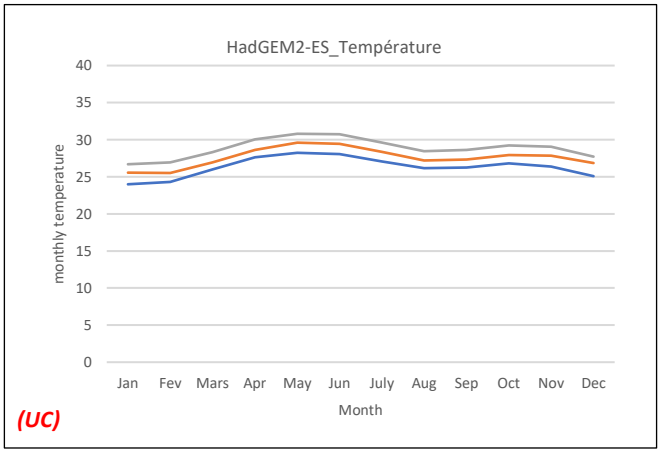
HadGEM2-ES_Température
monthly temperature
0
5
10
15
20
25
30
35
40
Jan Fev Mars Apr May Jun July Aug Sep Oct Nov Dec
Month
(UC)

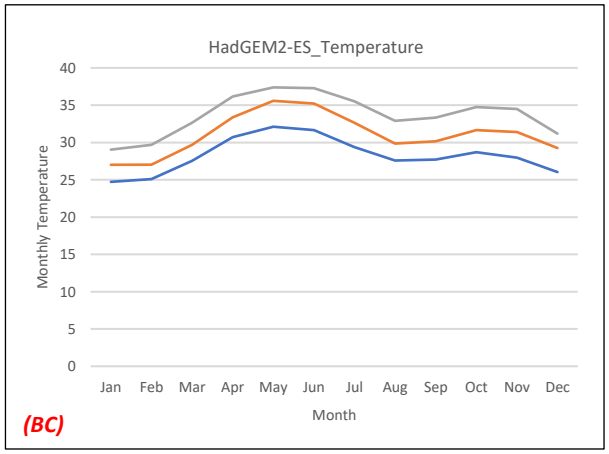
HadGEM2-ES_Temperature
Monthly Temperature
0
5
10
15
20
25
30
35
40
Jan Feb Mar Apr May Jun Jul Aug Sep Oct Nov Dec
Month
(BC)

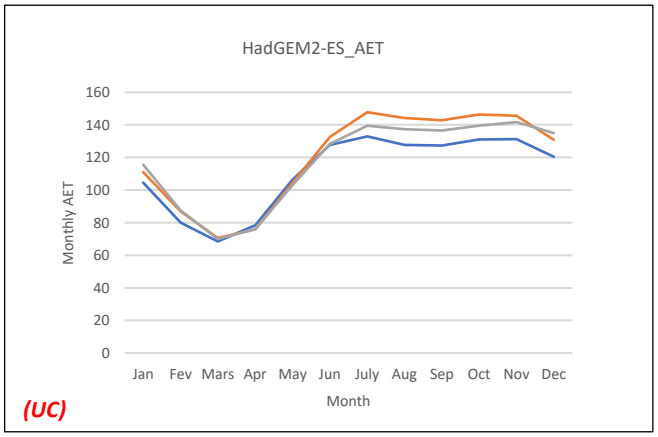
HadGEM2-ES_AET
Monthly AET
0
20
40
60
80
100
120
140
160
Jan Fev Mars Apr May Jun July Aug Sep Oct Nov Dec
Month
(UC)

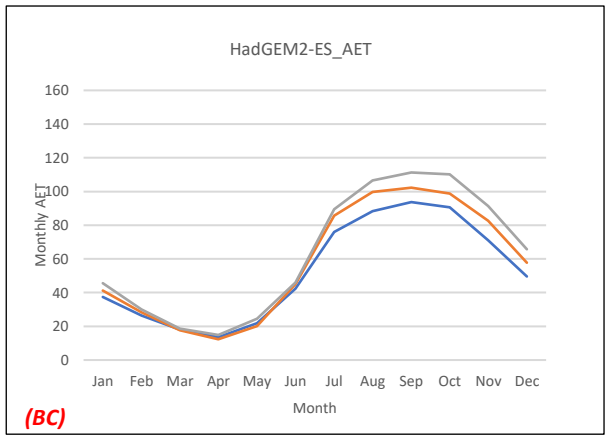
HadGEM2-ES_AET
Monthly AET
0
20
40
60
80
100
120
140
160
Jan Feb Mar Apr May Jun Jul Aug Sep Oct Nov Dec
Month
(BC)

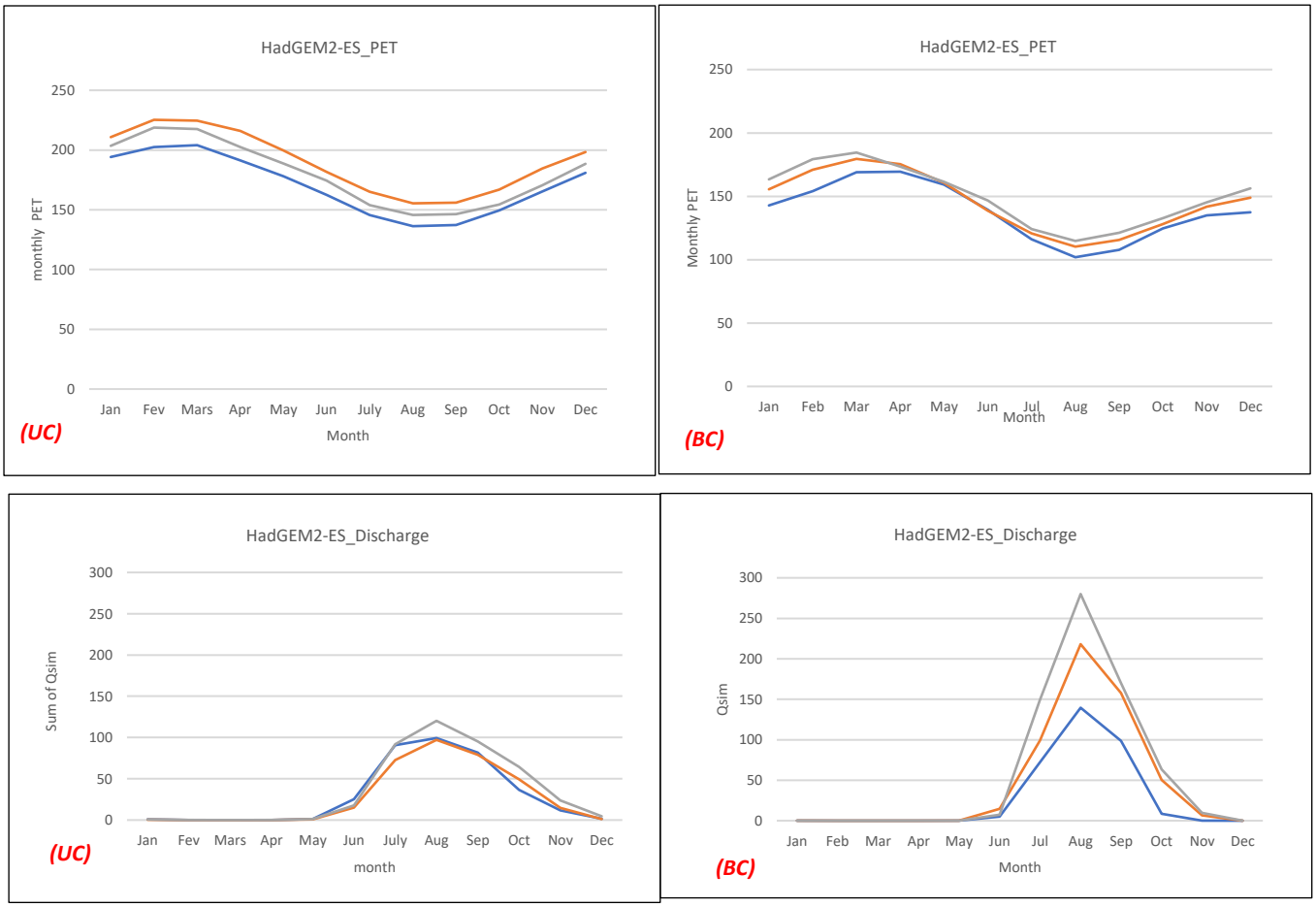

Fig 5.8 compares historical (1980-2005) and projected (2020-2049 and 2070-2099) average monthly precipitation, temperature, Potential evapotranspiration (PET), Actual Evapotranspiration (AET) and discharges (Qsim) under emission scenarios RCP4.5 (HadGEM2

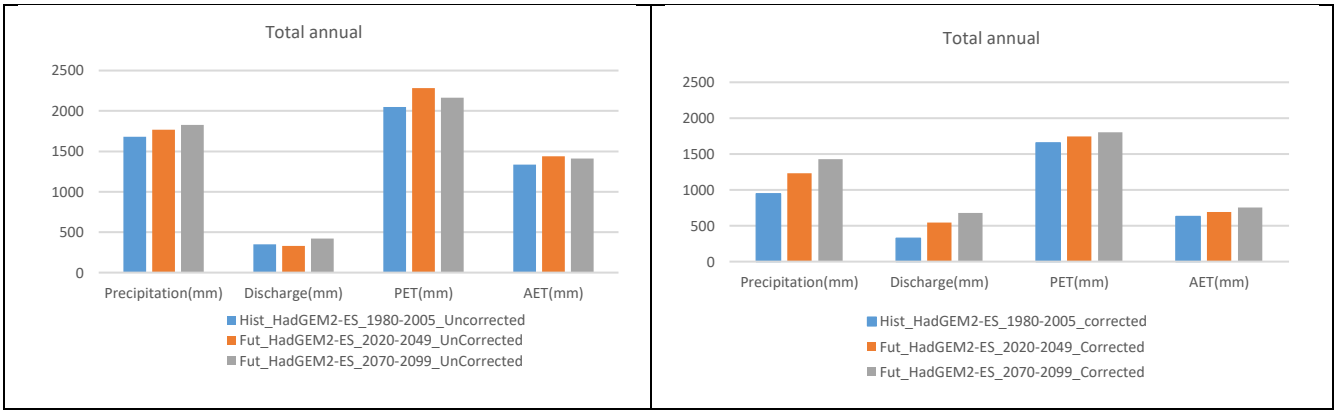

Fig 5.9: Comparison between the historical (1980-2005) and projected (2020-2049 and 2070-2099) mean annual precipitation, temperature, Potential evapotranspiration (PET), Actual Evapotranspiration (AET) and discharges (Qsim) climate model product RCP4.5

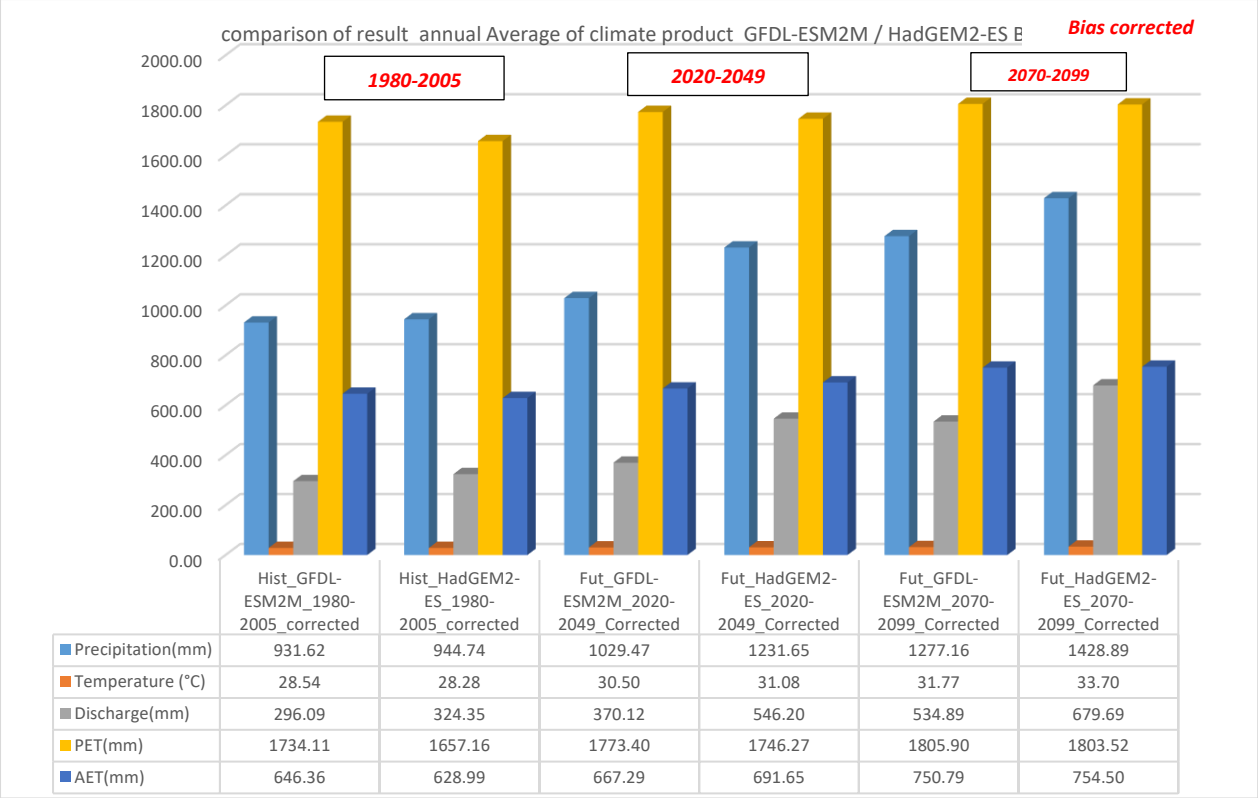

	Hist_GFDL-ESM2M_1980-2005_corrected	Hist_HadGEM2-ES_1980-2005_corrected	Fut_GFDL-ESM2M_2020-2049_Corrected	Fut_HadGEM2-ES_2020-2049_Corrected	Fut_GFDL-ESM2M_2070-2099_Corrected	Fut_HadGEM2-ES_2070-2099_Corrected
Precipitation(mm)	931.62	944.74	1029.47	1231.65	1277.16	1428.89
Temperature (°C)	28.54	28.28	30.50	31.08	31.77	33.70
Discharge(mm)	296.09	324.35	370.12	546.20	534.89	679.69
PET(mm)	1734.11	1657.16	1773.40	1746.27	1805.90	1803.52
AET(mm)	646.36	628.99	667.29	691.65	750.79	754.50

Fig 5.10 diagram comparing Historical (1980-2005) and projected (2020-2049 and 2070-2099) of annual Average of precipitation, temperature, Potential evapotranspiration (PET), Actual Evapotranspiration (AET) and discharges (Qsim) of two emission scenarios

5.4. Discussion

a) Data evaluation and correction

Bias correction using the quantile mapping clearly proved to improve the biases of raw RCMs For this reason the current study used and presented results for both bias corrected and non-bias corrected simulated climate datasets keeping in mind that bias correction can potentially affect climate change signal as reported by several studies. Despite being effective in general, the applied method showed limited results for precipitation and relative humidity for the HadGEM2-ES dataset.

b) Scenario Application in hydrological modelling, trend, Signal change and magnitude

The comparison between the historical period of 1980-2005, And the projection period (2020-2049 and 2070-2099) show a clear increase signal of the different variables that are temperature, Precipitation, Potential evapotranspiration and Actual evapotranspiration for both climates simulation product GFDL-ESM2M and HadGEM2-ES under RCP4.5.

These results are common the several studies carried out in the region. found that an increase in the frequency of heavy precipitation events is likely to occur for the West African region, while Patricola and Cook (2009, highlighted an increase in precipitation in general, but also noted drier

June and July months. this come to confirm the increasing precipitation in the projected period presented in the current study.

With regard to temperature, it is noticed a temperature increase signal for both climate models for the projections period (2020-2049 and 2070-2099) compared to the historical period. Yira et al. (2017) have reported the same results for studies conducted in the area with different climate models. According to the Fourth Assessment Report (AR4) of the Intergovernmental Panel on Climate Change (IPCC 2007), Africa is very likely to become much warmer than the rest of the Earth, with an increase in average surface temperature of about 3–4◦C by the end of the 21st century (Kankam-Yeboah et al. 2013) these results are consistent with the ones obtained in the current study. This increase in temperature will lead to an increase in PET. The IPCC reports that different climate models yield different trends and patterns of the West African climate however, an increased evapotranspiration is expected with a high level of confidence (IPCC, 2001)

The discharges got from hydrological modelling for the projected periods are in trend up for all climate simulation products, this trend agree with the study made by Aich et al. (2014) in the Niger basin finding an increase of 50% of the discharges at the end of the century(Aich et al. 2014). This is the consequence of precipitation increase combined to a less important increase in PET.

(Setegn et al. 2011) also investigated how changes in temperature and precipitation might translate into changes in streamflow and other hydrological components and found the direction of streamflow change generally followed the direction of changes in rainfall. According to (Tsolakis and Janson 2008) runoff in the Volta Basin is closely associated with the pattern of local precipitation, and changes in runoff frequency can reflect changes in climate

5.5. Conclusion

To determine the climate change and variability and it impact on hydrology there are different parameters that need to be analysed, among them are precipitation, temperature, relative humidity, wind speed and discharges. In order to assess the impact of climate change on streamflow, two climate simulation datasets over two projected periods compared to a historic one. The biases correction by the quantile mapping of the input data helped increasing the reliability of the results.

The results indicated an increasing trend for temperature, precipitation and other derivatives like potential evapotranspiration for both climate datasets (GFDL-ESM2M and HadGEM2-ES). Temperature is clearly expected to increase (by 2 to 3 °C for 2020-2049 and by4 to 5 °C at the end of the century) compared to historical period. For precipitation, the projections for this study indicate an increases reaching 10 to 30 % in the middle of the century and between 37 to 51.4% towards 2100.

Chapter 6: Climate change impact on Water Related Ecosystem Services (WRES)

6.1. Introduction

The concept of ecosystem services (ESs), understood as the contribution of the benefits derived passively or actively from ecosystems towards current and future human well-being (Fisher et al., 2009), has gained increasing recognition in the last decade. The availability of water, in terms of both its quantity and quality, is influenced heavily by ecosystem functioning(Coates et al. 2013). Knowing the importance of water in nowadays it is important to see how climate change can affect the services rely to water. This chapter aims to see how the application of climate simulation products (HadGEM2-ES and GFDL-ESM2M) under RCP 4.5 can help to see the future change on the provision of water related ecosystem services of water supply, hydropower and agriculture.

6.2. Methodologies

-Data requirements

In this study the data needed are (i) discharges obtaining from results of hydrological modelling using HBV Light(ii) information on per capita water demand, and (iii) total population and population growth rate. The simulated discharges from the application of simulated climate (HadGEM2-ES and GFDL-ESM2M) under RCP4.5 over the historical and future periods are used (refer to previous chapter for details)

-Indicators for Water Related Ecosytem services (WRES)

-Hydropower generation

Determining the hydropower potential requires to know the power that can derives from the streamflow. This power is determinized by streamflow, and others information like: hydropower plant efficiency, Head (m) density (Kg/m3). Eq 1 & 2 was applied for this purpose

$$Power(wh) = Qsim(m3/s) * Efficiency*Head\ (m) * density(\text{Kg/m3}) * g \quad \text{Eq.1}$$

$$Energie(Kw) = Power(wh) * time\ (h) \quad \text{Eq 2}$$

- Domestic water uses:

The second water use to be met is known as “primary water requirements”, which in the frame of the current study is restricted to domestic uses. In this study the domestic consumption has the highest priority, implying that all discharge is used for the domestic consumption until satisfied. Population density data was downloaded from world pop datasets: https://www.worldpop.org/geodata/summary?id=139 and extracted using borders of the Dano

catchment. The current population in the Dano catchment (for year 2015) was estimated using the mean density (inhabitant by square kilometer) * catchment area (in square-kilometer) (Eq. 3). As for the future population in the catchment, it was determined using the annual population growth rate to estimate the population by 2020-2049 and 2070-2099 (Eq. 4). The population growth rate was retrieved from https://data.worldbank.org/indicator/SP.POP.GROW?locations=BF and roughly equals 3%.

The formula used is

$$Population\ 2015 = \ Mean\ density\ * Area\ (km^2) \quad \text{Eq.3}$$

$$Population\ (future\ year) = \ Population\ (year\ 2015) * \ Population\ growth\ rate \quad \text{Eq.4}$$

Population per capita use (x l/day)

In rural areas, needs are estimated by unit consumption of 20 L / inhabitant / day, which is the highest level of the evolution of specific consumption planned by the DGRE (Direction Générale des Resources en Eau) between 2015 and 2030 (Mea 2016). This rate was applied.

-Ecological flow (95%)

The ecological flow or base flow is the water that must remain in the river system to preserve ecological functions. Q_{95}. was used in the frame of this study.

-Agricultural water availability

This is the amount of water remaining for agriculture after all uses and without interfering in ecological flow.

6.3. Results

Fig. 6.1, 6.2, 6.3 & 6.4shows comparison between Historical (1980-2005) and projected (2020-2049 & 2070-2099) monthly hydropower production, domestic water consumption, ecological flow, Crop water available, under emission scenarios RCP4.5 for the GFDL-ESM2M dataset.

Hydropower

The graph fig 6.1 shows an increase of the energy production capacity comparing the historical period to the projected period. For bias corrected data, the discharges start by April/May, with a production starting with 3.6 MegaWatt in April for projected period 1 (2020, 2049) and 0.89 MWatt in May for projected 2 (2070-2099). This capacity production increases until August where there is

the pics of energy production: 351.43 MWatt during (2020-2049) and 502.35 MWatt during (2070-2099), after August, the capacity of energy production decrease until zero in February to March and December to April respectively for futures periods (2020-2049) and (2070-2099). Annual increases of 25% (167.87 MWatt) and 80% (541.5 MWatt) are projected for the period (2020-2049) and (2070-2099) respectively. The uncorrected data have the same positive trend compared to bias corrected data but the magnitudes are different.

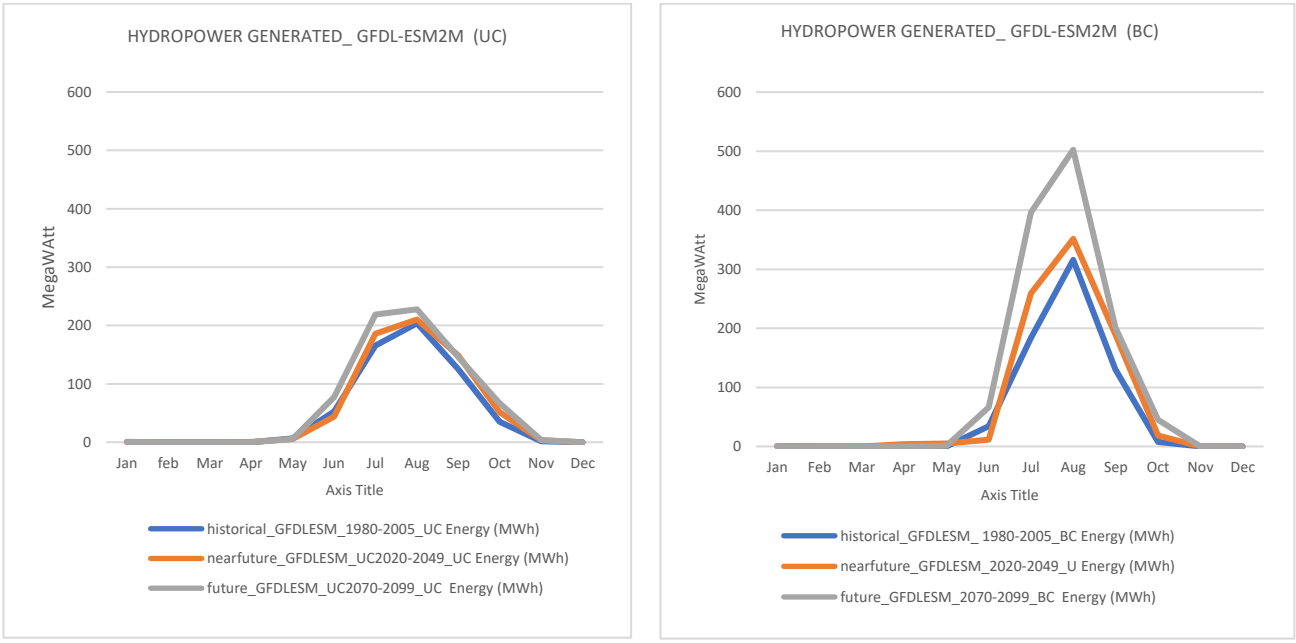

Fig 6.1 Projected hydropower generated use and demand for 2020-2049 and 2070-2099, under emission scenarios RCP4.5 (GFDL-ESM2M). UC refers to non-bias corrected, BC to bias corrected

Domestic Water use

When comparing the estimation of Additional domestic water demand and Additional domestic water used, one notices that it is only during certain months of the year where the discharges are high that all domestic consumptions are satisfied in the near future (Jun to October) and future (July to September). This implies that domestic water provision is worsening over time as from a full satisfaction over 5 months in 2020-2049 it decreases to five months in 2070-2099 despite an increase of discharge as already highlighted in the chapter. Non-bias corrected data shows an exacerbated situation as for the future (2070-2099) the additional domestic water demand is never satisfied. The pics of consumption are noticed in August in the future with 13047.35 m3 and 119540.47 m3 respectively toward the middle and the end century.

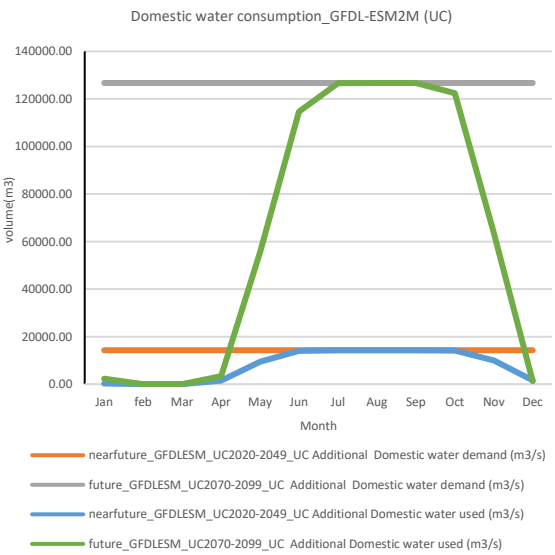

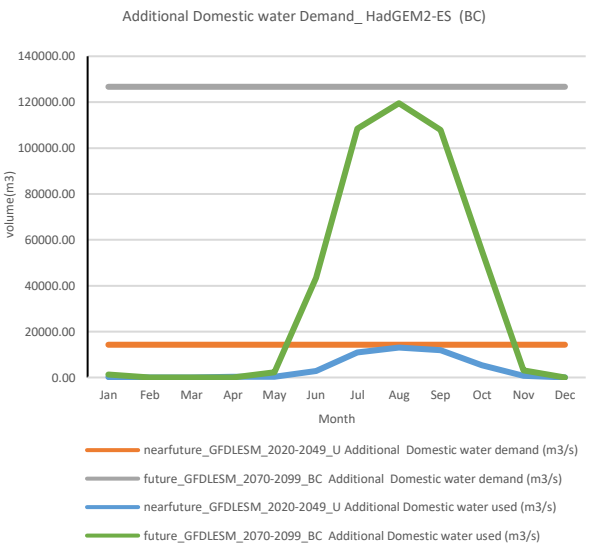

Fig 6.2: Projected additional domestic water use and demand for 2020-2049 and 2070-2099, under emission scenarios RCP4.5 (GFDL-ESM2M). UC refers to non-bias corrected, BC to bias corrected.

Ecological flow (95%)

Fig 6.3 shows a negative ecological flow provision trend over both future period considering uncorrected data. This projected is consistent with for the near future period using the bias corrected data, while the trend is opposite for the end of the century.

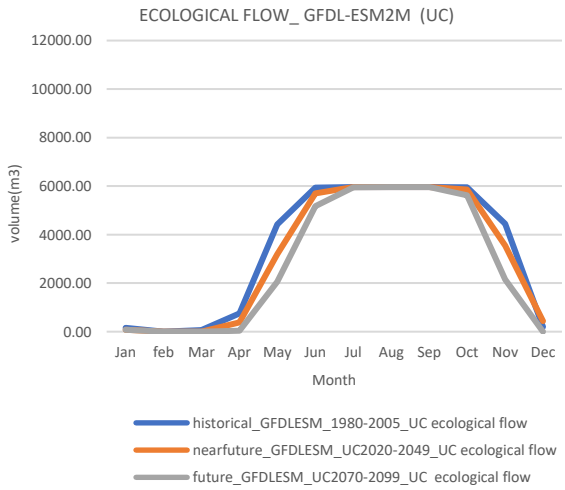

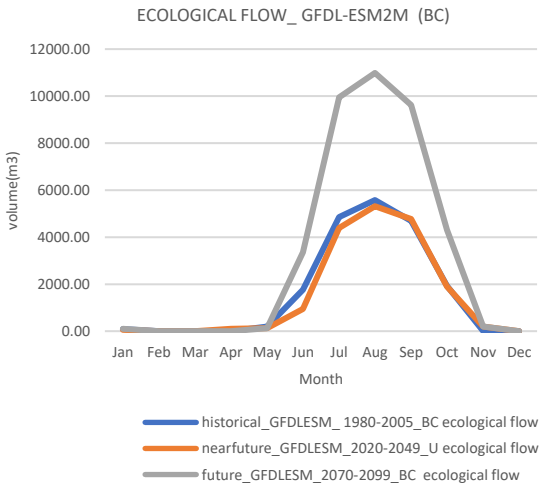

Fig 6.3: Monthly ecological flow for the historical and projected periods, under emission scenarios RCP4.5 (GFDL-ESM2M). UC refers to non-bias corrected, BC to bias corrected.

Agricultural water availability

Fig 6.4 shows a positive trend for available crop water in the future periods compared to the historic period. An annual increase of 25.6% (1189113.838 m^3) and 80.8 % (3753773.2 m^3) respectively

for projected period 2020-2049 and 2070-2099 compared to the historical period (1980-2005). The crop water will be available from May to November and the pics are recorded in August with 28792724.44 m3 in the near future (2020-2049) and 41053128.61 m3 towards the end of the century (2070-2099). The uncorrected data have the same trend up compared to bias corrected data but the magnitudes are different

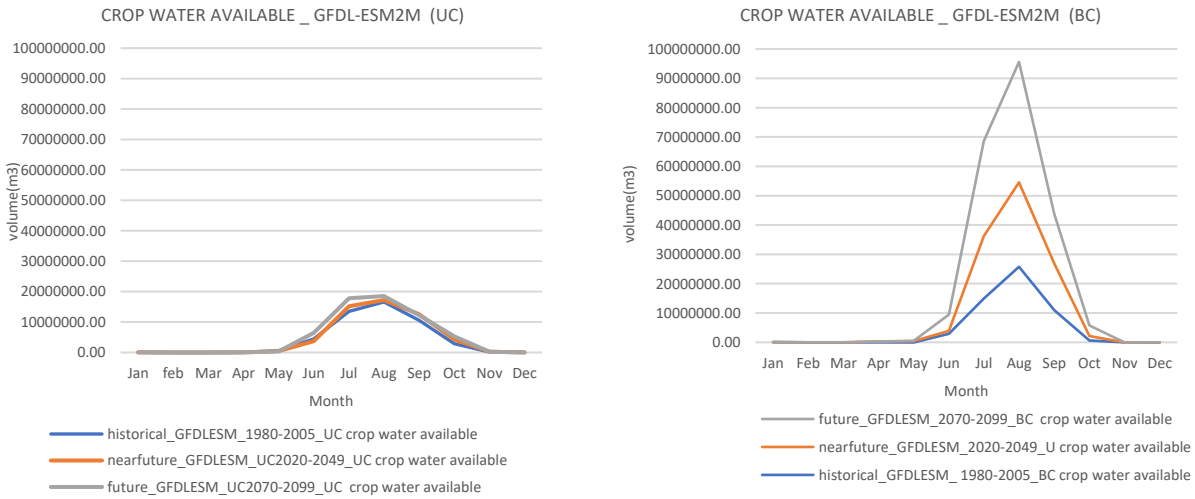

Fig 6.4: Monthly agricultural water availability for the historical and projected periods, under emission scenarios RCP4.5 (GFDL-ESM2M). UC refers to non-bias corrected, BC to bias corrected.

The Fig 6.5 show the evolution of annual hydropower production, domestic water consumption, ecological flow, Crop water available, under emission scenarios RCP4.5 (GFDL-ESM2M). bias corrected data of Historical (1980-2005) and projected (2020-2049 and 2070-2099). One notices that the trend is increasing for all of the ecosystems services comparing the historic period to the future period, only the ecological flow are showing a decrease in the projected period (2020-2049) but toward the end of the century the ecological flow increases.

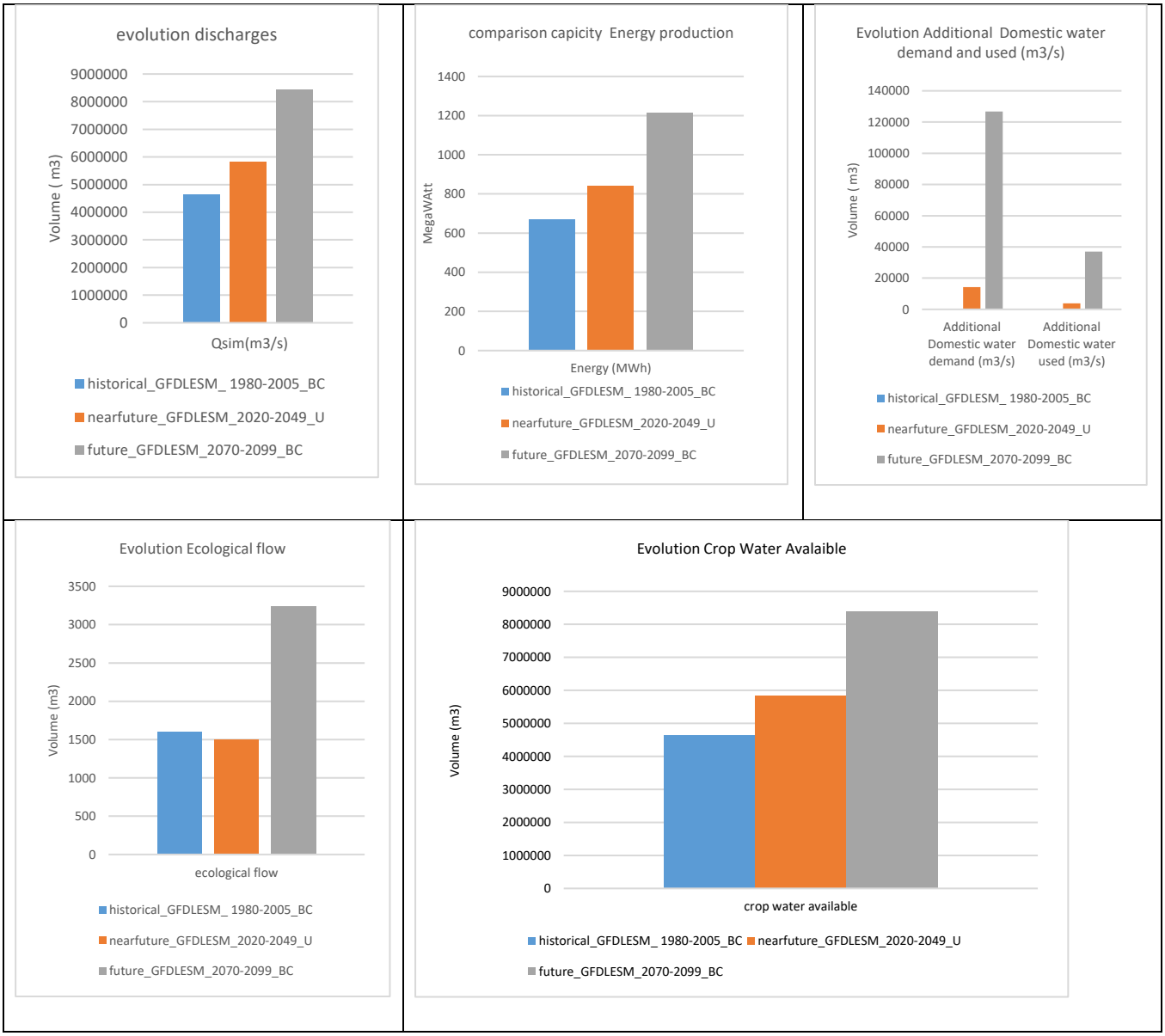

Fig 6.5: Graphs of evolution of Historical (1980-2005) and projected (2020-2049 and 2070-2099) annual hydropower production, domestic water consumption, ecological flow, Crop water available, under emission scenarios RCP4.5 (GFDL-ESM2M). bias corrected

The fig 6.6, 6.7,6.8 & 6.9 show the changement between Historical (1980-2005) and projected (2020-2049 / 2070-2099) of Average monthly hydropower production, domestic water consumption, ecological flow, Crop water available, under emission scenarios RCP4.5 (HadGEM2-ES).

In general, the results of the two climates simulation products RCP4.5 (HadGEM2-ES, GFDL-ESM2M) for the futures needs of water related ecosystems services, the graphs show the same trend only the magnitudes are different.

Hydropower

As for the first product the graphs of bias corrected data show an increase trend for energy production capacity comparing the historical period to the projected period. One notice that the production capacity increases until August where there is the peak of energy production: 495.3 MWatt during (2020-2049) and 648.1 MWatt during (2070-2099), these values are higher than the GFDL-ESM2M dataset. After August, the potential of energy production decrease until zero from November to May for futures periods (2020-2049)/ (2070-2099). It is observed a global annual increase of 63%, (480.72 MWatt) and 104.8 % (797.4 MWatt) respectively for projected period (2020-2049) and (2070-2099) compared to the historical period (1980-2005).

The uncorrected data have the same trend up compared to bias corrected data but the magnitudes are different and bias correction permitted to correct the underestimation of the hydropower capacity.

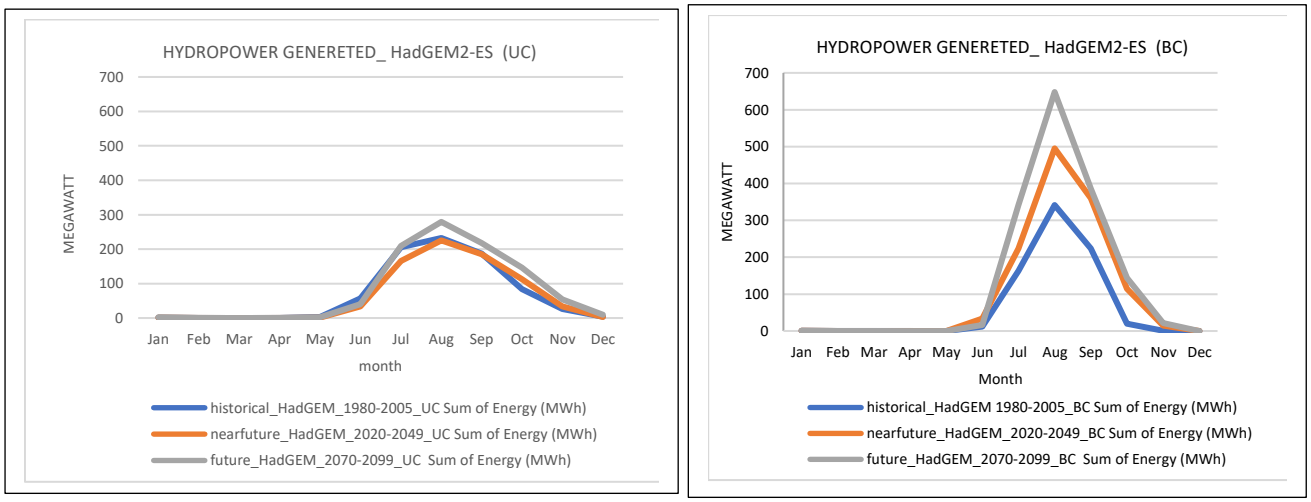

Fig 6.6: Projected hydropower generated use and demand for 2020-2049 and 2070-2099, under emission scenarios RCP4.5 (HadGEM2-ES). UC refers to uncorrected, BC to bias corrected.

Water domestic consumption

Fig 6.7 shows a positive trend in the future period compared to the historic period. As for the first product only, the magnitudes are different When comparing the estimation of Additional domestic water demand and Additional domestic water used, It can be seen that during some months of the year where the discharges are available (May to November) all domestic consumption are satisfied, the graph of Additional domestic water used are under Additional domestic water demand. The pics of consumption are noticed in August in the future with 13056.25 m^3 and 120305.48 m^3 respectively toward the middle and the end century almost the same with the first product

The uncorrected data have the same trend up compared to bias corrected data but the magnitudes are different and bias correction permitted to correct the underestimation of the hydropower capacity.

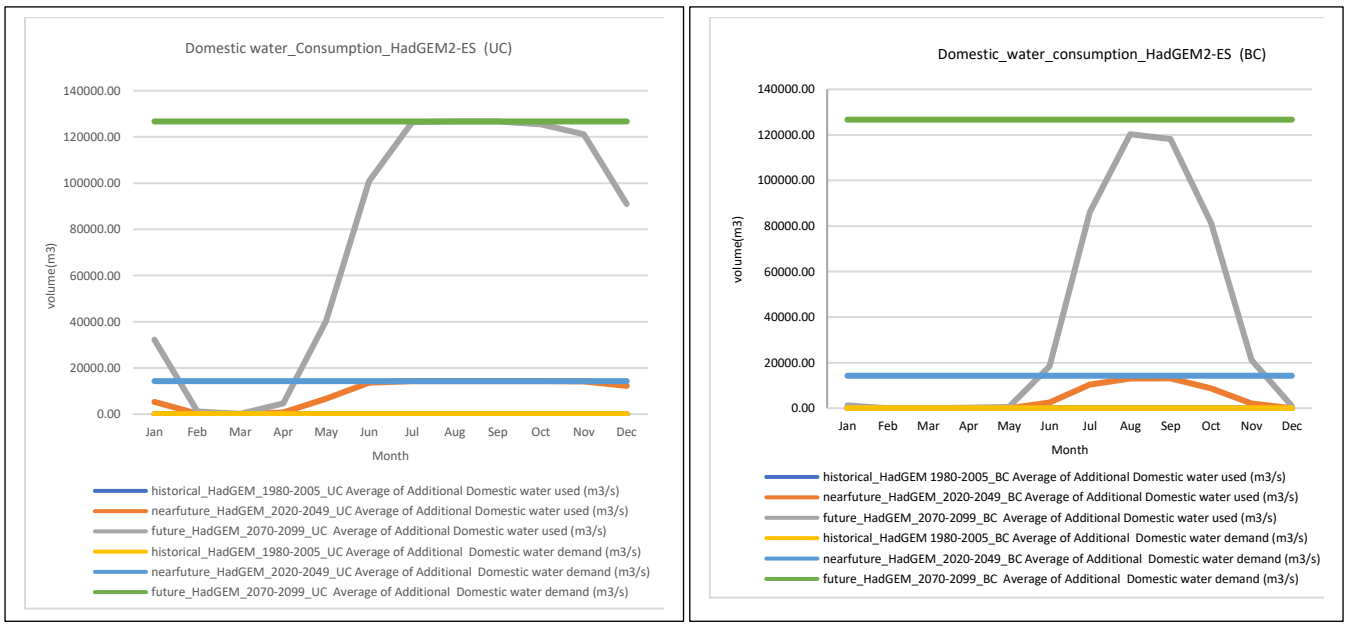

Fig 6.7: Projected additional domestic water use and demand for 2020-2049 and 2070-2099, under emission scenarios RCP4.5 (HadGEM2-ES). UC refers to non-bias corrected, BC to bias corrected.

Ecological flow (95%)

Fig 6.8 shows that there is a trend up in the future period compared to the historic period under emission scenarios RCP4.5 (GFDL-ESM2M). The 5 % of ecological flow correspond to an increase of 47.27m^3 (2.9%) and 1747.77 m3 (107.5%) of flow respectively for the projected period (2020-2049) and (2070-2099).

The uncorrected data have the same trend up compared to bias corrected data but the magnitudes are different and bias correction permitted to correct the underestimation of the ecological flow.

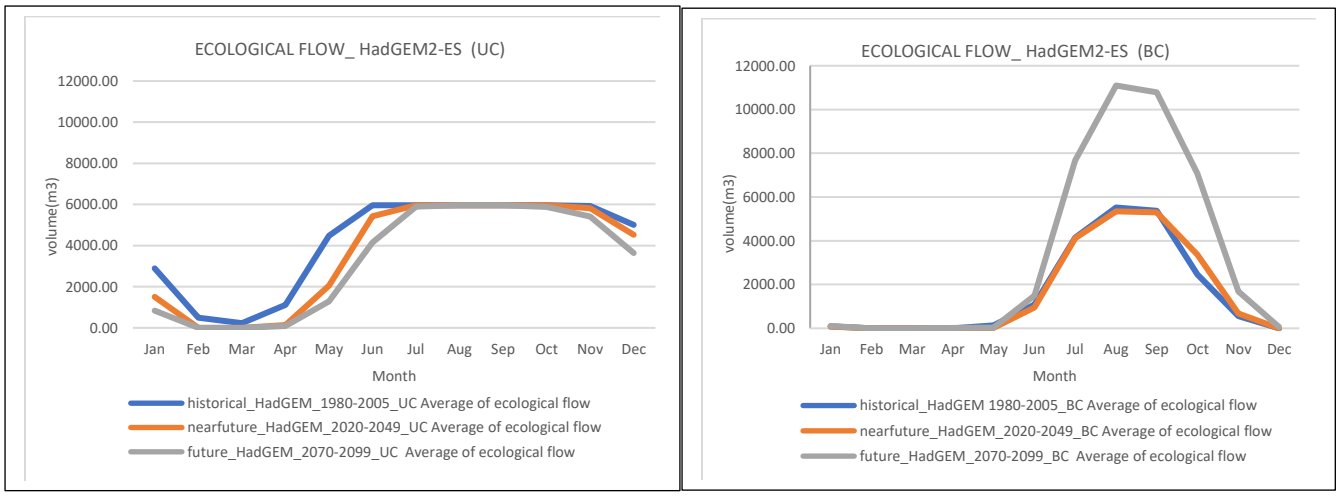

Fig 6.8: Monthly ecological flow for the historical and projected periods, under emission scenarios RCP4.5 (HadGEM2-ES). UC refers to non-bias corrected, BC to bias corrected.

Agricultural water availability

Fig 6.9 shows a positive trend in the future periods compared to the historic one. Annual increases of 64 % (3368613.492 m^3) and 105 % (5536912.584 m^3) respectively for projected periods 2020-2049 and 2070-2099 compared to the historical one (1980-2005). The crop water will be available from May to January and the peaks are recorded in August with 40541332.91 m^3 in the near future (2020-2049) and 52942448.41 m^3 towards the end of the century (2070-2099). Those values are higher with this product than the first. The uncorrected data have the same trend up compared to bias corrected data but the magnitudes are different and bias correction permitted to correct the overestimation and of the crop water availability.

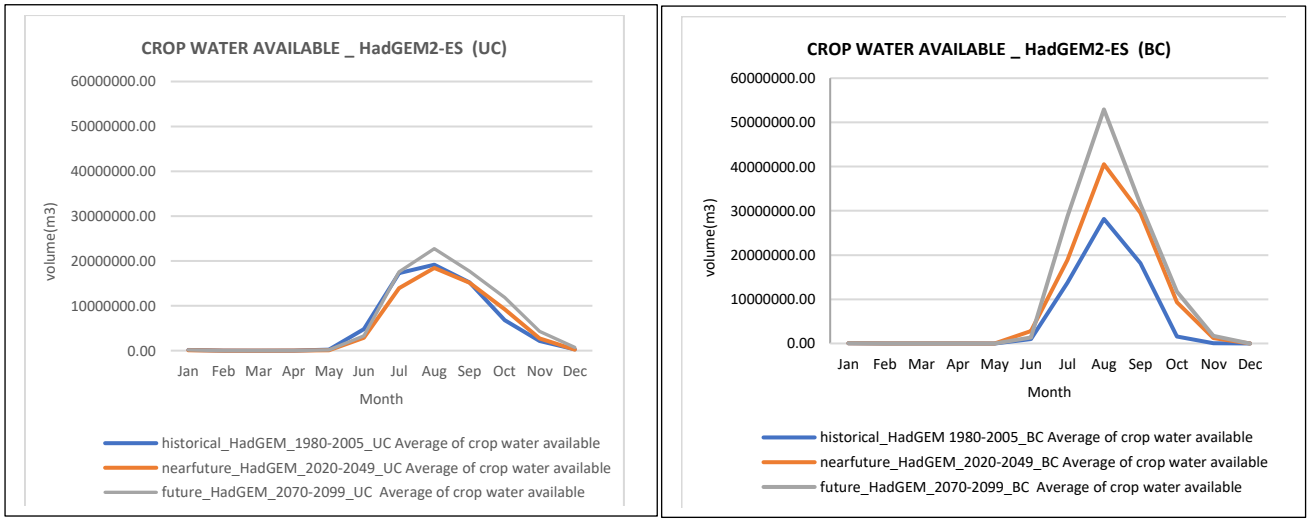

Fig 6.9: Monthly agricultural water availability for the historical and projected periods under emission scenarios RCP4.5 (HadGEM2-ES). UC refers to non-bias corrected, BC to bias corrected.

6.4. Discussion

Hydropower

With the two climates simulation product HadGEM2-ES and GFDL-ESM2M the results show an increase of hydropower production capacity. The impact of climate change is expected to be positive. This is mainly due to the increase in flowrate. A study made by et al., (2006) suggested that there are direct factors that rely to temperature or precipitation that could have an impact on hydropower production. A temperature degraded by 0.44 while precipitation increased by 0.77 yielded in their case an increase in hydropower potential. A similar process explains the achieve results of the current study. According to IPCC, indirect effects on water availability for energy purposes may occur if water demand for other uses such as irrigation and water supply for residential households and industry rises due to the climate change (IPCC, 2012). In our case the others demand (water supply, crop water demand) were assumed not affecting the production of hydropower as all the turbined water is release after use.

Domestic water demand and consumption

The future water consumption shows an increase of water demand, but the additional water needs will only be satisfied in certain periods of time in the year (May to December). This is linked to the runoff, so to the precipitation amount that is more important during these periods of the month. Domestic water supply will therefore get worst in the Dano catchment not due to climate change that increase the runoff but due to population and increase demand.

Ecological flow (95%)

The results show in general that for the months (from May to November) where there is runoff, the ecological flow (Q_{95}) is satisfied and this will in no way be negatively affected by climate change.

Agricultural water availability

Crop water availability need will increase in the future. This is essentially due to the projected increase in rainfall. (United et al. 2011) show that the agriculture is the largest user of water in Africa about 85% of the total available water. According to (Burke and Jean-Marc 2011) the factors affecting crop productivity are predominantly weather based: changes in mean weather (temperature and rainfall); changes in variability or distribution of weather, combinations of changes in the mean and changes in its variability. Increase of temperature and precipitation in the Dano catchment in the future are therefore expected to positively affected the crop production if the additional water is used for irrigation purposes.

6.5. Conclusion

Discharge generated from the application of two simulation climate datasets (GFDL-ESM2M and HadGEM2-ES) to the validated HBV model were used to assess the impact of climate change on water related ecosystem services. The results indicated positive trends for all the services (hydropower, crop water availability and the ecological flow) excepted additional domestic water use that is likely to worsen du to and increase demand (linked with population growth).These results show that climate change will have both positive and negatives impacts on WRES in the Dano catchment. The results also indicate that impact of climate change on water resources should be combined with other drivers affecting water demand (like population growth).

Chapter 7: Conclusion and recommendations

7.1. General conclusion

Dano is a small catchment of 196 Km² localised in west Africa. It is a subcatchment of the Volta basin one of the biggest basins in west Africa. The basin is reported to be vulnerable to climate change (Kumi M 2015). However, climate change related studies conducted in the basin have mainly addressed its impact on water resources, and not specifically on services like crop water supply, household water supply and hydropower.

This thesis was carried out to assess the impact of future climate change on water-related ecosystem services (WRES) in West Africa, particularly the Dano catchment. It intends to provide relevant information and prediction of future impact of climate change on WRES and would like to suggest solutions. From the initial specific objectives that were outlined in the general introduction, the following conclusion can be derived:

- How efficient is the HBV hydrological model in simulating the hydrology of the Dano catchment? The hydrological behaviour of the Dano catchment was modelled using the conceptual: HBV Light model developed by the Swedish Meteorological and Hydrological Institute (SMHI) at the daily time step. The criteria used to measure the performances of the model encompassed the Coefficient of determination, Model efficiency and the Kling-Gupta efficiency. The model was successfully validated for all these criteria. Acceptable to very good results during the calibration and validation were achieved and the model was deemed suitable for impact assessment

- What is projected climate change for the Dano catchment and w how will it affect the catchment hydrology? Several climate variables were used be analyse climate change, including precipitation, temperature, relative humidity, wind speed; while the change in discharge was used to analyze the hydrological impact on climate change. Two projected periods were compared to a historic one. Climate data were also bias corrected to increase confidence into the results. The results indicated a positive trend for all the variables and for the two climate datasets (GFDL-ESM2M and HadGEM2-ES). The temperature is expected to increase up to 2 to 3 °C by 2049 and 4 to 5 °C at the end of the century. Compared to historical period for precipitation is expected to increase by 10 to 30 % in the middle of the century and between 37 to 51.4% towards 2100. As a consequence, discharges will have a positive trend due to an amount of precipitation that is not counter balanced by the increase of PET.
- What is the expected impact of climate change on WRES what are the future WRES demand and challenges? The observed hydrological changes were translated into changes in WRES

provision (hydropower, domestic water consumption, crop water availability even the ecological flow). The projected discharge increase will result in an increase of all investigated WRES in the future except the satisfaction of additional domestic water use that will decrease due to population growth. The projected increase of discharge will not be enough to counter balance the increase in water demand associated to population growth.

7.2. Recommendations

The following recommendation can be formulated at the end of this study:

-As, the trend is showing a positive increase in the water resources, preventive measures need to be taken for the flood risk vulnerability in this area;

-There is a need to adopt technologies that reduce evaporation (because of trend up temperature);

- In order to explore the full range of the potential impacts of climate change WRES, studies with a larger number of regional models and greenhouse gas concentration scenarios should be conducted;

-The study revealed a large potential for the investigated WRES in the catchment, actions towards the harnessing this potential should be undertaken.

References

Achleitner, S., M. Rinderer, and R. Kirnbauer. 2009. “Hydrological Modeling in Alpine Catchments: Sensing the Critical Parameters towards an Efficient Model Calibration.” *Water Science and Technology* 60 (6): 1507–14. https://doi.org/10.2166/wst.2009.488.

Aich, V., S. Liersch, T. Vetter, S. Huang, J. Tecklenburg, P. Hoffmann, H. Koch, et al. 2014. “Comparing Impacts of Climate Change on Streamflow in Four Large African River Basins.” *Hydrology and Earth System Sciences* 18 (4): 1305–21. https://doi.org/10.5194/hess-18-1305-2014.

Akhtar, M, N Ahmad, and M J Booij. 2008. “The Impact of Climate Change on the Water Resources of Hindukush–Karakorum–Himalaya Region under Different Glacier Coverage Scenarios.” *Journal of Hydrology* 355 (1–4): 148–63. https://doi.org/10.1016/j.jhydrol.2008.03.015.

Almestad, Christian. 2015. “Modelling of Water Allocation and Availability in Devoll River Basin , Albania.” https://doi.org/10.1145/1321440.1321544.

Amengual, A., V. Homar, R. Romero, S. Alonso, and C. Ramis. 2012. “A Statistical Adjustment of Regional Climate Model Outputs to Local Scales: Application to Platja de Palma, Spain.” *Journal of Climate* 25 (3): 939–57. https://doi.org/10.1175/JCLI-D-10-05024.1.

Bhattarai, Santosh, Yihong Zhou, Narendra Man Shakya, and Chunju Zhao. 2018. “Hydrological Modelling and Climate Change Impact Assessment Using HBV Light Model : A Case Study of Narayani River Basin , Nepal.” *An International Quarterly Scientific Journal* 17: 691–702. http://iwra.org/member/congress/resource/ABSID119_ABSID119_Full_Paper_Abstract_ID_119_Feb_24.pdf.

Bodian, Ansoumana, Alain Dezetter, Lamine Diop, Abdoulaye Deme, Koffi Djaman, and Aliou Diop. 2018. “Future Climate Change Impacts on Streamflows of Two Main West Africa River Basins: Senegal and Gambia.” *Hydrology* 5 (1): 21. https://doi.org/10.3390/hydrology5010021.

Burke, Jacob, and Faurès Jean-Marc. 2011. “Climate Change, Water and Food Security,” no. c: 2–6.

Callo-concha, Daniel, Thomas Gaiser, and Frank Ewert. 2012. “Working Paper Series.” *Accounting & Finance* 20 (2): 146–146. https://doi.org/10.1111/j.1467-629X.1980.tb00220.x.

Chang, Heejun, and Matthew Ryan Bonnette. 2016. “Climate Change and Water-Related Ecosystem Services: Impacts of Drought in California, USA.” *Ecosystem Health and Sustainability* 2 (12): e01254. https://doi.org/10.1002/ehs2.1254.

Coates, David, Petina L Pert, Jennie Barron, Catherine Muthuri, Sophie Nguyen-Khoa, Eline Boelee, and Devra I Jarvis. 2013. “Water-Related Ecosystem Services and Food Security.” *Managing Water and Agroecosystems for Food Security*, 29–41. https://doi.org/10.1079/9781780640884.0029.

Devia, Gayathri K., B.P. Ganasri, and G.S. Dwarakish. 2015. “A Review on Hydrological Models.” *Aquatic*

Procedia 4 (July): 1001–7. https://doi.org/10.1016/j.aqpro.2015.02.126.

Driessen, T. L.A., R. T.W.L. Hurkmans, W. Terink, P. Hazenberg, P. J.J.F. Torfs, and R. Uijlenhoet. 2010. "The Hydrological Response of the Ourthe Catchment to Climate Change as Modelled by the HBV Model." *Hydrology and Earth System Sciences* 14 (4): 651–65. https://doi.org/10.5194/hess-14-651-2010.

European Small Hydropower Association. 2004. "Guide on How to Develop a Small Hydropower Plant." *European Small Hydropower Association*. http://citeseerx.ist.psu.edu/viewdoc/download?doi=10.1.1.172.1731&rep=rep1&type=pdf.

Fallis, A.G. 2013. "Model of Solar Tracker and Application." *Journal of Chemical Information and Modeling* 53 (9): 1689–99. https://doi.org/10.1017/CBO9781107415324.004.

Hagemann, Stefan, Jan O Haerter, and Claudio Piani. 2010. "Bias Correction of Climate Model Data – the Golden Solution for Impact Models or Cursed Black Magic ?" *Water and Global Change*.

Harlin, Joakim, and Göran Lindström. 1992. "Spillway Design Floods In Sweden : II . Applications and Sensitivity Analysis Applications and Sensitivity Analysis." *Hydrological Sciences Journal* 6667 (December). https://doi.org/10.1080/02626669209492616.

Harrison, G. P, H. W Whittington, and A. R Wallace. 2006. "Edinburgh Research Explorer Sensitivity of Hydropower Performance to Climate Change" 26 (1): 42–48.

Heinzeller, Dominikus, Diarra Dieng, Gerhard Smiatek, Christiana Olusegun, Cornelia Klein, Ilse Hamann, Seyni Salack, Jan Bliefernicht, and Harald Kunstmann. 2018. "The WASCAL High-Resolution Regional Climate Simulation Ensemble for West Africa: Concept, Dissemination and Assessment." *Earth System Science Data* 10 (2): 815–35. https://doi.org/10.5194/essd-10-815-2018.

Hundecha, Hirpa. 2005. *Regionalization of Parameters of a Conceptual \rRainfall-Runoff Model*. *Institut Für Wasserbau Der Universität Stuttgart*.

IPCC. 2007. *Climate Change 2007: Synthesis Report. Contribution of Working Groups I, II and II to the Fourth Assesment*. *Report of the Intergovernmental Panel on Climate Change*. https://doi.org/10.1256/004316502320517344.

IPCC, 2018. 2018. "No Titleหมู่บ้านหมอกควัน."

IWMI. 2007. *Comprehensive Assessment of Water Management in Agriculture. Water for Food, Water for Live*. *Water Management*. https://doi.org/10.1007/s10795-008-9044-8.

Johansson, Barbro, Johan Andreasson, and Johan Jansson. 2003. "Satellite Data on Snow Cover in the HBV Model. Method Development and Evaluation." *Hydrology* 90 (90): 32.

Kankam-Yeboah, Kwabena, Emmanuel Obuobie, Barnabas Amisigo, and Yaw Opoku-Ankomah. 2013.

"Impact of Climate Change on Streamflow in Selected River Basins in Ghana." *Hydrological Sciences Journal* 58 (4): 773–88. https://doi.org/10.1080/02626667.2013.782101.

KI, Francine Anthonia Lawagülou. 2009. "Etude D'Impact Environnemental De La Culture Du Jatropha Curcas Dans La Commune De Dano," 89.

Maraun, Douglas, Theodore G. Shepherd, Martin Widmann, Giuseppe Zappa, Daniel Walton, José M. Gutiérrez, Stefan Hagemann, et al. 2017. "Towards Process-Informed Bias Correction of Climate Change Simulations." *Nature Climate Change* 7 (11): 764–73. https://doi.org/10.1038/nclimate3418.

Mdemu, M. V., C. Rodgers, P. L G Vlek, and J. J. Borgadi. 2009. "Water Productivity (WP) in Reservoir Irrigated Schemes in the Upper East Region (UER) of Ghana." *Physics and Chemistry of the Earth* 34 (4–5): 324–28. https://doi.org/10.1016/j.pce.2008.08.006.

Mea, L Assainissement. 2016. "Programme National d ' Approvisionnement En Eau Potable 2016-2030 Table Des Matières."

Milano, Marianne, Denis Ruelland, Alain Dezetter, Julie Fabre, Sandra Ardoin-Bardin, and Eric Servat. 2013. "Modeling the Current and Future Capacity of Water Resources to Meet Water Demands in the Ebro Basin." *Journal of Hydrology* 500: 114–26. https://doi.org/10.1016/j.jhydrol.2013.07.010.

Mul, Marloes, Emmanuel Obuobie, Richard Appoh, Kwabena Kankam-Yeboah, Emmanuel Bekoe-Obeng, Barnabas Amisigo, Frederick Yaw Logah, Benjamin Ghansah, and Matthew McCartney. 2015. "Water Resources Assessment of the Volta River Basin." *IWMI Working Papers*. Vol. 166. https://doi.org/10.5337/2015.220.

N'Tcha M'Po, Yèkambèssoun. 2016. "Comparison of Daily Precipitation Bias Correction Methods Based on Four Regional Climate Model Outputs in Ouémé Basin, Benin." *Hydrology* 4 (6): 58. https://doi.org/10.11648/j.hyd.20160406.11.

OUICI, Fatima Zohra. 2018. "Etude de La Performance Du Modèle Hydrologique HBV Appliqué Au Bassin Versant d'oued Sebdou (Tafna, Algérie)." Université Aboubakr Belkaïd– Tlemcen.

Pachauri, Rajendra k, and Meyer Leo. 2014. "Climate Change 2014: Synthesis Report; Chapter Observed Changes and Their Causes." https://doi.org/10.1046/j.1365-2559.2002.1340a.x.

Patil, Sachin Ramesh. 2008. *Regionalization of an Event Based Nash Cascade Model for Flood Predictions in Ungauged Basins*. Vol. 3.

Qian, Wei Hong, Bo Lu, and Cong Wen Zhu. 2010. "How Would Global-Mean Temperature Change in the 21st Century?" *Chinese Science Bulletin* 55 (19): 1963–67. https://doi.org/10.1007/s11434-010-3258-5.

Ramirez-Villegas, Julian, Andrew J. Challinor, Philip K. Thornton, and Andy Jarvis. 2013. "Implications of Regional Improvement in Global Climate Models for Agricultural Impact Research." *Environmental*

Research Letters 8 (2). https://doi.org/10.1088/1748-9326/8/2/024018.

Seibert, J., and M. J.P. Vis. 2012. "Teaching Hydrological Modeling with a User-Friendly Catchment-Runoff-Model Software Package." *Hydrology and Earth System Sciences* 16 (9): 3315–25. https://doi.org/10.5194/hess-16-3315-2012.

Seibert, J. 1998. "HBV Light." *User's Manual, Department of Earth Science, Hydrology, Uppsala University*, no. November.

Setegn, Shimelis G., David Rayner, Assefa M. Melesse, Bijan Dargahi, and Raghavan Srinivasan. 2011. "Impact of Climate Change on the Hydroclimatology of Lake Tana Basin, Ethiopia." *Water Resources Research* 47 (4): 1–13. https://doi.org/10.1029/2010WR009248.

Sten, Bergström. 1976. *Development and Application of a Conceptual Runoff Model for Scandinavian Catchments by Sten Bergström*.

Su, Buda, Xiaofan Zeng, Jianqing Zhai, Yanjun Wang, and Xiucang Li. 2015. "Projected Precipitation and Streamflow under SRES and RCP Emission Scenarios in the Songhuajiang River Basin, China." *Quaternary International* 380–381: 95–105. https://doi.org/10.1016/j.quaint.2014.03.049.

"System of Accounting 2012 Experimental." 2012.

Taylor, Karl E., Ronald J. Stouffer, and Gerald A. Meehl. 2012. "An Overview of CMIP5 and the Experiment Design." *Bulletin of the American Meteorological Society* 93 (4): 485–98. https://doi.org/10.1175/BAMS-D-11-00094.1.

Taylor, Publisher, Rebekka Neumann, Gerlinde Jung, Patrick Laux, Harald Kunstmann, Rebekka Neumann, Gerlinde Jung, Patrick Laux, Harald Kunstmann, and Forschungszentrum Karlsruhe. 2010. "International Journal of River Basin Management Climate Trends of Temperature , Precipitation and River Discharge in the Volta Basin of West Africa Climate Trends of Temperature , Precipitation and River Discharge in the Volta Basin of West Africa," no. April 2013: 37–41.

Tazen, Fowe. 2015. "Simulation et Optimisation Du Fonctionnement Du Barrage de Boura En Zone Soudanienne Du Burkina Faso."

Tigkas, D, H Vangelis, and G Tsakiris. 2013. "The Drought Indices Calculator (DrinC)." *Proceedings of the 8th International Conference of …*, no. JUNE. http://scholar.google.com/scholar?hl=en&btnG=Search&q=intitle:The+Drought+Indices+Calculator+(+DrinC+)#0.

Tigkas, Dimitris. 2013. "D r i n C G e t t i n g S t a r t e d G u i d E."

Tsolakis, Apostolos V., and Eva T. Janson. 2008. "Endocrine Pancreatic Tumors: Diagnosis and Treatment." *Expert Review of Endocrinology and Metabolism* 3 (2): 187–205. https://doi.org/10.1586/17446651.3.2.187.

United, Nations, Economic, Commission, For, Africa, African, Climate, and Policy. 2011. “Climate Change and Water Resources of Africa: Challenges, Opportunities and Impacts. Working Paper 5.” *Working Paper 5*, no. 5: 26.

United Nations Environment Programme, Water Research Commission. 2014. “Assessment of Transboundary Freshwater Vulnerability in Africa to Climate Change.” http://wedocs.unep.org/handle/20.500.11822/7835.

Viney, Neil R, Helge Bormann, Lutz Breuer, Axel Bronstert, B F W Croke, H Frede, T Gräff, et al. 2009. “Assessing the Impact of Land Use Change on Hydrology by Ensemble Modelling (LUCHEM) II: Ensemble Combinations and Predictions.” *Advances in Water Resources* 32 (2): 147–58. https://doi.org/10.1016/j.advwatres.2008.05.006.

Vuuren, Detlef P. van, Jae Edmonds, Mikiko Kainuma, Keywan Riahi, Allison Thomson, Kathy Hibbard, George C. Hurtt, et al. 2011. “The Representative Concentration Pathways: An Overview.” *Climatic Change* 109 (1): 5–31. https://doi.org/10.1007/s10584-011-0148-z.

Wheater, Howard, Soroosh Sorooshian, and K.D Sharma. 2007. *Hydrological Modelling in Arid and Semi-Arid Areas*. Vol. 91.

Wilcke, Renate Anna Irma, Thomas Mendlik, and Andreas Gobiet. 2013. “Multi-Variable Error Correction of Regional Climate Models.” *Climatic Change* 120 (4): 871–87. https://doi.org/10.1007/s10584-013-0845-x.

Appendix

Appendix 1:

GFDL-ESM2M

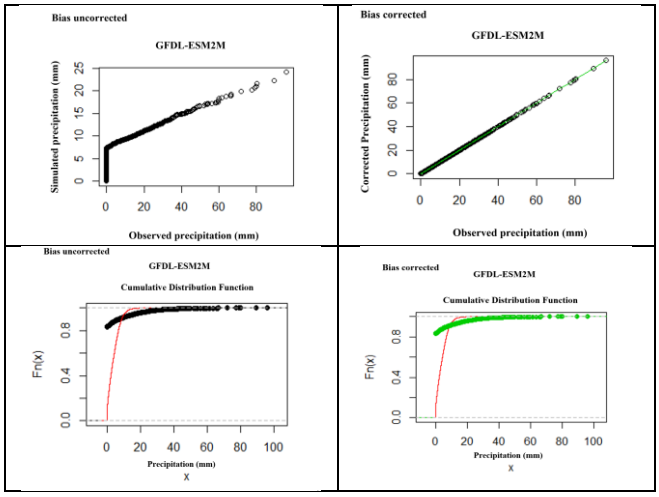

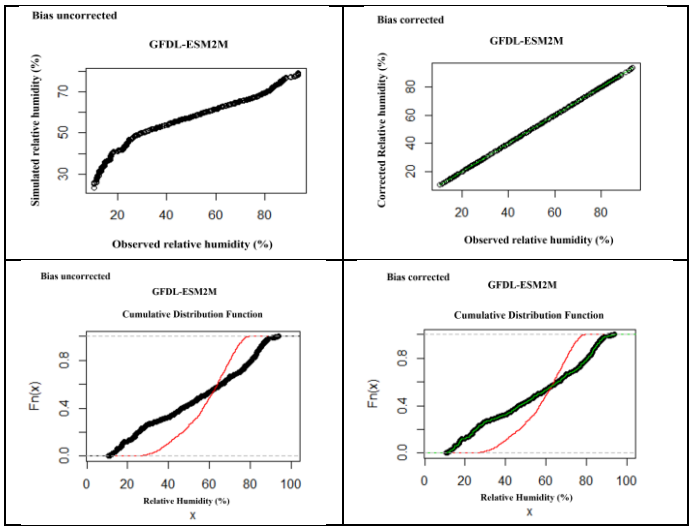

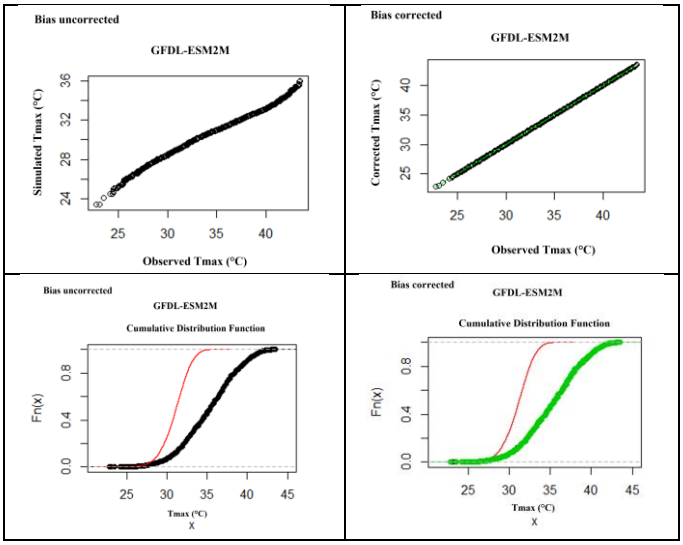
Bias uncorrected
GFDL-ESM2M
Simulated Tmax (°C)
Observed Tmax (°C)
Bias corrected
GFDL-ESM2M
Corrected Tmax (°C)
Observed Tmax (°C)
Bias uncorrected
GFDL-ESM2M
Cumulative Distribution Function
Fn(x)
Tmax (°C)
x
Bias corrected
GFDL-ESM2M
Cumulative Distribution Function
Fn(x)
Tmax (°C)
x

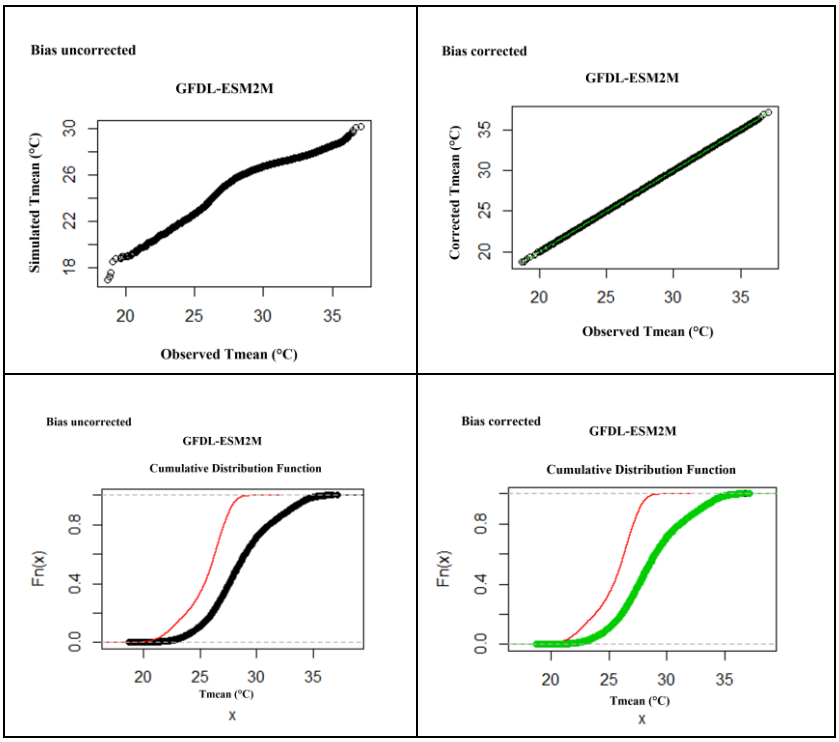
Bias uncorrected
GFDL-ESM2M
Simulated Tmean (°C)
Observed Tmean (°C)
Bias corrected
GFDL-ESM2M
Corrected Tmean (°C)
Observed Tmean (°C)
Bias uncorrected
GFDL-ESM2M
Cumulative Distribution Function
Fn(x)
Tmean (°C)
x
Bias corrected
GFDL-ESM2M
Cumulative Distribution Function
Fn(x)
Tmean (°C)
x

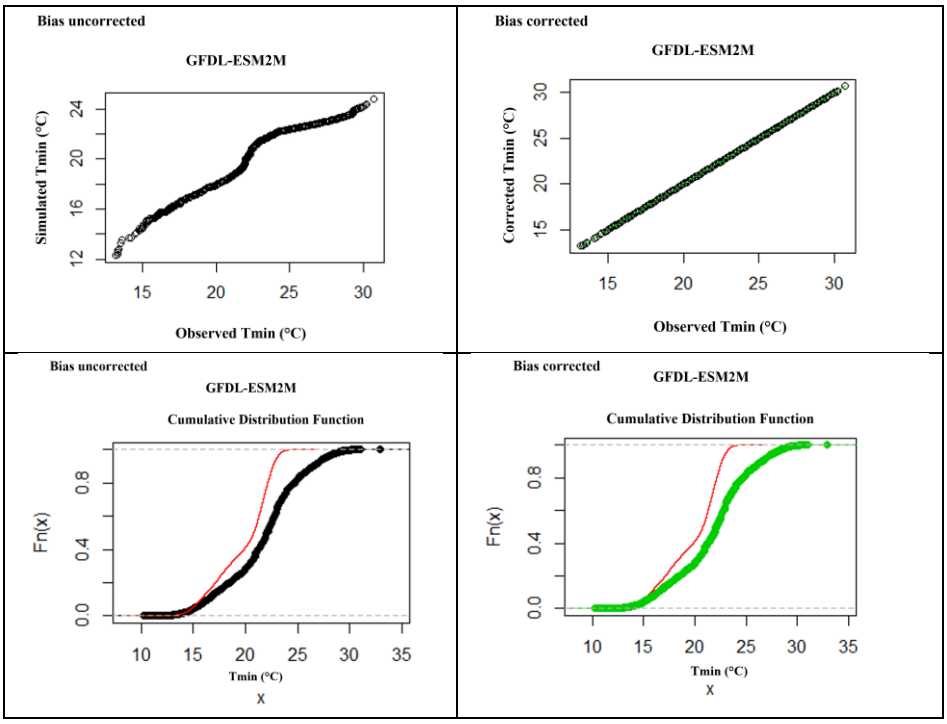
Bias uncorrected
GFDL-ESM2M
Simulated Tmin (°C)
Observed Tmin (°C)
Bias corrected
GFDL-ESM2M
Corrected Tmin (°C)
Observed Tmin (°C)
Bias uncorrected
GFDL-ESM2M
Cumulative Distribution Function
Fn(x)
Tmin (°C)
x
Bias corrected
GFDL-ESM2M
Cumulative Distribution Function
Fn(x)
Tmin (°C)
x

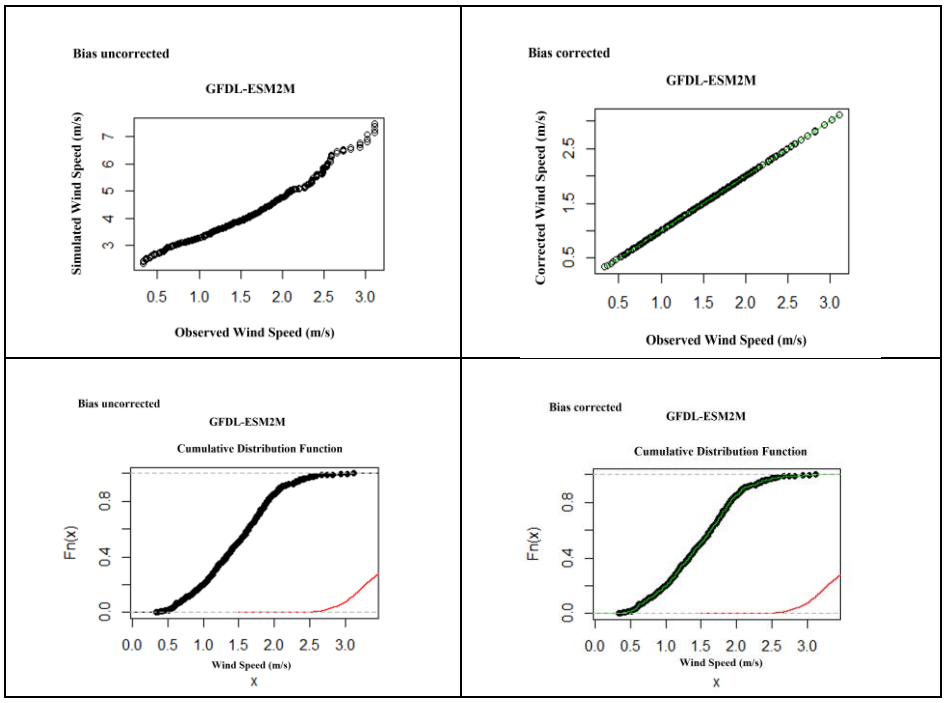
Bias uncorrected
GFDL-ESM2M
Simulated Wind Speed (m/s)
Observed Wind Speed (m/s)
Bias corrected
GFDL-ESM2M
Corrected Wind Speed (m/s)
Observed Wind Speed (m/s)
Bias uncorrected
GFDL-ESM2M
Cumulative Distribution Function
Fn(x)
Wind Speed (m/s)
x
Bias corrected
GFDL-ESM2M
Cumulative Distribution Function
Fn(x)
Wind Speed (m/s)
x

HadGEM2-ES

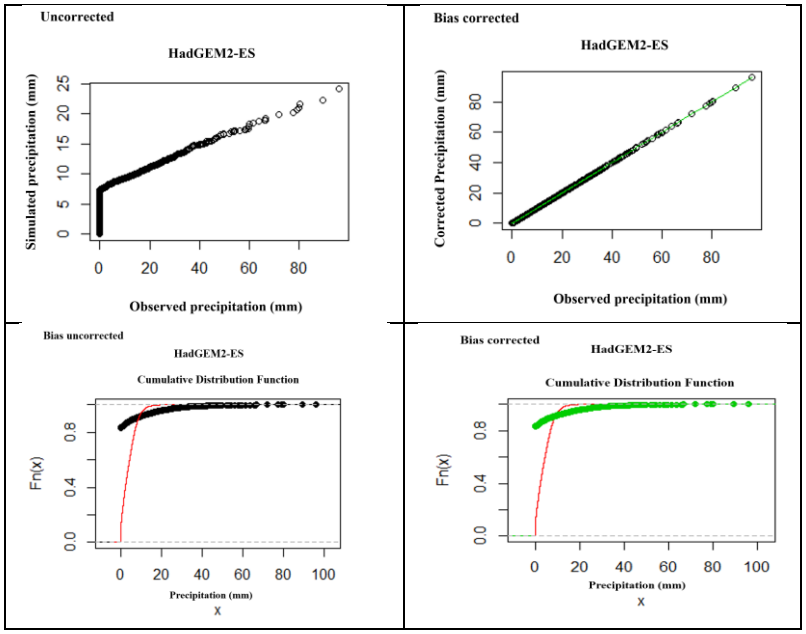
Uncorrected
HadGEM2-ES
Simulated precipitation (mm)
Observed precipitation (mm)
Bias corrected
HadGEM2-ES
Corrected Precipitation (mm)
Observed precipitation (mm)
Bias uncorrected
HadGEM2-ES
Cumulative Distribution Function
Fn(x)
Precipitation (mm)
x
Bias corrected
HadGEM2-ES
Cumulative Distribution Function
Fn(x)
Precipitation (mm)
x

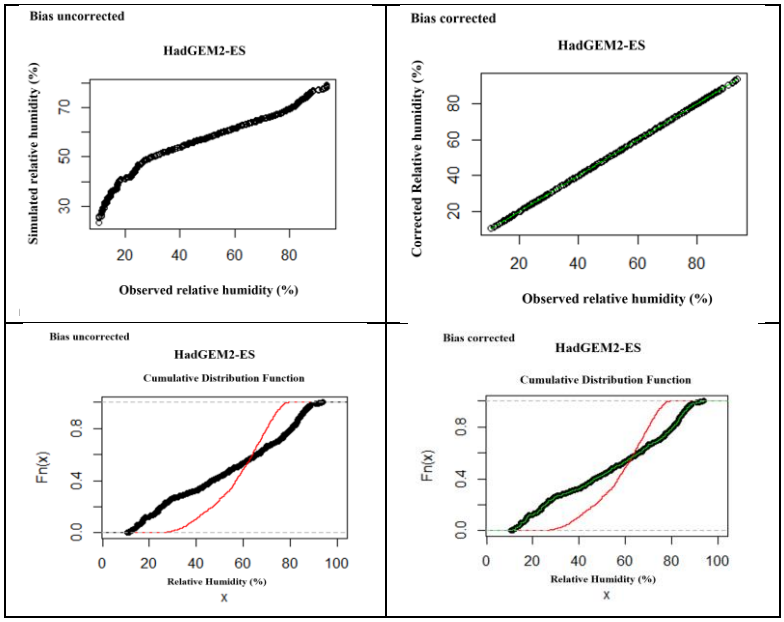
Bias uncorrected
HadGEM2-ES
Simulated relative humidity (%)
Observed relative humidity (%)
Bias corrected
HadGEM2-ES
Corrected Relative humidity (%)
Observed relative humidity (%)
Bias uncorrected
HadGEM2-ES
Cumulative Distribution Function
Fn(x)
Relative Humidity (%)
x
Bias corrected
HadGEM2-ES
Cumulative Distribution Function
Fn(x)
Relative Humidity (%)
x

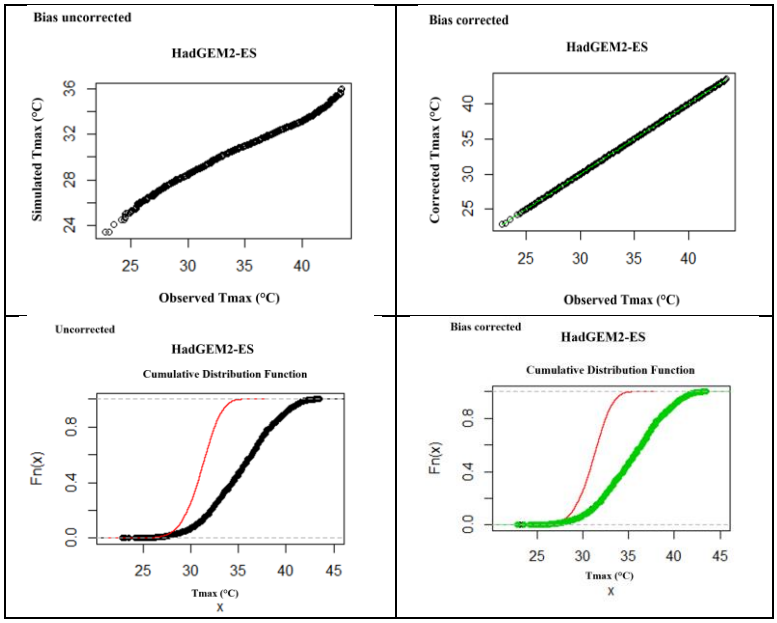
Bias uncorrected
HadGEM2-ES
Simulated Tmax (°C)
Observed Tmax (°C)
Bias corrected
HadGEM2-ES
Corrected Tmax (°C)
Observed Tmax (°C)
Uncorrected
HadGEM2-ES
Cumulative Distribution Function
Fn(x)
Tmax (°C)
x
Bias corrected
HadGEM2-ES
Cumulative Distribution Function
Fn(x)
Tmax (°C)
x

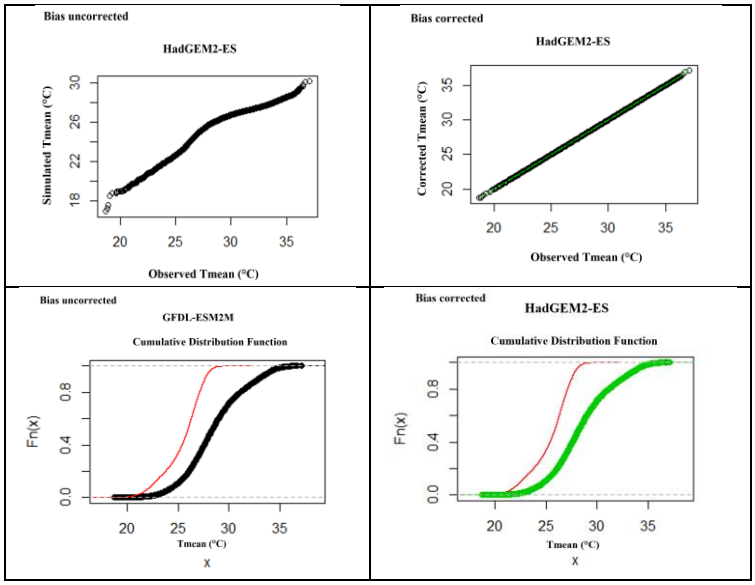
Bias uncorrected
HadGEM2-ES
Simulated Tmean (°C)
Observed Tmean (°C)
Bias corrected
HadGEM2-ES
Corrected Tmean (°C)
Observed Tmean (°C)
Bias uncorrected
GFDL-ESM2M
Cumulative Distribution Function
Fn(x)
Tmean (°C)
x
Bias corrected
HadGEM2-ES
Cumulative Distribution Function
Fn(x)
Tmean (°C)
x

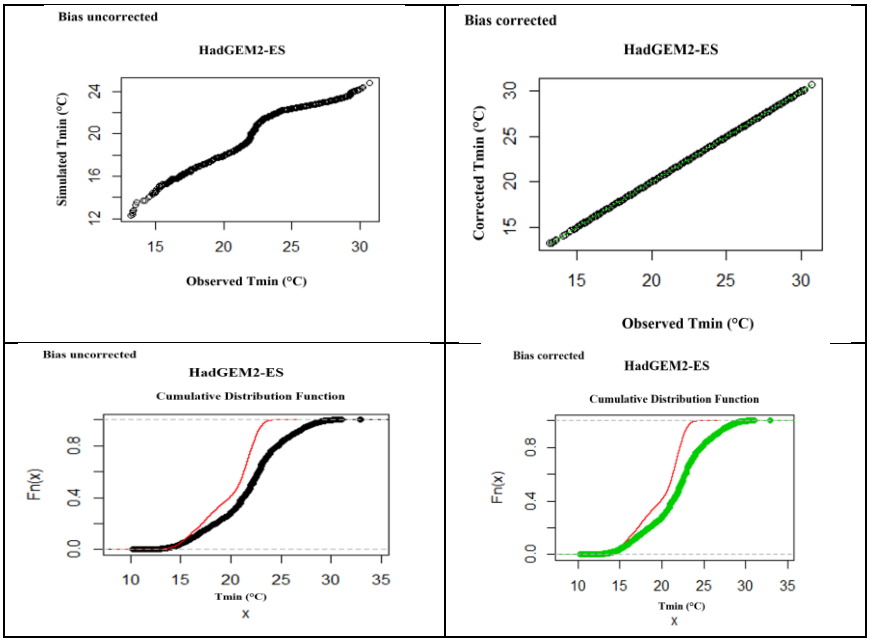
Bias uncorrected
HadGEM2-ES
Simulated Tmin (°C)
Observed Tmin (°C)
Bias corrected
HadGEM2-ES
Corrected Tmin (°C)
Observed Tmin (°C)
Bias uncorrected
HadGEM2-ES
Cumulative Distribution Function
Fn(x)
Tmin (°C)
x
Bias corrected
HadGEM2-ES
Cumulative Distribution Function
Fn(x)
Tmin (°C)
x

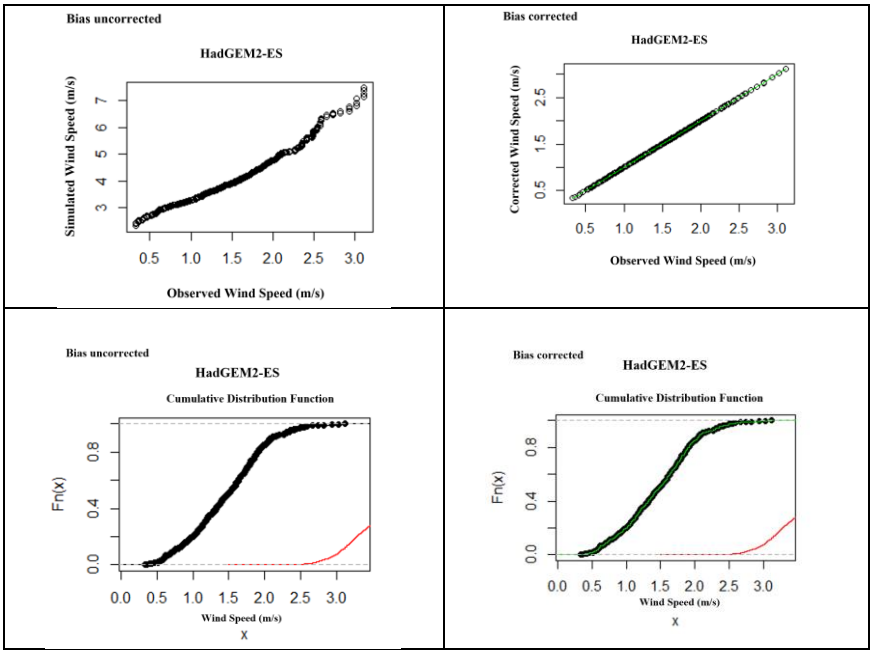
Bias uncorrected
HadGEM2-ES
Simulated Wind Speed (m/s)
Observed Wind Speed (m/s)
Bias corrected
HadGEM2-ES
Corrected Wind Speed (m/s)
Observed Wind Speed (m/s)
Bias uncorrected
HadGEM2-ES
Cumulative Distribution Function
Fn(x)
Wind Speed (m/s)
x
Bias corrected
HadGEM2-ES
Cumulative Distribution Function
Fn(x)
Wind Speed (m/s)
x